DISSERTATION

# AGENT-BASED MOVEMENT MODELS AND LANDSCAPE CONNECTIVITY

Submitted by
Jeff Alfred Tracey
Graduate Degree Program in Ecology

In partial fulfillment of the requirements
For the Degree of Doctor of Philosophy
Colorado State University
Fort Collins, Colorado
Fall 2006

COLORADO STATE UNIVERSITY

September 20, 2006

WE HEREBY RECOMMEND THAT THE DISSERTATION PREPARED UNDER OUR SUPERVISION BY JEFF ALFRED TRACEY ENTITLED AGENT-BASED MOVEMENT MODELS AND LANDSCAPE CONNECTIVITY BE ACCEPTED AS FULFILLING IN PART REQUIREMENTS FOR THE DEGREE OF DOCTOR OF PHILOSOPHY

Committee on Graduate Work

F. Jay Breidt

Barry Noon

Dave Theobald

**Adviser** Kevin R. Crooks

**Department Head/Director**

ABSTRACT OF DISSERTATION

AGENT-BASED MOVEMENT MODELS AND LANDSCAPE CONNECTIVITY

Human-caused changes in landscapes typically result in the loss, degradation, and fragmentation of animal habitats. One consequence of habitat fragmentation is changes in functional landscape connectivity, which, for animals, refers to their ability to move through a landscape among areas of suitable habitat. Our ability to anticipate the consequences of human-caused landscape change on connectivity depends in part on how well we are able to incorporate both animal movement behavior and landscape structure into predictive models for connectivity.

In my dissertation research, I have explored various approaches to modeling animal movement and how to use such models to evaluate functional connectivity. Four chapters are presented. The first chapter presents a simple model for studying animal movement response to a single type of landscape feature. We demonstrate the model using data from a red diamond rattlesnake. The second chapter describes an approach for modeling movement and using individual-based movement models to evaluate functional connectivity. Model formulation, computer implementation, and

application to connectivity evaluation are described and illustrated using a case study for puma in southern California. The third chapter presents a distance-weighted anisotropic detector model for perception that can be used in agent-based movement modeling. Modeling results suggest that increased anisotropy in the detection space leads to increased directional persistence and decreased use of the most suitable transition habitat. The fourth chapter describes a general approach to agent-based movement modeling and illustrates how to parameterize and evaluate these models using radio-tracking data. Forty-one models for three different puma were fit to data, and model selection was performed using $AIC_c$. The best models produced patterns that were consistent with observed data at the move level, but the patterns of nightly net displacement predicted by the best models were not consistent with the observed patterns at this scale; however, this nightly net displacement pattern may be produced by extending the current models to use spatial and temporal covariates. This work improves our ability to model individual-based movement and use such models to study functional landscape connectivity.

Jeff Alfred Tracey
Graduate Degree Program in Ecology
Colorado State University
Fort Collins, CO 80523
Fall 2006

## TABLE OF CONTENTS

## ACKNOWLEDGEMENTS

I thank my advisor, Dr. Kevin R. Crooks, who has helped to keep me focused on what this work is really about, provided much advice, and is a genuinely fine person. I have also enjoyed working with Dr. Jun Zhu, from the Department of Statistics at the University of Wisconsin-Madison. She was my co-advisor, along with Dr. Crooks, as I pursued a Master's of Science Degree in Biometry at UW. I plan to continue working with them both into the future. I have a fine committee, which includes Kevin Crooks, Barry Noon, Dave Theobald, and F. Jay Breidt. I admire and respect each of these men as scientists and human beings.

We have collaborated with, or will collaborate with, several researchers including: Paul Beier (Northern Arizona University), Lisa Lyren (US Geological Survey), Scott Morrison (The Nature Conservancy), Walter Boyce (UC Davis), and Seth Riley (National Park Service). I thank them for their work and their efforts in wildlife research and conservation.

I received research support from the US Geological Survey, The Nature Conservancy, the California Department of Fish and Game. This research is based upon work partially supported by the National Science Foundation under IGERT Grant No. DGE-0221595 through the PRogram for Interdisciplinary Mathematics,

Ecology, and Statistics (PRIMES) at Colorado State University.

The first chapter of this dissertation has been published in the *Journal of Agricultural, Biological, and Environmental Statistics*. The second chapter has been published in a book entitled *Connectivity Conservation*, edited by Kevin R. Crooks and M. Sanjayan, and published by Cambridge University Press. The third and fourth chapters will be submitted for publication within the year.

## DEDICATION

I dedicate this work to my wife, Rosana, and my children, Andrew and Marissa. They have made many sacrifices so that I might pursue graduate education, and have supported me through many challenging times. This achievement is as much theirs as it is mine.

# A Set of Nonlinear Regression Models for Animal Movement in Response to a Single Landscape Feature

J. A. TRACEY, J. ZHU, and K. CROOKS

The study of individual animal movement in relation to objects in a landscape is important in many areas of ecology and conservation biology. Yet, many of the models used by ecologists do not account for landscape features and thus may not be conducive to analysis of animal movement data. This article develops a set of nonlinear regression models for both move angles and move distances in relation to a single object in the landscape. Our models incorporate the concept of perceptual range from theories of animal movement behavior. We describe numerical methods for obtaining the maximum likelihood estimates of the model parameters. For illustration, we show results from both computer simulated data and real movement data collected for a red diamond rattlesnake (*Crotalus ruber*) via radio telemetry field techniques.

**Key Words:** Animal ecology; Circular data; Gamma distribution; Perceptual range; von Mises distribution.

## 1. INTRODUCTION

In spite of its importance in many areas of behavior, ecology, and wildlife conservation, the movement of individual animals in space remains a poorly understood process (Marsh and Jones 1988; Turchin 1998). Of particular importance is movement in relation to objects in a landscape, a process that has been called *object orientation* (Jander 1975). Objects include a wide range of point features such as prey or den sites, linear features such as rivers or roads, and polygon features such as an urban development or lake. Behavioral theory asserts that an animal may respond, through movement, to objects that are within its *perceptual range*, defined as the distance from which an animal can perceive a particular landscape element (Lima and Zollner 1996). The movement response to the object (or land-

J. A. Tracey is Research Assistant, Department of Fishery and Wildlife Biology, Colorado State University, Ft. Collins, CO 80523. J. Zhu is Assistant Professor, Department of Statistics and Soil Science, University of Wisconsin–Madison, 1300 University Avenue, Madison, WI 53706 (E-mail: jzhu@stat.wisc.edu). K. Crooks is Assistant Professor, Department of Fishery and Wildlife Biology, Colorado State University, Ft. Collins, CO 80523.


*Journal of Agricultural, Biological, and Environmental Statistics, Volume 10, Number 1, Pages 1–18*
*DOI: 10.1198/108571105X29056*

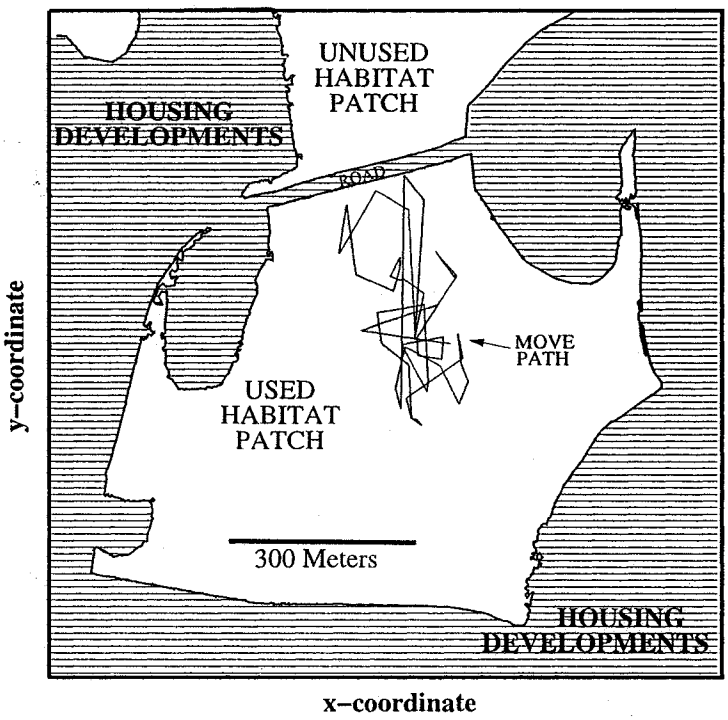


*Figure 1. A map of rattlesnake habitat and movement paths. The unfilled polygons are patches of rattlesnake habitat. The two largest habitat patches are separated by a two-lane road. The hatched areas are urban development or roads. The boundaries between habitat and urban development are shown as solid lines. The move paths for the rattlesnake are shown as solid lines in the central habitat patch.*

scape feature) may be qualitatively described as attractive, repulsive, or neutral. However, it remains a challenge to describe object orientation quantitatively based on empirical data.

Movement data are collected, for example, in behavioral ecology to study habitat use, and in conservation biology to study how animal behavior is affected by human-caused changes to a landscape. Data on the movement of individual animals are often collected using field techniques such as radio-telemetry, snow tracking, or continuous observation, where animal positions are taken at regular or irregular time intervals. Animal movement is inherently an individual-level process because it is the result of the capabilities, needs, experience, perception, information processing, and activity of individual animals. Further, due to considerations of time, effort, and cost in such studies, oftentimes there are many observations for an individual animal, but only for a very small number of individuals. Data on landscape features, in contrast, are more abundant and are collected via remote sensing or ground measurement using a global positioning system or other techniques.

In this article, we focus on an example of such movement and landscape data shown in Figure 1. The data were collected to study the effects of roads and housing developments on the movement of red diamond rattlesnakes (*Crotalus ruber*) in San Diego, CA (Tracey 2000;

Tracey and Case 2005). The figure shows the boundaries between two habitat patches and regions of urban development (hereafter referred to as *patch boundaries*). Within the central patch is a movement path of an individual adult male rattlesnake formed by joining observed locations with straight line segments (Figure 1). Even though there was an equally suitable habitat patch (Figure 1, upper part) that could have been reached by crossing a paved road approximately 20 meters in width, the animal did not use this neighboring patch. Within the used habitat patch, the rattlesnake was found in areas further away from the patch boundary more often than areas close to the patch boundary. There are at least two plausible conservation implications of such movement responses to the patch boundary. First, even narrow paved roads can act as barriers to movement, so there may be little movement of the rattlesnake between patches of habitat. Second, because areas near patch boundaries along urban development tend to be avoided, the amount of suitable habitat available within a habitat patch may depend on how much of its area is a sufficient distance from the patch boundary.

In practice, individual-based approaches are increasingly used in the fields of ecology and conservation (DeAngelis and Gross 1992), but movement and landscape data are rarely used together to quantitatively analyze movement responses of animals to landscape features. Recently, empirical studies have begun to focus on movement response of insects (Haddad 1999) and small mammals (Zollner 2000) to landscape features, but models and statistical methods for analyzing such data are not well developed. Here, we develop a set of statistical models for the analysis of individual animal movement data in relation to landscape feature data. Our intent in developing these models is to support individual-based models that will be used for conservation applications. The movement models we develop have several useful applications. First, the qualitative response of an individual animal to landscape features can now be inferred from the model parameters. Second, the models can be used to identify specifically which properties of movement change to produce attraction or avoidance as an animal approaches an object in the landscape (such as a patch boundary). Third, they can be used to quantify the distance from the object at which changes in an individual's movements first occur. That is, we incorporate into our models the notion of object orientation and perceptual range as in the ecological theories. Thus, the proposed models and methods will equip ecologists and biologists with more adequate tools for studying animal movement across the landscape and, hence, can impact future research in areas such as behavioral ecology and conservation biology.

In previous ecological studies that involve movement models, move angles have been modeled as a von Mises random variable with a constant mean angle and concentration parameter (Siniff and Jensen 1969; Batschelet 1981). Siniff and Jensen (1969) used gamma distributions to model rate of movement for an individual animal, and provided examples of empirical distributions of distance traveled per minute for red foxes and snowshoe hares to support their choice. Other studies, for example, of the butterfly *Danaus plexippus* (Zalucki and Kitching 1982), also have found that move distance distributions are consistent with the shape of gamma distributions. Unfortunately, most models of individual movement found

in the ecological literature, for example, simple random walk, correlated random walk, and directional bias models (Batschelet 1981; Kareiva and Shigesada 1983; Turchin 1998), do not describe movement in relation to landscape features, but rather model movement in a featureless landscape.

In order to model the response of an individual animal, through movement, to objects in the landscape, we let the parameters of the von Mises distribution and/or gamma distribution change based on the animal's location relative to the location of the object. In particular, for move angles, the von Mises distribution has a concentration parameter that changes as a function of the animal-to-object distance and a mean angle that changes as a function of the animal-to-object angle. For move distances, the gamma distribution has a mean move distance that changes as a function of the animal-to-object distance. Our approach bears similarity to generalized linear models, but we allow for more general nonlinear models which are sometimes necessary for the complex biological and ecological systems under study. Statistical inference herein is likelihood based and we use methods similar to those for generalized linear models to obtain the maximum likelihood estimates (MLE) (see, e.g., Thisted 1988; McCullagh and Nelder 1989). For move angle models, we also use results for circular statistics in Fisher (1993) and Mardia and Jupp (2000). In particular, Chapter 6 of Fisher (1993) provides regression models for von Mises distributions, which we specialize for modeling move angles in relation to landscape features, but also generalize to include intrinsically nonlinear models for the concentration parameters.

In Section 2, we propose the models and provide biological interpretation of the model parameters. In Section 3, we describe statistical inference via maximum likelihood. In Section 4, we demonstrate applications of the model using simulated data and the rattlesnake data. Finally, we provide a summary and further discussion in Section 5.

## 2. MODEL

For the $i$th observation, where $i = 1, 2, \ldots, n+1$, we let $\mathbf{s}_i = (s_{i,1}, s_{i,2})'$ denote the location of an animal and let $\mathbf{x}_i = (x_{i,1}, x_{i,2})'$ denote the location of an object. We let $T_i = \|\mathbf{s}_i - \mathbf{x}_i\|_2$ denote the animal-to-object distance and $D_i = \|\mathbf{s}_i - \mathbf{s}_{i+1}\|_2$ denote the move distance between animal locations $\mathbf{s}_i$ and $\mathbf{s}_{i+1}$, where $i = 1, \ldots, n$ (Figure 2). Further let $B_i = \text{ang}(\mathbf{s}_i, \mathbf{s}_{i+1})$ denote the $i$th move angle, and let $C_i = \text{ang}(\mathbf{s}_i, \mathbf{x}_i)$ denote the animal-to-object angle at the $i$th move (Figure 2), where for $\mathbf{u} = (u_1, u_2)'$ and $\mathbf{v} = (v_1, v_2)'$:

$$\text{ang}(\mathbf{u}, \mathbf{v}) = \begin{cases} \tan^{-1}\left((v_2 - u_2)/(v_1 - u_1)\right) & ; v_1 - u_1 > 0, \\ \tan^{-1}\left((v_2 - u_2)/(v_1 - u_1)\right) + \pi & ; v_1 - u_1 < 0, \\ \pi/2 & ; v_1 - u_1 = 0 \text{ and } v_2 - u_2 > 0, \\ -\pi/2 & ; v_1 - u_1 = 0 \text{ and } v_2 - u_2 < 0, \\ \text{undefined} & ; v_1 - u_1 = 0 \text{ and } v_2 - u_2 = 0. \end{cases} \tag{2.1}$$

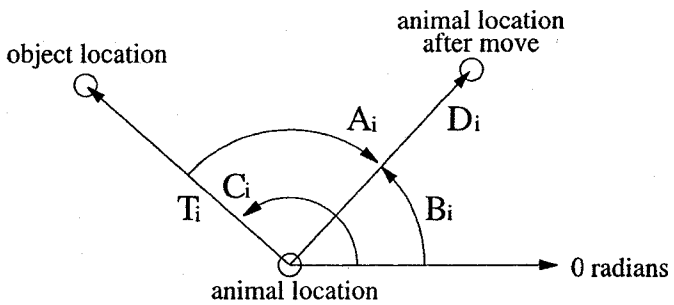


*Figure 2. Diagram illustrating movement in relation to an object in the landscape. The animal location ($\mathbf{s}_i$), the animal location after a move ($\mathbf{s}_{i+1}$), and the object location ($\mathbf{x}_i$) are shown as open circles. The animal-to-object angle in radians is $C_i$ and the animal-to-object distance is $T_i$. The move angle is $B_i$ and the move distance is $D_i$. The response angle is $A_i$.*

Thus, the $i$th move can be modeled as

$$\mathbf{s}_{i+1} = \mathbf{s}_i + D_i \begin{bmatrix} \cos(B_i) \\ \sin(B_i) \end{bmatrix}, \tag{2.2}$$

where $i = 1, \ldots, n$. We assume independence between $\{B_i\}$ and $\{D_i\}$ conditional on $\{T_i\}$ and $\{C_i\}$; therefore, we model $\{B_i\}$ and $\{D_i\}$ separately.

## 2.1 BASIC MOVE ANGLE MODEL

The basic move angle model does not incorporate the information on the object, but we describe it as a foundation for the responsive model in Section 2.2. We model the $i$th move angle, $B_i$, as a von Mises random variable:

$$[B_i|\mu, \kappa] \sim \text{vonmises}(\mu, \kappa), \quad B_i \in (-\pi, \pi], \tag{2.3}$$

where $i = 1, \ldots, n$, $\mu \in (-\pi, \pi]$ and $\kappa \geq 0$. The probability density is given by:

$$f(B_i|\mu, \kappa) = [2\pi I_0(\kappa)]^{-1} \exp(\kappa \cos(B_i - \mu)), \tag{2.4}$$

where $[2\pi I_0(\kappa)]$ is the normalizing constant and $I_0(\kappa)$ is a modified Bessell function of the first kind and zero order.

The von Mises distribution is a circular analogue to the normal distribution; it has two parameters, a mean angle $\mu$, and a concentration parameter $\kappa$ (Mardia and Jupp 2000). The mean angle is the angle of maximum probability density and the concentration parameter controls the dispersion of the distribution about the mean angle. The distribution is symmetric about the mean angle $\mu$. When the concentration parameter $\kappa = 0$, the distribution is uniform on $(-\pi, \pi]$. As $\kappa$ increases, the distribution becomes more concentrated about the mean angle.

## 2.2 RESPONSIVE MOVE ANGLE MODEL

To model move angle in response to the object, we modify the basic move angle model (2.3) and (2.4) as follows. We define the *response angle* as $A_i = (B_i - C_i) \text{mod}(-\pi, \pi]$, recalling that $B_i$ is the $i$th move angle and $C_i$ is the $i$th animal-to-object angle. We model $A_i$ by a von Mises distribution with a constant mean $\mu$ and a move-dependent concentration parameter $\kappa_i$. Here $\mu$ is the mean response angle that the animal prefers to move in relation to the animal-to-object angle. For example, if the animal is attracted to the object, then $\mu$ might be 0 radians, which indicates a tendency to move directly toward the object. On the other hand, if the animal is strongly repelled by the object, then $\mu$ might be $\pi$ radians, which would indicate a tendency to move directly away from the object. The mean response angle could depend on the animal-to-object distance $T_i$, but we assume a constant $\mu$ to yield a simpler but still realistic model. Next, we assume that the concentration parameter of $A_i$ depends on the animal-to-object distance $T_i$. We set $\kappa_i = g(T_i; \boldsymbol{\theta})$, where the "switch" function $g(T_i; \boldsymbol{\theta}) \geq 0$ for all $T_i > 0$ with parameters $\boldsymbol{\theta}$. The resulting probability density function is

$$f(A_i|T_i; \mu, \boldsymbol{\theta}) = \left[2\pi I_0(g(T_i; \boldsymbol{\theta}))\right]^{-1} \exp\left(g(T_i; \boldsymbol{\theta}) \cos(A_i - \mu)\right) . \tag{2.5}$$

We assume that $\kappa_i = g(T_i; \boldsymbol{\theta})$ is a decreasing function of $T_i$. If an animal responds to the object, then we expect the strength of the animal's response to increase as it gets closer to the object so that the animal has a greater tendency to move in the mean response angle $\mu$. Furthermore, we assume that as $T_i \to \infty$, $g(T_i; \boldsymbol{\theta}) \to 0$. That is, as the animal-to-object distance increases, the von Mises distribution becomes more uniform, and the animal moves in angles that depend less on the animal-to-object angle.

We consider two types of switch functions, namely, an exponential function and a logistic function (see, e.g., Seber and Wild 1989, chap. 7). The exponential function for $g(T_i; \boldsymbol{\theta})$ is

$$g(T_i; \boldsymbol{\theta}) = \theta_1 \exp(-\theta_2 T_i) , \tag{2.6}$$

where $\boldsymbol{\theta} = (\theta_1, \theta_2)'$, $\theta_1, \theta_2 > 0$. The exponential function (2.6) is monotone decreasing from $\theta_1$ to 0, at a rate of $\theta_2$. As $T_i \to 0$, $g(T_i; \boldsymbol{\theta}) \to \theta_1$; and as $T_i \to \infty$, $g(T_i; \boldsymbol{\theta}) \to 0$.

The logistic function for $g(T_i; \boldsymbol{\theta})$ is

$$g(T_i; \boldsymbol{\theta}) = \theta_1 \left[1 + \exp\left(\theta_2(T_i - \theta_3)\right)\right]^{-1} , \tag{2.7}$$

where $\boldsymbol{\theta} = (\theta_1, \theta_2, \theta_3)'$, $\theta_1, \theta_2, \theta_3 > 0$. The logistic function (2.7) is monotone decreasing, where the parameter $\theta_2$ controls the rate of decrease of the logistic function and $\theta_3$ is the inflection point. Thus, as $T_i \to 0$, $g(T_i; \boldsymbol{\theta}) \to \theta_1[1 + \exp(-\theta_2\theta_3)]^{-1}$; and as $T_i \to \infty$, $g(T_i; \boldsymbol{\theta}) \to 0$.

## 2.3 BASIC MOVE DISTANCE MODEL

We describe a basic move distance model as a foundation for the responsive move distance model in Section 2.4. We model the $i$th move distance, $D_i$, as a gamma random

variable:

$$[D_i|\alpha, \sigma^2] \sim \text{gamma}(\alpha, \sigma^2), \quad D_i > 0, \tag{2.8}$$

where $i = 1, \ldots, n$, the mean move distance $\alpha > 0$ and the variance in move distance $\sigma^2 > 0$.

We write the gamma distribution in terms of the mean and the variance because the meaning of these parameters is more intuitive. However, both the mean and variance of the move distance can be expressed in terms of the shape parameter $\iota$ and the inverse scale (or rate) parameter $\lambda$. The relations are: $\alpha = \iota/\lambda$ and $\sigma^2 = \iota/\lambda^2$, where $\iota > 0$ and $\lambda > 0$.

## 2.4 RESPONSIVE MOVE DISTANCE MODEL

To model move distance in response to the object, we modify the basic move distance model (2.8) by letting the mean move distance $\alpha$ depend on the animal-to-object distance. For the $i$th move, we set $\alpha_i = h(T_i; \boldsymbol{\eta})$, where the switch function $h(T_i; \boldsymbol{\eta}) > 0$ for all $T_i > 0$ with parameters $\boldsymbol{\eta}$. For simplicity, we assume a constant variance $\sigma^2$ for move distance. The resulting probability density function is

$$f(D_i|T_i; \boldsymbol{\eta}, \sigma^2) = \frac{\left(\frac{h(T_i;\boldsymbol{\eta})}{\sigma^2}\right)^{\left(\frac{h^2(T_i;\boldsymbol{\eta})}{\sigma^2}\right)}}{\Gamma\left(\frac{h^2(T_i;\boldsymbol{\eta})}{\sigma^2}\right)} D_i^{\left(\frac{h^2(T_i;\boldsymbol{\eta})}{\sigma^2}-1\right)} \exp\left(-\frac{h(T_i;\boldsymbol{\eta})}{\sigma^2} D_i\right). \tag{2.9}$$

Unlike the switch functions $g(T_i; \theta)$ for move angle, we assume that the mean move distance $\alpha_i = h(T_i; \boldsymbol{\eta})$ can either increase or decrease as the animal approaches the object. Again, we consider an exponential and a logistic function for $h(T_i; \boldsymbol{\eta})$. The exponential function for $h(T_i; \boldsymbol{\eta})$ is

$$h(T_i; \boldsymbol{\eta}) = (\eta_1 - \eta_2) \exp(-\eta_3 T_i) + \eta_2, \tag{2.10}$$

where $\boldsymbol{\eta} = (\eta_1, \eta_2, \eta_3)'$, $\eta_1, \eta_2, \eta_3 > 0$. As $T_i \to 0$, $h(T_i; \boldsymbol{\eta}) \to \eta_1$; and as $T_i \to \infty$, $h(T_i; \boldsymbol{\eta}) \to \eta_2$. The parameter $\eta_3$ controls the rate of changes. The logistic function for $h(T_i; \boldsymbol{\eta})$ is

$$h(T_i; \boldsymbol{\eta}) = (\eta_1 - \eta_2) \left[1 + \exp\left(\eta_3(T_i - \eta_4)\right)\right]^{-1} + \eta_2, \tag{2.11}$$

where $\boldsymbol{\eta} = (\eta_1, \eta_2, \eta_3, \eta_4)'$, $\eta_1, \eta_2, \eta_3, \eta_4 > 0$. As $T_i \to 0$, $h(T_i; \boldsymbol{\eta}) \to (\eta_1 - \eta_2)[1 + \exp(-\eta_3\eta_4)]^{-1} + \eta_2$; and as $T_i \to \infty$, $h(T_i; \boldsymbol{\eta}) \to \eta_2$. The parameter $\eta_3$ controls the rate of change, and $\eta_4$ is the inflection point. Both the exponential and the logistic function are monotone increasing if $\eta_1 < \eta_2$ and monotone decreasing if $\eta_1 > \eta_2$.

## 2.5 APPARENT PERCEPTUAL RANGE

Lima and Zollner (1996) defined perceptual range as the distance from which an animal can perceive a particular landscape feature. Based on the responsive models for

move angles and move distances in Section 2.2 and 2.4, we now propose an *apparent perceptual range* (APR) as follows. Let $\delta \in (0,1)$. We define two APRs: $T_A$ and $T_D$. For the move angle, $T_A$ is such that $g(T_A;\theta) = \delta g(0;\theta)$. For example, suppose $\delta = .05$ and the switch function is exponential, the APR $T_A$ is the distance at which the switch function achieves 5% of $\theta_1$, which is the total range of the switch function $g(\cdot;\theta)$. The specific formulas are $T_A(\theta) = -(\log\delta)/\theta_2$ for an exponential switch function and $T_A(\theta) = \left[\log\left(1+(1-\delta)\exp(\theta_2\theta_3)\right) - \log(\delta)\right]/\theta_2$ for a logistic switch function.

Similarly, for the move distance, $T_D$ is such that $h(T_D;\eta) = \delta(h(0;\eta)-\eta_2)+\eta_2$. The formulas for $T_D$ are the same as those for $T_A$, with $\theta_2$ replaced with $\eta_3$ and $\theta_3$ replaced with $\eta_4$. When the animal responds to the object through both the move angles and the move distances, we define an overall APR as $\max\{T_A, T_D\}$. The proportion $\delta$ serves as a threshold for identifying perceptual range and is user-specified. Our APR should be smaller than the theoretical perceptual range, since the animal may perceive the object at a greater distance than the distance at which the movement starts to respond to the object. Nevertheless the APRs provide a reasonable way to quantify the theoretical perceptual range.

## 3. STATISTICAL INFERENCE BY MAXIMUM LIKELIHOOD

In this section, we use maximum likelihood to estimate the parameters of the responsive models for move angles and move distances.

### 3.1 RESPONSIVE MOVE ANGLE MODEL

Let $\mathbf{A} = (A_1, A_2, \ldots, A_n)'$ denote the vector of observed response angles (i.e., move angle relative to the animal-to-object angle) and let $\mathbf{T} = (T_1, T_2, \ldots, T_n)'$ denote the vector of animal-to-object distances. Let $\xi_A = (\mu, \theta')'$ denote the parameters of the responsive move angle model (2.5), where recall that $\mu$ is the constant mean angle and $\theta$ are the parameters of a switch function $g(T_i;\theta)$. Assuming conditional independence among all $A_i$ given $T_i$ and $C_i$ and by (2.5), the log-likelihood function for $\xi_A$ is:

$$\ell(\xi_A;\mathbf{A},\mathbf{T}) = -n\log(2\pi) - \sum_{i=1}^{n}\log I_0(g(T_i;\theta)) + \sum_{i=1}^{n} g(T_i;\theta)\cos(A_i-\mu)\,. \quad (3.1)$$

Maximization of the log-likelihood function (3.1) can be performed using a Newton-Raphson type of optimization algorithm. In particular, the first partial derivatives of $\ell(\xi_A;\mathbf{A},\mathbf{T})$ are

$$\frac{\partial\ell}{\partial\theta} = \sum_{i=1}^{n}\left[\cos(A_i-\mu) - I^{(1)}(g(T_i;\theta))\right]\frac{\partial g(T_i;\theta)}{\partial\theta}, \quad \frac{\partial\ell}{\partial\mu} = \sum_{i=1}^{n} g(T_i;\theta)\sin(A_i-\mu),$$

where $I^{(1)}(\kappa) = d\log\left(I_0(\kappa)\right)/d\kappa = I_1(\kappa)/I_0(\kappa)$ and $I_1(\kappa)$ is the modified Bessell function of the first kind and first order. Furthermore, the second partial derivatives of $\ell(\xi_A;\mathbf{A},\mathbf{T})$ are

$$\begin{aligned}
\frac{\partial^2 \ell}{\partial \theta \partial \theta'} &= \sum_{i=1}^{n} \left[\cos(A_i - \mu) - I^{(1)}(g(T_i;\theta))\right] \frac{\partial^2 g(T_i;\theta)}{\partial \theta \partial \theta'} \\
&\quad - I^{(2)}(g(T_i;\theta)) \frac{\partial g(T_i;\theta)}{\partial \theta} \left(\frac{\partial g(T_i;\theta)}{\partial \theta}\right)', \\
\frac{\partial^2 \ell}{\partial \theta \partial \mu} &= \sum_{i=1}^{n} \frac{\partial g(T_i;\theta)}{\partial \theta} \sin(A_i - \mu), \\
\frac{\partial^2 \ell}{\partial \mu^2} &= \sum_{i=1}^{n} -g(T_i;\theta) \cos(A_i - \mu),
\end{aligned}$$

where $I^{(2)}(\kappa) = d^2 I_0(\kappa)/d\kappa^2 = \left[I_0(\kappa)\left(I_0(\kappa) - I_1(\kappa)/\kappa\right) - I_1(\kappa)^2\right]/I_0(\kappa)^2$.

Because $E[\cos(A_i - \mu)] = I^{(1)}(g(T_i;\theta)$ and $E[\sin(A_i - \mu)] = 0$ (Mardia and Jupp 2000), one can apply the Fisher scoring algorithm to obtain the MLE $\hat{\theta}$ and $\hat{\mu}$ with relative ease (see, e.g., Thisted 1988). The asymptotic variance for the MLE $\widehat{\theta}$ is

$$\left[\sum_{i=1}^{n} I^{(2)}(g(T_i;\theta)) \frac{\partial g(T_i;\theta)}{\partial \theta} \left(\frac{\partial g(T_i;\theta)}{\partial \theta}\right)'\right]^{-1}$$

and the asymptotic variance for the MLE $\hat{\mu}$ is

$$\left[\sum_{i=1}^{n} g(T_i;\theta)\cos(A_i - \mu)\right]^{-1}.$$

For an exponential switch function, the expressions can be further simplified (see, e.g., Fisher and Lee 1992; Fisher 1993).

The von Mises distributions belong to the exponential family and under mild regularity conditions (including the smooth condition for the switch function), similar arguments as in Section 5.3 of Mardia and Jupp (2000) ensure the asymptotic normality of the MLEs. Simulation was conducted and verified the asymptotic properties of the MLEs as the sample size increased. To save space, we omit presenting the standard simulation results.

### 3.2 RESPONSIVE MOVE DISTANCE MODEL

Let $\mathbf{D} = (D_1, D_2, \ldots, D_n)'$ denote the vector of observed move distances and again recall that $\mathbf{T} = (T_1, T_2, \ldots, T_n)'$ denotes the vector of animal-to-object distances. Let $\boldsymbol{\xi}_D = (\boldsymbol{\eta}', \sigma^2)'$ denote the parameters of the responsive move distance model (2.9), where recall that $\boldsymbol{\eta}$ are the parameters of a switch function $h(T_i;\boldsymbol{\eta})$ and $\sigma^2$ is the constant variance of the move distances. Assuming conditional independence among all $D_i$ given $T_i$ and by (2.9), the log-likelihood function for $\boldsymbol{\xi}_D$ is

$$\begin{aligned}
\ell(\boldsymbol{\xi}_D; \mathbf{D}, \mathbf{T}) &= \sum_{i=1}^{n} \frac{h^2(T_i;\boldsymbol{\eta})}{\sigma^2} \left(\log h(T_i;\boldsymbol{\eta}) - \log \sigma^2 + \log D_i\right) \\
&\quad - \sum_{i=1}^{n} \log \Gamma\left(\frac{h^2(T_i;\boldsymbol{\eta})}{\sigma^2}\right) - \sum_{i=1}^{n} \log D_i - \sum_{i=1}^{n} \frac{h(T_i;\boldsymbol{\eta})}{\sigma^2} D_i \,. \quad (3.2)
\end{aligned}$$

We omit presenting the standard results of the first and second partial derivatives of the log-likelihood function $\ell(\xi_D; \mathbf{D}, \mathbf{T})$, but note that the expectation of the second derivative does not have a closed form. Thus, it would be easier to use the observed information matrix instead of the Fisher information matrix in the iterations of a Newton-Raphson algorithm. Because the gamma distribution is in the exponential family and under the usual regularity conditions (Shao 1999), the MLEs are asymptotically normal. Simulation was also conducted and verified the asymptotic properties of the MLEs as the sample size increased.

### 3.3 STARTING VALUES

We obtain initial parameter estimates using descriptive statistics and visual inspection of data figures. For the responsive move angle model, we plot the observed response angles $\{A_i\}$ versus the animal-to-object distance $\{T_i\}$. For the exponential function, first visually estimate $T_{\max}$, the animal-to-object distance where the response angles appear to become uniform. Then using the observations at the small animal-to-object distances, estimate the mean angle $\mu^{(0)}$ and concentration parameter $\theta_1^{(0)}$. Finally, calculate $\theta_2^{(0)} = [\log(\theta_1^{(0)}) - \log(s)]/T_{\max}$ where $s$ is a small number such as .1. For the logistic function, first visually estimate $T_{\min}$, the animal-to-object distance at which the dispersion of response angles appears to stop changing as the animal-to-object distance is further decreased. Then visually estimate $T_{\max}$, the animal-to-object distance at which the dispersion of response angles appears to become uniform. Now, make point estimates for the mean angle $\mu^{(0)}$ and concentration $\theta_1^{(0)}$ for moves where the animal-to-object distance is smaller than $T_{\min}$. Finally, calculate $\theta_2^{(0)} = 4/[T_{\max} - T_{\min}]$ and $\theta_3^{(0)} = .5(T_{\max} + T_{\min})$. For the responsive move distance model, similar techniques as for the move angle model can be applied. We omit the details.

## 4. APPLICATIONS

This section illustrates the methods developed in Sections 2 and 3 with both simulated data and the rattlesnake data introduced in Section 1. By using simulated data we demonstrate the behavior of the models under different parameters and assess properties of the parameter estimates. By using data from a biological system we demonstrate the usefulness of the models and some of the practical issues involved in actual application.

### 4.1 SIMULATED DATA

We produced simulated datasets by modeling movement in relation to a point, a line, and a polygon. The point object is defined by spatial coordinates (100, 100). The line feature is defined by a line segment connecting (80, 80) and (120, 120), in which case the location of the object was determined as the point on the line feature closest to the animal's location.

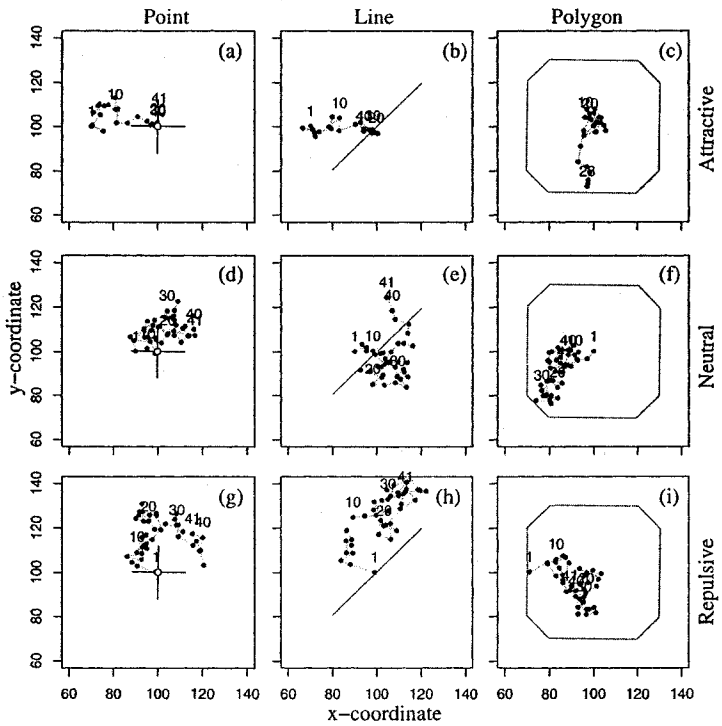


*Figure 3. Examples of simulated movement paths. Movements were simulated in relation to point ((a), (d), (g)), line ((b), (e), (h)), and polygon ((c), (f), (i)) features. The landscape features (or objects) are shown as black solid lines. The location of the point object is shown as "cross-hairs." Parameters were selected to produce attractive ((a)–(c)), neutral ((d)–(f)), and repulsive ((g)–(i)) responses. In the polygon case, attraction was to the polygon boundary, and the simulation was terminated when the simulated animal left the polygon. Conversely, repulsion was to the polygon boundary. The simulated animal locations are shown as filled circles joined by gray lines to show the movement order. Numbers above some locations also indicate movement order.*

The polygon feature is delineated by a closed set of eight line segments defined by the sequence of vertexes (80, 130), (120, 130), (130, 120), (130, 80), (120, 70), (80, 70), (70, 80), (70, 120), (80, 130). Again, the location of the object was determined to be the point on the polygon boundary closest to the animal location. Movement in relation to these objects was simulated according to the responsive models for move angles (2.5) with a logistic switch function (2.7) and for move distances (2.9) with a logistic switch function (2.11).

Examples of the simulated movement paths are shown in Figure 3. For movement that is attracted to an object (Figure 3(a)–(c)), we selected the following parameter values for the response angle model: $\mu = 0, \theta_1 = 4, \theta_2 = 1.2, \theta_3 = 10$; and the following parameter values for the move distance: $\eta_1 = 1, \eta_2 = 5, \eta_3 = 1.2, \eta_4 = 5, \sigma^2 = 2$. Starting far from the object at (70, 100) (Figure 3(a) and 3(b)) and at the center of the polygon (100, 100) (Figure 3(c)), the simulated movement tends toward the object. The clear tendency to move toward the object is because of the zero mean response angle $\mu = 0$. For movement that does not relate to an object (Figure 3(d)–(f)), we selected the following parameter values

for the response angle: $\mu = 0, \theta_1 = 0, \theta_2 = 1.2, \theta_3 = 10$; and those for the move distance $\eta_1 = 5, \eta_2 = 5, \eta_3 = 1.2, \eta_4 = 5, \sigma^2 = 2$. Starting at (90, 100) (Figure 3(d) and 3(e)) and at (100, 100) (Figure 3(f)), the simulated movement wanders around the object,

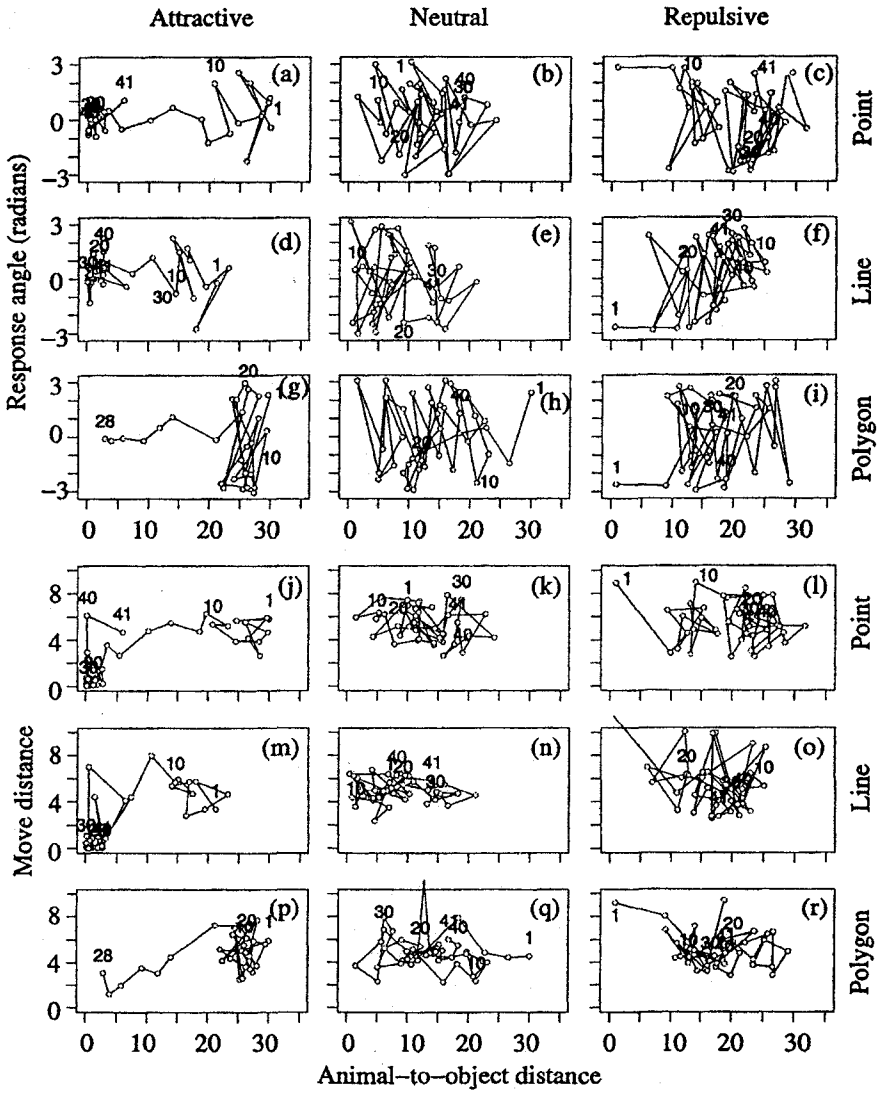


*Figure 4. Display of the simulated movement data. Subfigures (a)–(i) show the simulated response angles versus the animal-to-object distance, and subfigures (j)–(r) show the simulated move distances versus the animal-to-object distance. Simulated movements were in relation to point ((a)–(c), (j)–(l)), line ((d)–(f), (m)–(o)), and polygon ((g)–(i), (p)–(r)) features. The relation was attractive ((a), (d), (g), (j), (m), (p)), neutral ((b), (e), (h), (k), (n), (q)), and repulsive ((c), (f), (i), (l), (o), (r)) responses. The simulated observations are shown as circles joined by solid lines to show movement order. Numbers above some observations also indicate movement order.*

without an obvious tendency toward or away from the object. Finally, for movement that is repelled by an object (Figure 3(g)–(i)), we selected the following parameter values for the response angle: $\mu = \pi, \theta_1 = 4, \theta_2 = 1.2, \theta_3 = 10$; and those for the move distance $\eta_1 = 9, \eta_2 = 5, \eta_3 = 1.2, \eta_4 = 5, \sigma^2 = 2$. Starting near the object at (99, 100) (Figure 3(g) and 3(h)) and at (71, 100) (Figure 3(i)), the simulated movement moves away from the object. The clear tendency to move away from the object is produced by setting the mean response angle $\mu = \pi$.

For both the attractive and repulsive move angle response, the concentration parameter increases as a function of the animal-to-object distance from 0 at a large distance to approximately 4 at a distance of 0. For the move distance response, we set the mean move distance at large animal-to-object distances as $\eta_2 = 5$. For the attractive case, the mean move distance declines as the animal approaches the object, as would be expected if the animal prefers to be near the object. In contrast, for the repulsive examples, the mean move distance increases as the animal-to-object distance decreases, because the animal could avoid the object more effectively if it moves more quickly away when the object was nearby.

Corresponding to these movement patterns, we plotted the response angles $\{A_i\}$ versus the animal-to-object distances $\{T_i\}$ (Figure 4(a)–(i)). For movement attracted to an object, the response angles are more concentrated around 0 radians as the animal-to-object distances are decreased, whereas the response angles are more concentrated around $\pi$ radians for movement repelled by an object. No obvious pattern is seen for movement nonresponsive to an object. In the polygon case, the movement response is to the nearest point on the polygon boundary. In the attractive case, the animal tends to move toward the boundary and quickly leaves the polygon (Figure 3(c) and Figure 4(g)). For the repulsive case the animal tends to move away from the polygon boundary, and its movements are confined to within the polygon (Figure 3(i) and Figure 4(i)).

In addition, we plotted the move distances $\{D_i\}$ versus $\{T_i\}$ (Figure 4(j)–(r)). For the repulsive cases (Figure 4(l), (o), and (r)), the tendency to avoid the object is increased by larger move distances for small animal-to-object distances. In the neutral cases (Figure 4(k), (n), and (q)), the mean move length does not depend on the animal-to-object distance. In the attractive cases (Figure 4(j), (m), and (p)) the tendency to remain near the object is increased by smaller move distances for small animal-to-object distances.

The models produced the desired behavior in all cases. One important point is that for the simulations with a repulsive response, shorter animal-to-object distances are underrepresented in the simulated data. It is reasonable to expect this from real data where the animal is repelled by the object, which can pose difficulties in parameter estimation for a small sample size.

### 4.2 RATTLESNAKE MOVEMENT DATA

We return to the rattlesnake data presented in Section 1 to demonstrate the application of our models to real movement and landscape data. The data were obtained using radiotelemetry for a single adult male red diamond rattlesnake (*Crotalus ruber*; Tracey 2000;

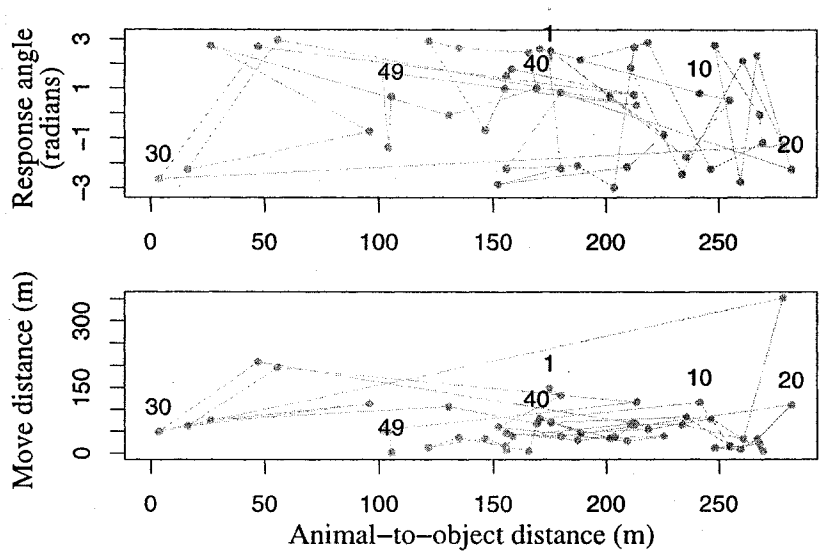


*Figure 5. Display of the rattlesnake movement data. The top figure shows the observed response angle versus the animal-to-object distance in meters. In this case, the location of the object is the nearest point on the habitat patch boundary. The bottom figure shows the move distance in meters versus the animal-to-object distance in meters. In both figures, the observations are shown as filled circles joined by gray lines to show their movement order. Numbers above some observations also indicate movement order.*

Tracey and Case 2005). Red diamond rattlesnakes, a species of pit viper, can be found only in coastal southern California and the Baja California, and are primarily active in spring and summer. They are referred to as *mobile ambush predators* because they move to a suitable ambush site, wait until a small mammal comes within striking range, and then strike the prey delivering venom through retractable fangs. Much of its habitat in the United States is being severely impacted by urban and agricultural development, but few studies of this species have been conducted by ecologists. The objective of the radio-telemetry study was to improve our understanding of the effects of urban development on the habitat use, movement, and home range sizes of red diamond rattlesnakes (Tracey 2000; Tracey and Case 2005).

The particular animal that is the focus of this analysis inhabited a fragment of natural vegetation isolated by roads and urban development (Figure 1). The rattlesnake was radio-tracked by surgically implanting a small transmitter in the snake's body, and then locating the transmitter by a receiver attached to a directional antenna. The study animal was located at two- to three-day intervals during the late spring and summer months of 1999 and 2000, the seasons when rattlesnakes are most active. Because the relocation time intervals were fairly regular, we may assume that the move duration (i.e., the time interval between two consecutively sampled locations) did not influence move distance. Universal Transverse Mercator (UTM) coordinates accurate to within 1.7 meters were obtained using a Global Positioning System receiver and differential correction techniques. A total of $n = 49$ moves were observed (Figure 1). Data for relocation intervals during which the animal did not move

Table 1. Maximum Likelihood Estimates of Model Parameters From Rattlesnake Movement Data

*Move angle models*

| Model | $\hat{\mu}$ | $\hat{\kappa}$ | $\hat{\theta}_1$ | $\hat{\theta}_2$ | $\hat{\theta}_3$ |
|---|---|---|---|---|---|
| basic | 2.77 | .45 | — | — | — |
| responsive (exponential) | −2.74 | — | 17.25 | .06 | — |
| responsive (logistic) | −3.09 | — | 4.14 | .53 | 74.19 |

*Move distance models*

| Model | $\hat{\alpha}$ | $\hat{\sigma}^2$ | $\hat{\eta}_1$ | $\hat{\eta}_2$ | $\hat{\eta}_3$ | $\hat{\eta}_4$ |
|---|---|---|---|---|---|---|
| basic | 65.45 | 3198.70 | — | — | — | — |
| responsive (exponential) | — | 3101.58 | 96.07 | 61.70 | .017 | — |
| responsive (logistic) | — | 2767.29 | 109.51 | 59.52 | 1.92 | 101.42 |

were excluded from this analysis. During the study, the animal was not observed moving beyond the boundary between the natural vegetation and urban development.

The boundary of the habitat fragment was digitized from high-resolution aerial imagery (U.S. Geological Survey DOQQs), resulting in a polygon defined by a closed set of line segments (Figure 1). We computed the distance $T_i$ and angle $C_i$ from each animal location to the nearest point on the habitat patch boundary, the distance the animal moved $D_i$, the angle the animal moved $B_i$, and the response angle $A_i$ for each observation $i$. In Figure 5, we plotted the response angles $\{A_i\}$ and the move distances $\{D_i\}$ versus the animal-to-object distances $\{T_i\}$. The plot of the response angles (Figure 5) are remarkably similar to the simulated data for repulsion to a polygon boundary (Figure 4(i)). Most notably, in both plots the distribution of response angles becomes more uniform as $T_i$ increases and there are relatively fewer observations for small values of $T_i$.

We analyzed the response angle data $\{A_i\}$ using a basic move angle model (i.e., von Mises distribution with constant mean and concentration), a responsive move angle model with an exponential switch function of the animal-to-object distance $\{T_i\}$ for the von Mises concentration parameter, and a response move angle model with a logistic switch function (Table 1). Similarly we analyzed the move distance data $\{D_i\}$ using a basic move distance model (i.e., gamma distribution with constant mean and variance), a responsive move distance model with an exponential switch function of the animal-to-object distance $\{T_i\}$ for the mean move distance, and a responsive move distance model with a logistic switch function (Table 1). We used likelihood ratio tests (LRT) and Akaike's information criterion (AIC) for model selection (Table 2). All data were analyzed using functions written by the authors in R (R Development Core Team 2003). These functions can be obtained from the authors upon request.

For the move angles, the LRT for the basic model versus the responsive model with an exponential switch function had a $\chi^2 = 4.22$ on 1 df with a $p$ value of .04. Similarly, the LRT for the basic model versus the responsive model with a logistic switch function had a $\chi^2 = 5.64$ on 2 df with a $p$ value of .06. Thus, there is some evidence that the basic model is not adequate and the animal's response to the patch boundary did change with the animal-to-boundary distances. Between the two switch functions, the AIC values were close

Table 2. Model Selection for Move Angle and Move Distance Models. Likelihood ratio test is used to compare a basic model and a responsive model, whereas Akaike's information criterion (AIC) is used to compare a responsive model with an exponential switch function and that with a logistic switch function.

| *Move angle models* | | | | | |
|---|---|---|---|---|---|
| *Full model* | *AIC* | *Reduced model* | $\chi^2$ | *df* | *p value* |
| basic | 179.25 | — | — | — | — |
| responsive (exponential) | 177.04 | basic | 4.21 | 1 | .040 |
| responsive (logistic) | 177.61 | basic | 5.64 | 2 | .060 |
| *Move distance models* | | | | | |
| *full model* | *AIC* | *reduced model* | $\chi^2$ | *df* | *p value* |
| basic | 509.40 | — | — | — | — |
| responsive (exponential) | 511.97 | basic | 1.43 | 2 | .488 |
| responsive (logistic) | 509.11 | basic | 6.30 | 3 | .098 |

with 177.04 for the exponential switch and 177.61 for the logistic switch. Nonetheless, we selected the exponential function because of its simplicity. Given the final exponential responsive angle model, the parameter estimates and their standard errors (in the parentheses) are $\hat{\mu} = -2.74\ (.050), \hat{\theta}_1 = 17.25\ (8.10), \hat{\theta}_2 = .056\ (.0081)$. The estimated mean response angle $\hat{\mu} = -2.74$ indicates that the animal tends to move away from the nearest point on the habitat patch boundary. Recall that $\theta_1$ is the concentration of the von Mises distribution when $T_i = 0$. Because the estimate $\hat{\theta}_1$ is large, the tendency to move away from the patch boundary became very strong as the animal approached the boundary. The strength of the tendency decreased exponentially at a rate of $\hat{\theta}_2 = .056$ as the animal moved away from the patch boundary. These results indicate that this rattlesnake had a strong repulsive response to the patch boundary.

In contrast, for the move distance models, the LRT for the basic model versus the responsive model with an exponential switch function had a $\chi^2 = 1.43$ on df $= 2$ with a $p$ value of .49; whereas the LRT for the basic model versus the responsive model with a logistic switch function had a $\chi^2 = 6.30$ on df $= 3$ with a $p$ value of .10. For both types of switch functions, there is no evidence against the basic unresponsive model. Given the final basic move distance model, the parameter estimates and their standard errors (in the parentheses) are $\hat{\alpha} = 65.45\ (.78), \hat{\sigma}^2 = 3198.70\ (106.32)$. The results indicate that the animal did not alter the move distance deliberately as it approached the patch boundary. In summary, altering the move angles rather than the move distances was the primary mechanism that this particular rattlesnake used to avoid approaching the patch boundary and possibly crossing into roads or urban areas, thereby avoiding the risks involved in moving through the human-dominated landscape elements.

Furthermore, based on the final move angle model, we could compute the apparent perceptual range (APR) $T_A$ for this individual as defined in Section 2.5. With the threshold set at $\delta = .05$, the estimated APR is $\hat{T}_A = 53.57$ meters, the distance from the patch boundary where the rattlesnake showed avoidance of the patch boundary. Using a parametric bootstrap, we further computed a 95% confidence interval for the APR, which ranged between 40.47 meters and 72.37 meters (see, e.g., Manly 1997). From a conservation

perspective, this means that habitat within at least 40.47 meters and as much as 72.37 meters of the nearest roads and urban development is avoided by this rattlesnake. This kind of information can be taken into account in designing reserves (e.g., buffer zones) and is useful in determining how much habitat is available.

Analysis based on our models yield useful results even though the number of observations in this example were moderate. We determined that the rattlesnake responded to the habitat patch boundary and the response was one of avoidance. Moreover, the changes in the move angle as the animal approached the boundary were the primary mechanism of avoidance and the avoidance response was evident at roughly 53.57 meters from the patch boundary. We have obtained a parameterized model for how the angular response changed with distance to the boundary. The results are consistent with the visual inspection of the data (Figure 5) and are sensible from a biological and ecological perspective.

## 5. CONCLUSIONS AND DISCUSSION

This article proposes a set of statistical models for individual animal movement in response to a single type of landscape feature. The models are useful for simulating animal movement in response to a landscape feature and for statistical analysis of movement path data such as the kind obtained through a radio telemetry study. We defined *apparent perceptual range*, and provided formulas to calculate this quantity based on the model parameters. We demonstrated the application of the model to simulated data for movement in response to point, line, and the boundary of polygon features. Further, we applied the methods to analyze a radio telemetry dataset collected from a rattlesnake in relation to a boundary between natural habitat and urban development.

The methods presented in this article also serve as a basis for further work on modeling animal movement. In our analysis of the rattlesnake data, we assumed that the move distance was not dependent on the move duration, because the relocation time intervals were fairly regular. In general, regular relocation time intervals can be incorporated into the study design. However, when this assumption is not met, a correction should be applied to the move distance by calculating, for example, a move rate based on both move distance and move duration. We also assumed conditional independence among the sequence of move angles and among the sequence of move distances given the animal-to-object angles and distances. More complicated dependence structures might sometimes arise in practice. For example, temporal autocorrelation may still be present in the move angle or move distance data even after the animal-to-object relations have been accounted for. Such dependence can be detected by plotting the auto-correlation among "residuals" at different time lags (Turchin 1998). Further, we assumed conditional independence between the response angle and move distance within a move given the animal-to-object angles and distances. It is possible that residuals in response angle and move distance are cross-correlated within a move, which can be tested using, for example, circular-linear correlations (Batschelet 1981). The present models can be extended to account for more complicated dependence structures. Finally, our methods for an individual animal can be extended to population-level inference based on data from a set of individuals. Random-effects type of models will be

suitable. We are currently investigating this and the other possible extensions of our current models.

## ACKNOWLEDGMENTS

We gratefully acknowledge Ted Case from the University of California, San Diego, for his guidance and support of the rattlesnake telemetry study. We would also like to thank The U.S. Geological Survey, California Department of Fish and Game, and the Nature Conservancy for funding. We thank Murray Clayton of the University of Wisconsin–Madison Department of Statistics for his helpful comments on the article.

*[Received January 2004. Revised September 2004.]*

## REFERENCES

Batschelet, E. (1981), *Circular Statistics in Biology*, New York: Academic.

DeAngelis, D. L., and Gross, L. J. (eds.) (1992), *Individual-Based Models and Approaches in Ecology*, New York: Chapman and Hall.

Fisher, N. I. (1993), *Statistical Analysis of Circular Data*, New York: Cambridge University Press.

Fisher, N. I., and Lee, A. J. (1992), "Regression Models for an Angular Response," *Biometrics*, 48, 665–677.

Haddad, N. M. (1999), "Corridor Use Predicted from Behaviors at Habitat Boundaries," *The American Naturalist*, 153, 215–227.

Jander, R. (1975), "Ecological Aspects of Spatial Orientation," *Annual Review of Ecology and Systematics*, 6, 171–188.

Kareiva, P. M., and Shigesada, N. (1983), "Analyzing Insect Movement as a Correlated Random Walk," *Oecologia*, 56, 234–238.

Lima, S. L., and Zollner, P. A. (1996), "Towards a Behavioral Ecology of Ecological Landscapes," *Trends in Ecology and Evolution*, 11, 131–135.

Manly, B. F. J. (1997), *Randomization, Bootstrap, and Monte Carlo Methods in Biology* (2nd ed.), New York: Chapman and Hall.

Mardia, K. V., and Jupp, P. E. (2000), *Directional Statistics*, New York: Wiley.

Marsh, L. M., and Jones, R. E. (1988), "The Form and Consequences of Random Walk Models," *Journal of Theoretical Biology*, 133, 113–131.

McCullagh, P., and Nelder, J. A. (1989), *Generalized Linear Models* (2nd ed.), New York: Chapman and Hall.

R Development Core Team (2003), *R: A Language and Environment for Statistical Computing*, Vienna, Austria: R Foundation for Statistical Computing.

Seber, G. A. F., and Wild, C. J. (1989), *Nonlinear Regression*, New York: Wiley.

Shao, J. (1999), *Mathematical Statistics*, New York: Springer.

Siniff, D. B., and Jensen, C. R. (1969), "A Simulation Model of Animal Movement Patterns," *Advanced Ecological Research*, 6, 185–217.

Thisted, R. A. (1988), *Elements of Statistical Computing*, London: Chapman and Hall.

Tracey, J. A. (2000), "Movement of Red Diamond Rattlesnakes (*Crotalus ruber*) in Heterogeneous Landscapes in Coastal Southern California," Master's thesis, University of California, San Diego.

Tracey, J. A., and Case, T. (2005), "Movement of Red Diamond Rattlesnakes *Crotalus ruber* in Southern California: A Test of Alternative Models," in preparation.

Turchin, P. (1998), *Quantitative Analysis of Movement*, Sunderland: Sinauer Associates.

Zalucki, M. P., and Kitching, R. L. (1982), "The Analysis and Description of Movement in Adult *Danaus plexippus l.* (lepidoptera: Danainae)," *Behaviour*, 80, 174–198.

Zollner, P. A. (2000), "Comparing the Landscape Level Perceptual Abilities of Forest Sciurids in Fragmented Agricultural Landscapes," *Landscape Ecology*, 15, 523–533.

in *Connectivity Conservation*, K. R. Crooks
and M. Sanjyan editors. Cambrdige
University Press. 2006.

14

# Individual-based modeling as a tool for conserving connectivity

JEFF A. TRACEY

## INTRODUCTION

### Animal movement

*Functional* (or *behavioral*) connectivity has been defined as "the degree to which the landscape facilitates or impedes movement among resource patches" (Taylor *et al.* 1993; Forman 1997; Taylor *et al.* Chapter. 2). When an animal moves, it must expend energy and it may take risks such as being more visible to predators. So why should an animal move at all? The reason is that the landscape in immediate proximity to an animal may not satisfy its present or anticipated needs. Therefore, we would expect movement to have some purpose for animals; in other words, it is a goal-oriented and behavior-mediated search. Bell (1990) suggests three factors that determine searching behavior: the characteristics and abilities of the animal, the resources and risks in the external environment, and resource requirements as determined by the internal state of the animal. We could think of movement as an activity that allows an animal to match its internal needs to its external environment: if it is threatened it finds safety, if it is hungry it finds food, if it is cold it finds warmth, and if it is ready to reproduce it finds a mate. An animal, however, must weigh all of these needs simultaneously each time it moves based on which needs are most important and what it knows about the landscape. An ordered set of these decisions, which results in a movement path, determines in large part the success of the individual. And the set of movement paths for all individuals in a landscape at a given point in time determines the functional connectivity of that landscape.

**Background**

Functional landscape connectivity is directly related to animal movement responses to landscapes. Most approaches for evaluating functional connectivity focus on the landscape, and only implicitly consider animal movement. I believe that animal movement behavior warrants equal and explicit evaluation in studies of functional connectivity. From this perspective, we consider the interaction of individual animals with the landscape; that is, how it is perceived by and affects movement behavior of individuals, and the costs and benefits the local landscape provides to them.

Before proceeding further, I will define some terminology and present some basic concepts related to landscapes and animal movement. First, we are interested in two kinds of spatial variation: discrete and continuous. We conceptualize discrete landscape variation in terms of distinct entities in space, such as an individual animal or a highway. I will refer to these entities as *objects*, but they are sometimes referred to as landscape features or landscape elements. Objects are often represented via vector-based models in which the geometry of objects are described by points, lines, or polygons. For example, we may represent animal locations as points, rivers or roads as lines, and urban development or lakes as polygons. Several important concepts related to the perception of objects by animals have been developed. Movement in relation to objects in a landscape has been called *object orientation* (Jander 1975). Further, Jander (1975) defined *detection space* as "the area around the searcher within which it detects objects." Later, Lima and Zollner (1996) defined *perceptual range* as the distance from which an animal can perceive a particular landscape element. More recently, Olden and others (2004) discuss concepts pertaining to the relation between the strength of environmental stimulus and components of perceptual range. In the absence of spatial learning, we assume that an object must be within an animal's detection space before it will respond to it through movement. These movement responses to objects (or landscape features) may be qualitatively described as attractive, repulsive, or neutral. Animals also respond to continuous landscape variation, often referred to as *fields*, and represented by raster (e.g., grid-based) models. Examples of landscape variables that might be represented with raster models are elevation and temperature. Movement in response to continuous landscape variation, depending on the mechanism of orientation, has been described by *taxis* and *kinesis* models (Jander 1975; Benhamou and Bovet 1992; Turchin 1998).

The effects of human-made (or built) objects on animal movement are the primary focus of movement-based evaluation of landscape

connectivity. For some species, human-made objects may be attractive, such as newly sprouted corn fields to feeding sandhill cranes or trash bins to foraging racoons. In some cases human-made structures can provide shelter; for example, rattlesnakes may overwinter in piles of concrete debris left behind following housing construction. But for many species and in many cases, human-made objects are avoided or hazardous. Some objects, such as urban development and its associated night-time illumination, may have no natural analogue. Objects such as freeways can reduce connectivity by restricting movement due to behavioral avoidance as well increasing mortality due to vehicle collisions when animals do risk a crossing (Clevenger and Wierzchowski Chapter 20).

The effects of a particular type of object on functional connectivity may not necessarily be inferred from habitat utilization studies. For example, suppose an animal encounters an urban development that it wants to avoid. Such avoidance can be achieved in many ways:

- the animal may avoid crossing the boundary into the urban area (and perhaps have to circumvent it),
- it may immediately leave the urban area if it is entered,
- it may decrease time in the urban area by moving more often, moving at a greater rate, or moving in straighter paths, or
- some combination of the above.

Each of these responses can produce low utilization of the urban development. However, the different kinds of avoidance responses can have different effects on landscape connectivity. In the first two responses, the urban development acts as a barrier to movement, and therefore, may reduce connectivity or alter connectivity by redirecting movement to other areas. In the third response, due to the rapid movement through urban development, could actually promote connectivity among core habitat areas if the risk of mortality in the urban area is not too high.

Animal movement is poorly understood (Marsh and Jones 1988; Turchin 1998; Van Vuren 1998), and in spite of some promising conceptual and empirical work (Jander 1975; Lima and Zollner 1996; Haddad 1999; Zollner 2000), there is a notable lack of models that are useful for analyzing movement in relation to objects. In general, it is important not to construct models that are more complicated than necessary for a particular application. But if the model leaves out essential features of the system, it will not be useful. Animal movement models (often with much biological realism) are frequently used in simulations employed for conservation purposes, but they are generally based on rules

of movement and parameter estimates that seem reasonable (this has been called a *standard of plausibility*: Lima and Zollner 1996), rather than those that have are based on analysis of movement data. On the other hand, very simple models of movement (e.g., simple or correlated random walks: Turchin 1998) are not useful by themselves because they do not include the responses to objects and fields that are central to functional connectivity. An important part of my research is to develop animal movement models that are sufficiently biologically realistic and yet simple enough that their parameters can be estimated from empirical data.

In the models I describe, I consider movement occurring in discrete (but potentially small) time intervals which can be conceptualized as an iterative process in which the animal cycles through three basic steps: (1) collecting information on the animal's needs and the landscape, (2) information processing, and (3) using the processed information to make a movement. Notice here that the animal is the system under consideration: information is input to the system (the animal), it is processed (which is a form of computation), and the output is a movement and/or other actions such as feeding. These processes occur within individual animals, and so I take an individual-based approach (Huston *et al.* 1988) to modeling movement.

#### Preview

In this section I have presented a background on the relation of animal movement to functional connectivity. In the remainder of this chapter, I give a brief introduction to statistical models of animal movement that my colleagues and I have developed, and an overview of a computer program that I have constructed for simulating animal movement on data layers derived in a geographic information system (GIS). We are applying these models to the evaluation of landscape connectivity for large carnivores, and I provide a case study for pumas (*Puma concolor*) in coastal southern California. I conclude with a brief summary and recommendations for future modeling, empirical, and applied work.

## GENERAL APPROACH

The approach I describe involves three general areas of research. First, I develop alternative mathematical models of movement in relation to landscape features and develop statistical procedures for parameter estimation and model selection. Second, I construct programs for simulating animal movement on GIS models of landscapes using the models

we have developed. Third, I develop the application of the statistical models and simulation programs so that they can be used to quantify and visualize connectivity from simulation output and to evaluate landscape connectivity in support of reserve design and other conservation efforts. Simulations can be run on current or alternative landscapes. Movement can even be simulated on models of potential future landscapes, such as those produced by urban growth models, providing proactive guidance to conservation planning. Therefore, this approach provides a framework for data supported evaluation of connectivity using models that include the essential features of connectivity. In the remainder of this section I will describe each of these areas of research in more detail, and in the next section I will present a case study that illustrates our approach.

#### Animal movement data

The models I present are designed for data on the movement paths of individual animals such as the type collected via radiotelemetry, global positioning system (GPS) tracking, snow tracking, direct observation, and other methods in which locations are sampled at discrete time intervals. Ideally, these time intervals should be regular. These data consist of spatial coordinates $(x, y)$ and a time at which the location was sampled (Fig. 14.1). From these data we can calculate the move distance and move angle between each pair of consecutive locations. The *turn angle* can also be calculated as the difference between consecutive move angles. These measurements serve as dependent variables in our statistical models.

Data on objects are required to quantify the relation of the animal locations to the landscape. These data are usually in the form of GIS layers (Fig. 14.1). For polygon data (e.g., land cover), we identify the type of polygon that each animal location falls within and the type of the nearest neighboring polygon. This allows us to identify the type of patch boundary to which the animal may be responding. We combine the movement and landscape data to obtain measurements of the angle and distance from each animal location to the nearest point on the boundary of each type of object in the landscape (Fig. 14.1). I refer to these as animal-to-object angles and distances. For continuous landscape variation, such as elevation, we might calculate the slope (which consists of the *gradient*, or steepness, and the *aspect*, or orientation) of the terrain at the animal's location. These measurements are related to the animal's perception of the landscape, and are predictor variables (or covariates) in our statistical models.

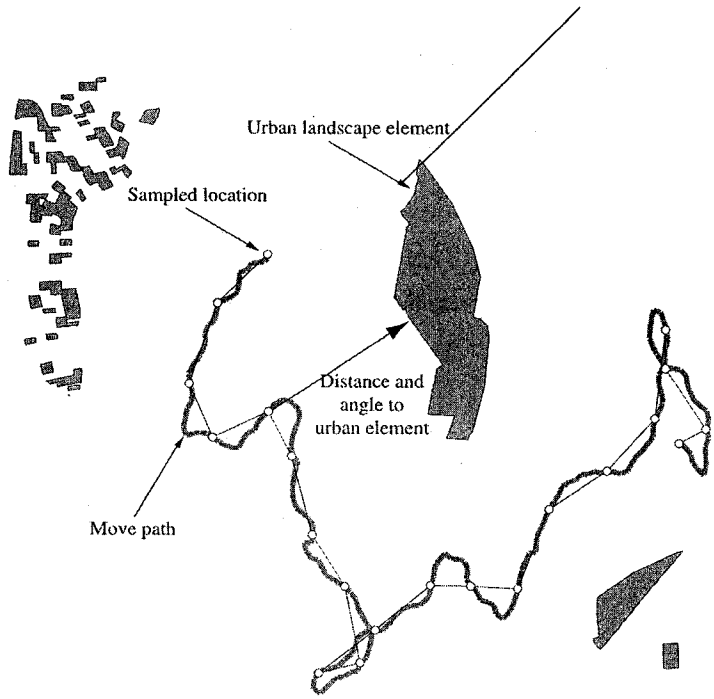


**Fig. 14.1.** Using radio or GPS telemetry data and geographic information system layers we can quantify animal movement in relation to landscape features (or objects). The gray polygons represent urban landscape elements. The thick dark gray line is the animal's true movement path, and the thin black lines show the approximated movement path formed by joining the sample locations (white-filled circles) with straight line segments. The animal-to-object angle for one of the locations is shown as an arrow. In this case the object is the closest point on the urban boundary to each animal location. This example was produced by simulation.

For each animal location, we also subtract animal-to-object angles and aspects from the move angle to obtain angle of movement relative to each object and field, which I refer to as a *response angle* (Fig. 14.2). For example, if the animal moves directly toward an object, its response angle is 0.0 degrees; alternatively, if it moves directly away from the object its response angle is 180.0 degrees. The response angle is also considered a dependent variable in the statistical models.

Careful consideration should be given to the kinds of movement and landscape data that are analyzed. Large-scale movements might be more important to connectivity than small-scale movements. Ranging,

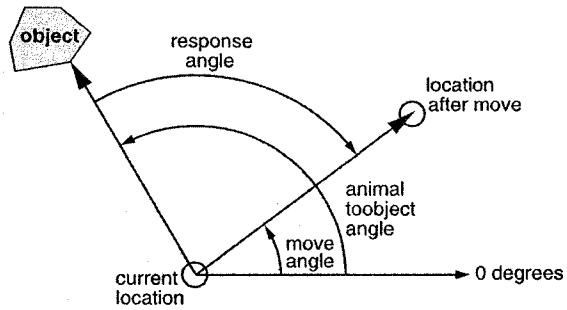


Fig. 14.2. Response angle. We calculate the *animal-to-object angle* from the animal's current location to the nearest point on the object, and the *move angle* from the animal's current location to its location after the move (the next observed location). The *response angle* for a move is the move angle minus the animal-to-object angle constrained to the interval from 0 to 360 degrees (or in radians, 0 to $2\pi$).

topographic orientation (Jander 1975), migration, and dispersal probably contribute more to connectivity among core areas in a reserve network than most other kinds of movements. We may also want to narrow our focus to particular kinds of animals. It may be reasonable to assume that newborn, dispersing, or relocated animals are moving primarily in response to their immediate perceptions rather than spatial memory. Furthermore, not all types of landscape features need to be included. The number of categories in landcover layers might be reduced to a smaller number of meaningful classes based on the particular application and the results of previous habitat utilization studies and analysis of movement data. Some data, such as the distribution of prey, might be important to determine where animals might establish home ranges, but might be less important to understanding movement across a landscape between core areas. One should select data that matches the assumptions of the statistical models used for analysis and that matches the connectivity evaluation objectives.

#### Statistical models of animal movement

The statistical models of movement I present in this section are a mathematical description of how the dependent variables (e.g., move distance, and move turn, and response angles) are related to the predictor variables

(e.g., animal-to-object distance and angle, slope). As such, they represent information processing and decision-making within individual animals. For this reason, the models are designed to make inferences about individual animals, not a population of animals. Parameters are estimated for each alternative model and the best model is selected separately for each individual. Since the animal movement simulation program I describe (see p. 000) is also individual-based, this is all we need. For some applications, population-level inference may be desirable, and the models I present in this section can be extended to do so, but an explanation is beyond the scope of this chapter. Here, I briefly describe two distinct approaches for modeling animal movement in relation to landscapes: non-linear regression models and finite mixture models. In general, rather than modeling movement on a grid, we allow the animals to draw response angles and distances from continuous distributions.

Our first approach to modeling animal movement in relation to landscape features is a *non-linear regression model* framework (Tracey *et al.* 2005). We first propose a theoretical distribution for both the response angle and the move distance. For the response angle model, we assume that an animal has a fixed mean response angle for movement in relation to a particular type of object. For example, if the animal tends to move away from the object it will always do so "on average." However, we assume that the strength of the response (which depends on a distribution parameter called *concentration* and can be thought of as the inverse of the variance) increases as the animal gets close to the object. In other words, when the animal is far from the object, the response angle distribution is less clustered about the mean response angle, and the animal is more free to choose response angles far from the mean. If the animal is very far enough from the object, the response angle will become uniform, and the animal will no longer move in relation to the object at all. But as the animal approaches the object, the distribution becomes more clustered about the mean response angle, and the animal will be more likely to choose a response angle close to the mean. We fit the model by estimating the mean response angle and regressing the *concentration* parameter on the animal-to-object distance using a non-linear function. For the move distance models, we assume that the variance of the theoretical move distance distribution remains constant, but that the mean move length of the distribution may potentially change as the animal approaches the object. For example, if the animal is repulsed by the object then its mean move length may increase, but if the animal is attracted to the object its mean move length may decrease. Again, the mean move

length is modeled as a non-linear function of the distance to the object. The assumptions mentioned above may be relaxed by extending the model structure; for example, we can make the mean move distance dependent upon the response angle. We are currently extending these non-linear regression models to account for movement in relation to multiple types of objects and fields in the landscape, and to allow population-level inference.

Our second approach to modeling animal movement in response to landscapes might be called *decision tree models*, but statistically they are called *finite mixture models* (McLachlan and Peel 2000). In these models, an animal is confronted with one or more objects or fields. It also has one or more possible responses to each object or field. For each move, the animal makes a series of decisions that eventually lead to selection of one type of movement response to one of the objects or fields. The probability of making each choice is a non-linear function of the predictor variables such as distance to each object or the slope of a field. For each possible choice, there is a corresponding response angle distribution and move distance distribution with fixed parameters. A movement is made by selecting the response, and then drawing a response angle and move distance from the corresponding distribution.

In both approaches, we must account for cases when the animal does not respond to *any* of the types of objects or fields that we include in the model. When this occurs, we assume that the animal moves according to a *default rule*. The default rule acts as a null model. For example, in the non-linear regression response angle models, the response angle becomes uniform (flat) as the animal-to-object distance becomes large and the animal moves according to a simple random walk where all directions of movement are equally likely. In the finite mixture models, an animal may "decide" not to respond to any of the objects or fields. For the finite mixture models, more types of default rules can be used, including a simple random walk, a correlated random walk, and directional bias. In a correlated random walk, which models the distribution of turn angles described above (p. 000), an animal has a tendency to move in a direction that is related to its previous direction of movement. An animal with directional bias has a higher probability of moving in a fixed compass direction. In both the non-linear regression approach and the finite mixture approach, when certain model parameter estimates are close to 0.0, the entire model reduces to the default rule, which suggests that an individual animal may not be responding to the types of objects or fields we have included in the model.

Above, I have presented two general approaches to modeling animal movement in response to landscape variation. Within each of these approaches, we can propose many specific alternative models for movement that vary in terms of the types of objects and fields included, the functional relation between response and predictor variables, and whether or not to include temporal autocorrelation in movements. When using the finite mixture approach, we can also vary the number of possible responses to each type of field or object, and the type of default rule used. Given sufficient real-world movement data for each individual, parameters can be estimated for each model for each animal using numerical optimization of the corresponding likelihood functions, and then the best alternative model for each animal can be selected using likelihood ratio tests (LRT, for nested models) or Akaike information criterion (AIC, for non-nested models). Then we can use these parameterized, selected models to evaluate connectivity.

#### Individual-based movement simulations

In order to use these statistical models to evaluate connectivity, we must have computational tools that can extract data from animal locations and GIS data layers and that can simulate animal movement on GIS landscape models. The structure of the individual-based movement simulation program I have developed has four basic parts: (a) a *main* function that can be thought of as the final executable program, (b) a *landscape component*, (c) an *animal component*, and (d) a *simulation control component*. Here I will review these parts of the simulation program.

The landscape component of the simulation program reads GIS data files into spatial data structures that support efficient search and retrieval and provides functions that query the spatial data structures. It can handle both raster-based data for continuous variation and vector-based data for discrete objects. This component is used both in the simulations and in programs that extract covariates that quantify the relation between animal locations and landscape elements from movement data and GIS data layers. The landscape model component performs queries that are used by the individuals in the animal component of the model. Two types of GIS data are managed by the landscape component: landscape data and core habitat data. The landscape data (for landcover, roads, terrain, and so on) represent the landscape variation to which the animals respond through movement. The core habitat specify where individuals begin their simulated paths and also play a role in the stopping conditions for a movement path (see below). The core habitat data *does not* play a role in how the

animal moves across the landscape; rather, we are concerned with predicting connectivity among the core habitat areas.

The animal component keeps track of the state and movement history of each individual and is responsible for simulating movement behavior. Each individual in the simulation corresponds to one of the real individuals in our data set, and its movement behavior is specified by the statistical model that has been selected and parameterized using field data from that individual. For each movement model there is a *perceive* function that calculates animal-to-object distances and angles and the gradient and aspect of the fields using landscape component query functions, and a *move* function that uses this information to generate a move angle and distance according to the individual's statistical movement model. The simulation generates movement paths for each individual by iteratively applying the perceive and move functions.

Interactions between individuals and the landscape are coordinated by the simulation control component. This component also sets the initial state of the simulation, controls the ordering of events within a time step and the number of realizations and time steps that the model will be run, and initiates the writing of output files at the end of the simulation.

Running a movement simulation consists of three basic steps, which are orchestrated by the main function. First, we set up the landscape and individuals. The GIS data layers are read by the landscape component, while the individual component creates a fixed number of each type of individual in each core area (each "type" of individual corresponds to a model that has been selected and parameterized from data from a real animal). Second, we simulate movement by allowing each individual to make one move per time step. An individual's movement path terminates when one of three stopping conditions is met: (a) the simulated animal moves outside the boundary of the landscape, (b) the simulated animal reaches a maximum number of moves (based on a realistic upper bound on dispersal path length), or (c) it successfully reaches another core area. Third, a *path summary file* and a *move summary file* are written. The path summary file contains information on each simulated movement path. Each record in this file includes the individual identification number, initial core, stopping condition, number of moves, total path length, final core. The move summary file contains information on each location occupied by each individual. Each record in this file includes the individual identification number, path number, move number, landcover type occupied, animal-to-object distances and angles, slope and aspect of fields, move distances and angles, and response angles. Records in the path

summary file can be matched to records in the move summary using the identification numbers. We can use this output to evaluate functional connectivity.

#### Evaluating functional connectivity

We use the movement simulation output to evaluate functional landscape connectivity by comparing alternative landscapes, determining how each alternative landscape meets specified connectivity objectives, and identifying functional corridors (movement routes between core habitat areas). When preparing to evaluate connectivity, we first select the focal species based on conservation status, ecological role, or other factors. We also take data availability into account. We select and parameterize models using movement data from the focal species according to the methods outlined above (pp. ooo–ooo). We must select the alternative landscapes upon which we will run the simulations; for example, we might be interested in how the current landscape compares to landscapes that might result from implementing different reserve network designs or future land use patterns. For each alternative, we develop GIS data layers containing information needed for each movement model used in the simulations. It is useful (if not essential) to develop clear objectives for conserving connectivity for the focal species. Core habitat areas must be identified; for the sake of comparison, the same core habitat areas should be used with all of the alternative landscapes. The role of connectivity between each pair of core areas in species conservation (based on genetics, demographics, and other considerations) should be described and prioritized. We could even use population viability analysis (PVA) models to specify dispersal rates between core areas that will be likely to ensure species persistence. This provides a basis for determining how well each alternative landscape satisfies our conservation objectives. Once we have finished preparing the models and alternative landscapes, we run the movement simulations on each alternative landscape as described above (p. ooo).

We use the output produced from the movement simulations to quantify and visualize functional connectivity. We quantify connectivity between pairs of core habitat areas in terms of *success*, *risk*, and *cost* and we may combine these quantities into a single pair-wise connectivity measure. If a simulated animal reaches a core other than the one from which it began, it is considered a *successful* disperser. Otherwise, it is considered *unsuccessful*. We can think of success as the probability that an individual will find its way from one specific core habitat area to another specific core area given that it survives the journey.

The probability of survival is related, in part, to the anthropogenic risks it encounters along its path and how much energy it must expend during dispersal. We quantify risks due to human-caused mortality in terms of numbers of road crossings (perhaps categorized by types of roads) and numbers of encounters with urban areas. We quantify cost as the length of the movement path outside of core habitat areas. All of the information we need to determine these quantities is contained in the path summary files output by the movement simulations. We may combine success, risk, and cost for each simulated movement path into a single probability of dispersal between a pair of core habitat areas:

Pr(successful *and* survives)
= Pr(success *given* survives) Pr(survives risks and survives cost)

where the event that an animal successfully moves from one core area to another and survives the journey is a Bernoulli random variable; that is, it takes on a value of either success (1) or failure (0). Here, we assume that mortality from natural causes, other than those related to movement costs, are negligible. For each pair of core areas, we can add up the number of simulated paths between the pair with a path connectivity value of 1, and divide each result by the total number of simulated paths to obtain a final pair-wise connectivity measure.

Methods for visualizing connectivity from simulation output are varied, and the method we should use depends on our objectives. If we want to get a general sense of connectivity across a landscape or visually compare alternative landscapes, we can use connectivity graphs. A graph consists of nodes that are connected by edges (see Fagan and Calabrese Chapter 12; Theobald Chapter 17). In our case, the nodes correspond to core habitat areas, and might be visually represented as circles or polygons depicting the shape of the core area. The edges correspond to connectivity. Connectivity is directional (Gustafson and Gardner 1996); therefore, these edges can be depicted by arrows (one in each direction) between each pair of core areas. We can visually depict the degree of connectivity between pairs of core areas by plotting numerical values (for success, risk, cost, or pair-wise connectivity measure) next to the corresponding edges, or by varying the widths of the arrows according to these values. In order to visualize movement routes through *functional corridors* between a pair of core areas, we can plot the movement paths between them using the information in the move summary files. However, not all of the movements in a successful movement path, such as moving into and back out of

cul-de-sacs, contribute equally to connectivity and may detract from identifying functional corridors. Therefore, an important area of future work will be to develop techniques to identify functional corridors from simulation output. As a final example, if we are interested in areas of high risk, we can plot locations where simulated movement paths intersect roads and urban areas (see Clevenger and Wierzchowski (Chapter 20) for an example for roads).

We can directly compare connectivity between pairs of core areas within or among alternative landscapes and how well an alternative landscape satisfies our connectivity conservation objectives using the quantities described above. Further, we can gain an overall sense of patterns of connectivity at broad scales, where land ought to be protected (as predicted from the simulations) in order to preserve connectivity at finer scales, and how differences in the alternative landscapes alter predicted patterns of movement between core habitat areas by visualizing connectivity in different ways. We can use these results as a basis for selecting alternative reserve designs, identifying weakness in existing or future landscapes, and for identifying and prioritizing areas for protection to help ensure the conservation of connectivity.

## CARNIVORE MOVEMENT IN SOUTHERN CALIFORNIA

### Background

In areas with increasing urbanization, the loss and fragmentation of habitat is virtually inevitable (Soulé 1991; Beier *et al.* Chapter 22). In coastal southern California, intensive development over the past century has fragmented the landscape and has helped create a "hotspot" of endangerment and extinction in the region (Myers 1990; Dobson *et al.* 1997). Pumas (*Puma concolor*) are the largest predator remaining in the region and are particularly sensitive to habitat fragmentation (Beier 1993; Crooks 2000, 2002). Pumas are an "area-dependent" species, requiring large areas for home ranges and dispersing long distances. For example, female pumas in the Santa Ana Mountains of southern California occupied minimum convex polygon home ranges that average an estimated 218 $km^2$ (Beier and Barrett 1993), and juveniles had an average estimated dispersal distance of 63 km (Beier 1995). Because fragmentation of the natural landscape of coastal southern California is continuing at a rapid rate, large-scale assessments of regional connectivity are critical. I conducted a pilot study, which used the methods outlined above (pp. 000–000), to evaluate landscape connectivity for pumas in relation

to an existing landscape, a habitat conservation plan landscape, and a worst-case landscape in the Southern California Ecoregion (Tracey and Crooks 2004). Here I use results for the existing and worst-case landscapes to illustrate the approach described above.

#### Alternative landscapes

For the movement simulations, I constructed GIS land cover layers for an existing landscape and a worst-case landscape scenario (Fig. 14.3). The existing landscape layer serves as a baseline for comparison. This layer was constructed from Southern California Association of Governments (SCAG) and San Diego Association of Governments (SanDAG) land-use layers, which were created in approximately 1995. Landcover in the existing landscape layer (and all other alternative landscape layers) was categorized into four types: habitat, disturbed, urban, and water. So-called "vacant" areas, undeveloped local and regional parks, and open space preserves were classified as habitat landcover. Housing, commercial, industrial, developed military, and other such areas were classified as urban landcover. Water consists of lakes, reservoirs, and the Pacific Ocean. All other land use types were classified as disturbed landcover, and include such areas as roads, rural residential areas, local developed parks, and agricultural lands. I constructed the worst-case landscape layer by regarding all public land as "protected" and assigning it to the habitat landcover type (Fig. 14.3). I used polygons for bodies of water from the existing landcover layer, and all private lands within the Southern California Ecoregion were assumed to be completely converted to the urban landcover type.

I constructed a GIS layer for puma core habitat areas from a protected lands data layer and a mountain lion wildlife habitat relation data layer. Protected lands layers were obtained from the California Spatial Information Library and The Nature Conservancy. I assumed all government land was adequately protected, although this is probably overly inclusive. I selected the two highest-quality habitat categories from layers for mountain lion wildlife habitat suitability (Hunter *et al.* 2003). The protected lands and suitable habitat layers were intersected to produce a layer of potential mountain lion core areas. From this layer, I selected polygons larger than 90 $km^2$, which is about 20 $km^2$ less than the smallest female minimum convex polygon home range reported by Beier and Barrett (1993). The result was a layer of 12 core habitat polygons (Table 14.1, Fig. 14.4).

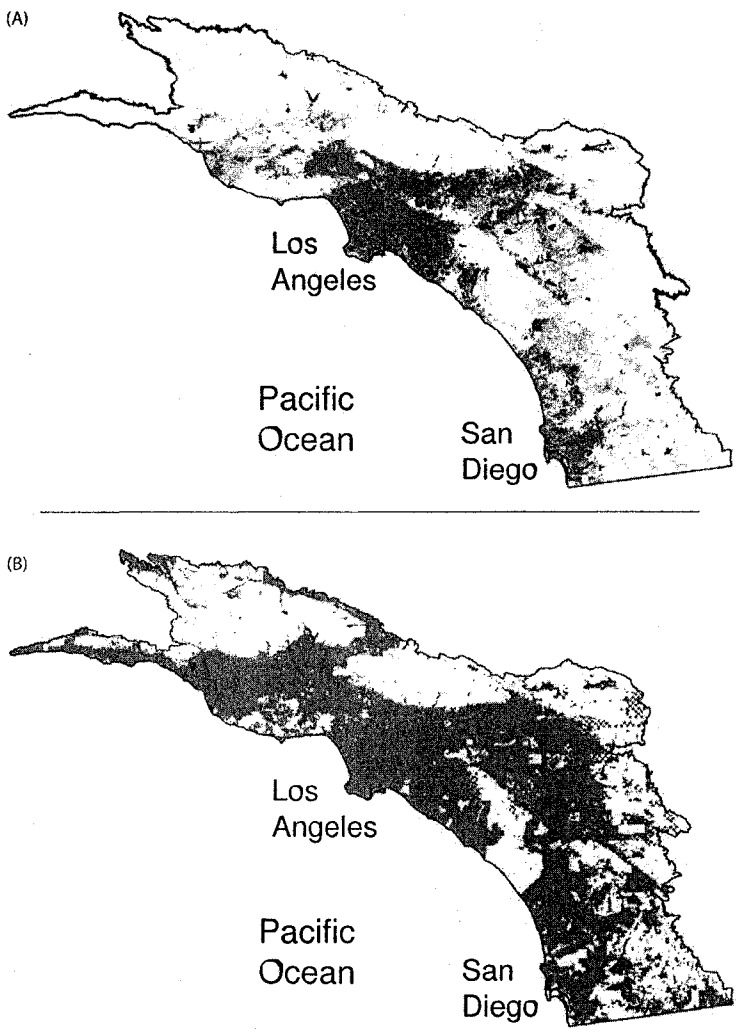


Fig. 14.3. A GIS representation of the existing (A) and worst-case (B) land cover scenarios used in the simulations. White areas indicate habitat, light gray indicates disturbed, dark gray indicates urban, and black indicates water. The black boundary delineates the Southern California Ecoregion.

**Table 14.1.** *A list of core areas used in the simulations*

| Number | Name | Area ($km^2$) |
|---|---|---|
| 1 | Los Padres NF 1 | 1115 |
| 2 | Los Padres NF 2 | 102 |
| 3 | San Bernadino NF | 213 |
| 4 | Santa Ana Mountains | 508 |
| 5 | Palomar Mountains | 583 |
| 6 | Los Coyotes | 301 |
| 7 | Cleveland NF | 1343 |
| 8 | Miramar | 98 |
| 9 | Otay Mountain | 122 |
| 10 | Angeles NF | 1791 |
| 11 | Santa Monica Mountains 1 | 116 |
| 12 | Santa Monica Mountains 2 | 273 |

### Data

For the pilot study, I estimated model parameters using radiotelemetry data from two subadult dispersing male pumas and landcover data. The movement data were collected by Paul Beier and his colleagues in the Santa Ana Mountains of coastal southern California (Beier 1995) between October 1990 and September 1992 (animals M8 and M10). In the analysis, I used data from 143 movements made by M8 and 260 movements made by M10. These data were collected during 12-h or 24-h monitoring sessions during which animals were located every 15 min, and the locations were rounded to the nearest 100 meters in a Universal Transverse Mercator (UTM) coordinate system. I used landscape data for the existing landscape to analyze movement in response to landcover polygons. Therefore, we had to test models for six boundary types: habitat–disturbed, habitat–urban, disturbed–habitat, disturbed–urban, urban–habitat, and urban–disturbed. I used a computer program that I constructed, which utilized the landscape component of the simulation program (p. 000), to derive the response (dependent) variables and covariates (independent variables) from the movement and landscape data (p. 000). The animal-to-object angles and distances were the points on the land cover polygon boundary closest to the animal locations (Fig. 14.1). I assumed that the animal responded to the nearest boundary type.

I proposed a total of 30 alternative finite mixture models for movement in each landcover type for response to each boundary type. Each model varies the kind of default model (simple random walk, correlated random

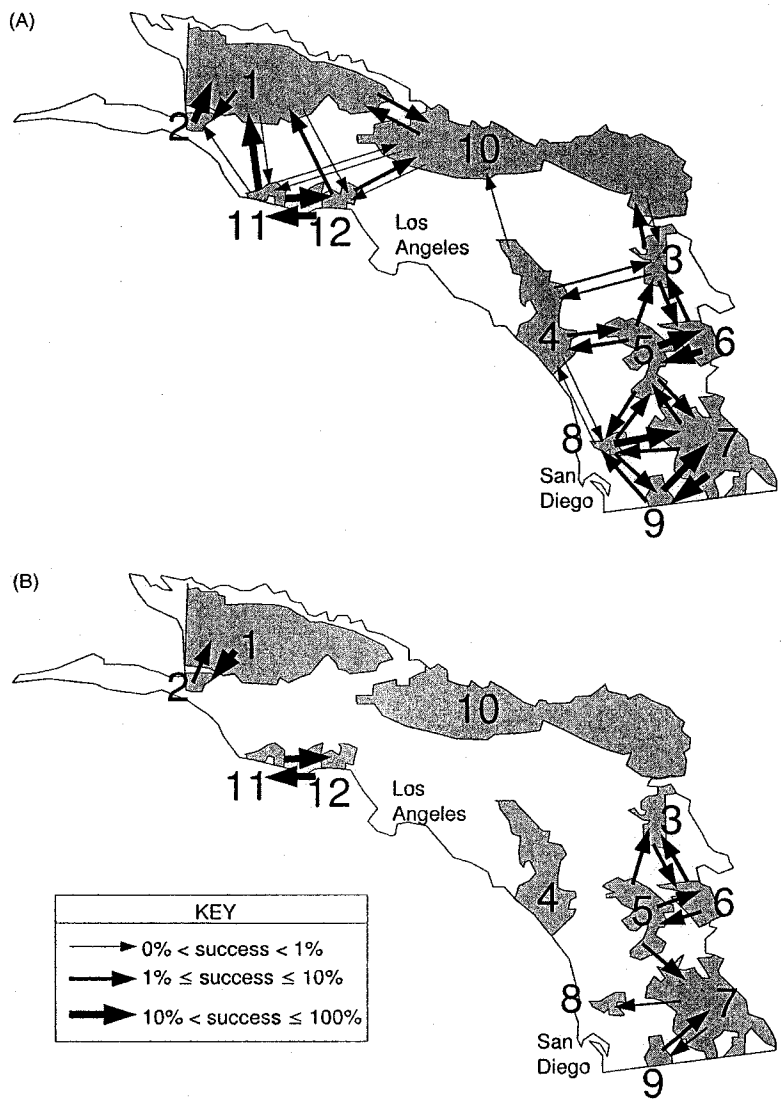


**Fig. 14.4.** Connectivity of existing (A) and worst-case (B) southern California landscapes. Connectivity, as measured by successful simulated dispersal among pairs of puma core areas (in gray), is depicted by arrows. The width of the arrow indicates the category derived from the number of successful simulated paths. The absence of an arrow between a pair of core areas indicates that no successful simulated dispersal occurred between them.

walk, and directional bias), whether there is no response, a single response, or two responses to a boundary type, and whether the probability of response was a constant, exponential, or logistic function of the distance to the boundary. In the single-response models, the animal has a tendency to move in one mean angle in relation to the boundary type (e.g., toward or away). In the two-response models the animal can move in two mean directions in relation to the boundary type, with each mean direction selected with some probability; for example, a rule might be to move parallel to the boundary to the left with probability Pr(left) and to the right with probability Pr(right). I also included two variations of the two response models, each with the two responses being either symmetric or asymmetric about a 0.0 degree response angle. I estimated the parameters for each model for each puma using programs that I have written in the R statistical language (R Development Core Team 2004), and then selected the best model for each animal using AIC or LRTs.

The analysis of the data using the models indicated that the two pumas generally moved according to a correlated random walk when they were in habitat. When they were in habitat near the urban edge, they tended to move parallel to it (either left or right), probably in an attempt to circumvent an urban area. They did not seem to avoid the habitat–disturbed boundary, but if they entered a disturbed area they tended to move back toward the habitat. Parameters were estimated and models were selected for two pumas, but since the results were very similar, simulations for only one puma (M10) are presented below. Recall that the statistical models I described above (p. 000) are designed to make individual-level inferences; hence, the number of individuals for which we have data is not relevant to making such inferences. When evaluating connectivity, however, we would like to have data from many animals so that we have a sample of movement behaviors representative of the animal population in our region. Our ongoing modeling efforts are incorporating data from more radio-collared animals in the region, including animals fitted with GPS collars.

#### Simulation results

We started with 250 individuals in each of the 12 core areas, for a total of 3000 simulated individuals. We allowed them to make a maximum of 7200 moves, which (at 15-min time steps) translates to 75 days of continuous movement. However, if a simulated animal left the boundary of the Southern California Ecoregion or successfully reached another core area, that individual's dispersal was terminated.

In the existing landscape, 1471 individuals (49%) left the Southern California Ecoregion, 792 individuals (26.4%) reached the maximum number of moves, and 737 individuals (24.6%) successfully reached another core area. Of the 132 possible linkages between cores ((number of cores)$^2$ − number of cores), 35 were realized in the simulations on the existing landscape. Of these, nine of the linkages had ≤2 successful paths, seventeen had from 3 to 24 successful paths, and nine of the linkages had ≥25 successful paths. In the worst-case landscape, 1238 individuals (41.3%) left the Southern California Ecoregion, 1518 individuals (50.6%) reached the maximum number of moves, and 244 individuals (8.1%) successfully reached another core area. Of the 132 possible linkages, twelve were realized in the simulations on the worst-case landscape. Of these, two of the linkages had ≤2 successful paths, eight had from 3 to 24 successful paths, and two of the linkages had ≥25 successful paths. A landscape connectivity graph showing the number of successful simulated movement paths between core areas in each landscape is shown in Fig. 14.4. By comparing the connectivity graphs for the existing and worst-case landscapes, we can see that the model predicts a near-complete breakdown in connectivity should the worst-case landscape be realized in coastal southern California.

### Objectives for connectivity conservation

It is constructive to interpret the simulation results in light of a clear set of objectives for conserving connectivity. Below, I suggest five connectivity objectives for the Southern California Ecoregion and use the model output to identify vulnerabilities and to provide guidance for improving and conserving connectivity. The connections associated with each objective

**Table 14.2.** *A list of connections related to each connectivity strategy goal*

| Goal number[a] | Linkages[b] |
|---|---|
| 1 | 1⇔10, 3⇔5, 3⇔6, 3⇔10, 5⇔7, 6⇔7 |
| 3 | 1⇒11, 1⇒12, 3⇒4, 5⇒4, 10⇒11, 10⇒12 |
| 4 | 1⇔2, 5⇔6, 7⇔9, 11⇔12 |
| 5 | 4⇒3, 4⇒5, 4⇒10, 5⇔8, 7⇔8, 11⇒1, 11⇒10, 12⇒1, 12⇒10 |

[a]Each goal is described in detail in the text. Goal 2 is omitted from this table because it depends on evaluation of connectivity in neighboring regions.

[b]A double arrow (⇔) indicates connectivity in both directions is related to the goal. A single arrow (⇒) indicates connectivity only in one direction is related to the goal. The numbers connected by arrows are the core area numbers in table 14.1.

are listed in Table 14.2. Connections between a pair of core habitat areas can contribute to more than one objective.

Objective 1: Conserve connectivity among large core areas

*Description* If we are to ensure that mountain lions have a continued presence in coastal southern California, then it will be essential to maintain connectivity among the larger core areas in the eastern parts of the Southern California Ecoregion. This includes connectivity between pairs of large habitat core areas (cores 1, 3, 5, 6, 7, 10) in both directions.

*Results* In the existing landscape, the simulations predict low to medium connectivity among large cores. Several critical weaknesses exist, most notably movement in the southern direction from core 10 to core 3 and from core 3 to core 5. In the worst-case landscape, connections among the large core areas in the northern part of the study area were predicted to be lost, essentially fragmenting the landscape at a regional scale.

Objective 2: Connectivity throughout California

*Description* By maintaining connectivity between large core habitat areas in the Southern California Ecoregion and large core habitat areas in adjacent ecoregions, we can help conserve connectivity at larger spatial scales. Important benefits of this connectivity are demographic and genetic exchange among mountain lion populations in neighboring ecoregions, and preserving opportunities for range shifts for mountain lions and other species in the face of regional or global climate change. Achieving this goal is also dependent upon successfully conserving connectivity among large core habitat areas.

*Results* This goal can not be addressed directly without conducting connectivity evaluations in neighboring regions. Using information from the move summary files, we can identify areas on the boundary of the Southern California Ecoregion what were encountered by simulated animals. We also note that more individuals left the confines of the Ecoregion in the existing landscape scenario compared to the worst-case scenario, suggesting that exchange of individuals with adjacent ecoregions would be reduced in the worst-case landscape.

Objective 3: Connectivity for important coastal core areas

*Description* Several coastal core areas, most notably the Santa Ana Mountains (core 4) and the Santa Monica Mountains (cores 11 and 12), can still support mountain lions. However, for these populations to persist,

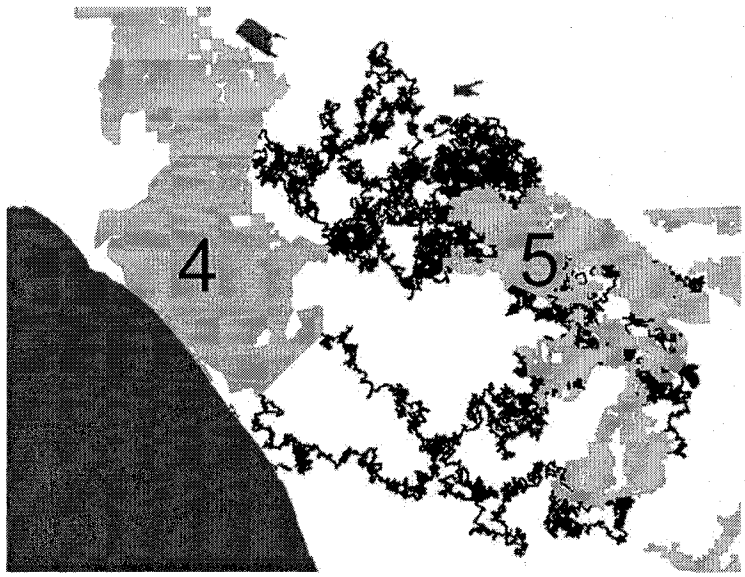


**Fig. 14.5.** Simulated locations for lowest-cost successful dispersal locations from the Palomar Mountains (core 5) to the Santa Ana Mountains (core 4). The core areas are shown in light gray, water in dark gray, and the simulated lowest-cost successful dispersal paths are shown in black.

connectivity from larger eastern cores *into* the coastal cores must be maintained. On the other hand, the coastal core habitat areas, due to the relatively small puma populations they contain, probably will make little contribution to the long-term viability of the larger core areas (but see Objective 5), so successful dispersal from these areas to the larger eastern cores is less essential.

*Results* In the existing landscape scenario, connectivity from larger inland cores to the coastal core areas is low. Therefore, it is critical to protect such connectivity immediately. In Fig. 14.5, we show predicted low-cost movement paths from the Palomar Mountains (core 5, an inland core) to the Santa Ana Mountains (core 4, a coastal core). Such predictions can help identify areas that should be immediately protected to conserve connectivity. In the worst-case landscape scenario, all connectivity from inland to coastal core areas is predicted to be lost.

Objective 4: Connectivity for nearby small cores

*Description* By connecting small nearby core habitat areas to other core habitat areas (large or small) we can increase the effective area of both core

areas. Some smaller core habitat areas, such as the two protected regions of the Santa Monica Mountains (cores 11 and 12), will require connectivity with each other in order to form a single larger core habitat area. Some small core habitat areas can add to the effective area of larger, nearby core habitat areas. For example, the Chino Hills (not listed as a core) are in very close proximity to the Santa Ana Mountains (core 4), and can make additional habitat available to pumas in the Santa Ana Mountains (this particular corridor is discussed further in Beier *et al.* Chapter 22). Other small core areas are strategically important because they help achieve other connectivity objectives; for example, Otay Mountain (core 9) is important in achieving Objectives 1 and 2.

*Results* In the existing landscape, many of the small core habitat areas show high connectivity to nearby large core habitat areas, and this connectivity changes little in the worst-case landscape.

Objective 5: Create redundant connections

*Description* In some cases, connectivity between pairs of core habitat areas may create redundancy in linkages among other core areas. The coastal core habitat areas, such as Santa Ana Mountains, Santa Monica Mountains, and Otay Mountain, can play a role in maintaining alternate, albeit less viable, connections among the large cores.

*Results* Most of the redundant connections occur through coastal areas (except for connections from core 5 to 8 and from core 7 to 8) so the results for Goal 3 also pertain to this objective.

## CONCLUSION

Modeling is by nature an iterative process in which models are proposed, evaluated, and then revised or replaced. Therefore, the existing models need to be applied to data for a range of species and landscapes and then evaluated. We need to develop variations and extensions of existing models, and propose new types of models. Another important area of work is to develop better methods for visualizing connectivity from the large volumes of output produced by the movement simulation programs.

In field studies, careful consideration must be given to the scale (both grain and extent) of landscape change with which we are concerned. The scale of landscape change and the scale of movement behavior of the focal animals will dictate the frequency at which we should sample movements.

Additionally, there must be correspondence between the grain of the landscape data and the frequency of sampling locations. In general, most tracking studies relocate animals too infrequently to give useful information about local movement responses to landscape variation. With new GPS tracking collars, however, it is practical to obtain this information for larger species. Another advantage of GPS methods is that we often obtain many more animal locations, which can permit us to use more detailed movement models. For other species, field sessions involving more frequent relocations can be conducted using traditional radiotelemetry techniques (similar to Beier *et al.* 1995). It is also important to try to collect movement data that occur in a variety of landscape contexts, and over a range of the covariates such as distances to objects. Otherwise, we may not be able to fit models that include responses to all of the landscape variation we judge important to our specific application. Finally, it may be helpful to collect behavioral information associated with movements or segments of individual movement pathways.

Conservation practitioners should prepare to use this approach in several ways. First, important focal species for connectivity studies should be identified. Second, GIS data for the region of interest, including elevation, roads, vegetation and landcover, streams or riparian zones, bridges and road undercrossings, and other relevant information should be acquired, evaluated for accuracy, and prepared for use in movement simulation models. Third, information on projected land-use trends and conservation plans should be acquired and studied. In some cases, GIS layers for projected land use can be obtained from local governments, resource agencies, or universities. This information should be used to create GIS layers for possible future alternative landscapes. It is important that the alternative future landscapes are similar to the GIS data used to analyze the movement data (for example, with respect to spatial resolution, landcover categories, and ranges of continuous spatial variation). Finally, objectives for conserving connectivity for each focal species should be developed to guide interpretation of the simulation results. The use of data-supported, individual-based movement models has the potential to be a useful addition to our conservation toolkit.

## ACKNOWLEDGEMENTS

I dedicate this chapter to my wife, Rosana, and my children Andrew and Marissa. I thank them for their love and support. I am grateful to my advisors which include Kevin Crooks, Jun Zhu, and Ted Case and

to collaborators that include Paul Beier, Robert Fisher, Lisa Lyren, Seth Riley, Ray Sauvajot, Ken Logan, Walter Boyce, and Steve Torres. I thank Scott Morrison of The Nature Conservancy, and Colleen Miller and Dave Lawhead of the California Department of Fish and Game. This project was funded by the US Geological Survey, the California Department of Fish and Game, The Nature Conservancy, the University of Wisconsin—Madison, and Colorado State University.

## REFERENCES

Beier, P. 1993. Determining minimum habitat areas and habitat corridors for cougars. *Conservation Biology* 7:94–108.

Beier, P. 1995. Dispersal of juvenile cougars in fragmented habitat. *Journal of Wildlife Management* 59:228–237.

Beier P., and R. H. Barrett. 1993. *The Cougar in the Santa Ana Mountain Range, California*, Final Report. Sacramento, CA: California Department of Fish and Game.

Beier, P., D. Choate, and R. H. Barrett. 1995. Movement patterns of mountain lions during different behaviors. *Journal of Mammalogy* 76:1056–1070.

Bell, W. J. 1990. *Searching Behavior.* New York: Chapman and Hall.

Benhamou, S., and P. Bovet. 1992. Distinguishing between elementary orientation mechanisms by means of path analysis. *Animal Behavior* 43:371–377.

Crooks, K. R. 2000. Mammalian carnivores as target species for conservation in southern california. Pp. 105–112 in J. E. Keeley, M. Baer-Keeley, and C. J. Fotheringham (eds.) *Second Interface between Ecology and Land Development in California*, Open-File Report 00-62. Sacramento, CA: US Geological Survey.

Crooks, K. R. 2002. Relative sensitivities of mammalian carnivores to habitat fragmentation. *Conservation Biology* 16:488–502.

Dobson, A. P., J. P. Rodriguez, W. M. Roberts, and D. S. Wilcove. 1997. Geographic distribution of endangered species in the united states. *Science* 275:550–553.

Forman, R. T. T. 1997. *Land Mosaics.* New York: Cambridge University Press.

Gustafson, E. J., and R. H. Gardner. 1996. The effect of landscape heterogeneity on the probability of patch colonization. *Ecology* 77:94–107.

Haddad, N. M. 1999. Corridor use predicted from behaviors at habitat boundaries. *American Naturalist* 153:215–227.

Hunter, R., R. Fisher, and K. Crooks. 2003. Landscape-level connectivity in coastal southern california as assessed by carnivore habitat suitability. *Natural Areas Journal* 23:302–314.

Huston, M., D. DeAngelis, and W. Post. 1988. New computer models unify ecological theory. *BioScience* 38:682–691.

Jander, R. 1975. Ecological aspects of spatial orientation. *Annual Reviews of Ecology and Systematics* 6:171–188.

Lima, S. L., and P. A. Zollner. 1996. Towards a behavioral ecology of ecological landscapes. *Trends in Ecology and Evolution* 11:131–135.

Marsh, L. M., and R. E. Jones. 1988. The form and consequences of random walk models. *Journal of Theoretical Biology* 133:113–131.

McLachlan, G., and D. Peel. 2000. *Finite Mixture Model.* New York: John Wiley.

Myers, N. 1990. The biodiversity challenge: expanded hot-spots analysis. *Environmentalist* 10:243–256.

Olden, J. D., R. L. Schooley, J. B. Monroe, and N. L. Poff. 2004. Context-dependent perceptual ranges and their relevance to animal movements in landscapes. *Journal of Animal Ecology* 73:1190–1194.

R Development Core Team. 2004. *R: A Language and Environment for Statistical Computing.* Vienna, Austria: R Foundation for Statistical Computing. Available online at http://www.R-project.org/

Soulé, M. E. 1991. Land use planning and wildlife maintenance: guidelines for conserving wildlife in an urban landscape. *Journal of the American Planning Association* 57:313–323.

Taylor, P. D., L. Fahrig, and G. Merriam. 1993. Connectivity is a vital element of landscape structure. *Oikos* 68:571–573.

Tracey, J. A., and K. R. Crooks. 2004. *Evaluating Landscape Connectivity in Coastal Southern California using Individual-Based Movement Models,* Final Report. San Diego, CA: The Nature Conservancy and the California Department of Fish and Game.

Tracey, J. A., J. Zhu, and K. R. Crooks. 2005a. A set of nonlinear regression models for animal movement in response to a single landscape feature. *Journal of Agricultural, Biological, and Environmental Statistics* 10:1–24.

Turchin, P. 1998. *Quantitative Analysis of Movement.* Sunderland, MA: Sinauer Associates.

Van Vuren, D. 1998. Mammalian dispersal and reserve design. Pp. 369–393 in T. Caro (ed.) *Behavioral Ecology and Conservation Biology.* New York: Oxford University Press.

Zollner, A. P. 2000. Comparing the landscape level perceptual abilities of forest sciurids in fragmented agricultural landscapes. *Landscape Ecology* 15:523–533.

# Animal Perception in Agent-based Models

Jeff A. Tracey

## 1 Introduction

Although it is poorly understood, understanding how animals move through a landscape is essential to conservation efforts in increasingly reduced, hazardous, and fragmented habitats (Van Vuren, 1998; Zollner and Lima, 2005). Through movement, animals gather information and find resources that are essential to their survival and reproduction. During movement, animals are also more vulnerable to risks such as predators (Zollner and Lima, 2005) and may traverse unknown or hazardous areas. This individual-level behavior affects higher-level population dynamics, population genetics, and community interactions (Wiens et al., 1993; Ims, 1995; Zollner and Lima, 1999*b*). In fragmented landscapes, the interaction between movement behavior and the landscape determines functional connectivity (Taylor et al., 1993; Forman, 1997), which may be critical to a species' persistence (Soulé and Terborgh, 1999; Crooks and Sanjayan, 2006). Animal perception of its surrounding environment is an essential process in movement-landscape interaction because it is the means by which an animal obtains information about its local environment (Olden et al., 2004). A greater understanding of the interaction among animal behavior, perception, and landscape structure, and the ability to incorporate this knowledge into models, will benefit our ability to conserve biodiversity and ecological complexity in the face of anthropogenic change (Zollner and Lima, 2005).

Agent-based models (Grimm et al., 2005) have been used in many fields including conservation and resource management (Gimblett, 2002; Weigand et al., 2003), and may continue to be more useful in the future as such models improve. Although

there is no generally accepted definition of what constitutes an agent (d'Inverno and Luck, 2001; Jiang and Gimblett, 2002), at minimum an agent is an entity situated in an environment which it may perceive and to which it may react and possibly act upon. In ecological models, agents often represent individual organisms and are therefore referred to as *individual-based models* (DeAngelis and Gross, 1992). Many advantages of individual-based models have been described (Huston et al., 1988; Judson, 1994), and they are consistent with the notions of individual variability and local interactions that are typically violated by state variable models (Huston et al., 1988). Their usefulness, however, may be limited by our understanding of individual-level perception and movement and empirical support to guide modeling efforts (Zollner and Lima, 1999*b*; Weigand et al., 2003).

In an agent-based model, stimuli from a simulated environment must pass through some kind of perceptual component before the agent can respond. These stimuli are translated to a corresponding response by a *response function* (Enquist and Ghirlanda, 2005). This response function may be as simple as a look-up table (Enquist and Ghirlanda, 2005) and as complicated as classifier or neural network systems with adaptive capabilities (Holland, 1992; Strand et al., 2002; Enquist and Ghirlanda, 2005). More potential stimuli are available in a real or simulated environment than can be detected by an animal or agent, and information conveyed by the stimuli that are detected must be reduced before a response can be made. When we build a model, we implicitly filter out some of this information when we decide what constitutes the simulated environment and how it is represented. Further, many of our ideas about perception serve to filter out information that is assumed to be unimportant to animal decisions. In the ecological literature attention has been devoted to delineating a region in space within which an animal (or agent) perceives its environment (Jander, 1975; Lima and Zollner, 1996; Schooley and Wiens, 2003; Olden et al., 2004). By delineating such a space, we ignore what falls outside of it.

The aim of this paper is to address perception in ecological agent-based models

and consequences for movement that arise from the manner in which perception is modeled. My specific objectives in this paper are to (1) synthesize some concepts important in modeling perception within agent-based models, (2) provide a mathematical description of a perception model that can be used in studies and simulations of animal movement, (3) explore some properties of the model, (4) demonstrate the use of the perception model as part of an agent-based movement model, and (5) present computer experiments that show some of the consequences of how we model perception on simulated dispersal in different landscapes.

## 2 Concepts

Jander (1975), in his paper on spatial orientation, describes *object orientation* as spatial orientation in relation to objects. Objects are resources or stress sources restricted to a point or area (patch) in space (Jander, 1975). The term *object* has also been applied to passive entities in agent-based models that do not react to stimuli (Jiang and Gimblett, 2002). When modeling perception, objects are often assigned to *types*. Objects of the same type are assumed to be similar with respect to how they are perceived and responded to by animals. Jander (1975) defines *detection space* as "the area around the searcher within which it detects objects." Later, Lima and Zollner (1996) define *perceptual range* as the distance at which an animal can perceive or detect a given type of landscape feature. Although this definition does not explicitly refer to a region about the animal, this distance implies a radius and hence a circular detection space, while detection space seems to be a more general concept because it refers to any region surrounding the animal. Lima and Zollner's definition also indicates that perceptual range is dependent upon the type of object being perceived (Lima and Zollner, 1996). This is a critical point, because perception depends on both the capabilities of the observer and properties of the object being observed. I acknowledge Jander's (1975) earlier contribution and use the more general term "detection space" to refer the the region around the animal within which it

perceives objects, while recognizing that the detection space is specific to the type of objects being perceived, environmental conditions, and the observing animal (or agent). The original definition of "perceptual range" identified a maximum distance from an animal to an object rather than an area about the animal (Lima and Zollner, 1996), so I will retain this meaning of perceptual range.

In subsequent work (Zollner and Lima, 1997, 1999*a*; Schooley and Wiens, 2003), effects of environmental conditions on perceptual range were explored. Hence, perceptual range is dependent on conditions intrinsic and extrinsic to the animal. Recently, others extended the idea of perceptual range to an anisotropic case in which the perceptual range depends on direction (Schooley and Wiens, 2003; Olden et al., 2004). Olden et al. (2004) proposed three properties of a detection space: perceptual distance, perceptual horizon, and perceptual breadth. The term "perceptual distance" is redundant with perceptual range, and will not be used in this paper. Since the detection space is not necessarily circular, the perceptual range will depend on the angle from the animal, and I will operationally define perceptual range as the distance from the animal to the boundary of the detection space at a given angle (Figure 1a). The term "perceptual horizon" (Olden et al., 2004) refers to an angular range of the detection space. This range may be dependent on the distance from the observer, depending on the shape of the detection space, so I suggest that the definition of perceptual horizon take into account the dependence of this quantity on distance (Figure 1b). Finally, the meaning of "perceptual breadth," the area of the detection space, is clear as originally stated (Olden et al., 2004).

Objects initiate signals that are propagated through the environment (Reiners and Driese, 2001). These signals are potential stimuli that may consist of, for example, light waves, sound waves, or chemical compounds and may provide information to an animal about its environment. The strength of a signal will generally decrease as the distance between an animal and the source of a signal increases. For example, light and sound waves emitted from a point source decrease in intensity as distance to

the source increases by an inverse-square relation (Serway, 1990), and concentration of chemicals diffusing from a point source decrease with distance as described by diffusion equations (Berg, 1993). Characteristics of the environment will further alter (attenuate) the propagation of the signal (Reiners and Driese, 2001). There are more opportunities for the environment to obscure detection as distance between the animal and the object increases. Terrain, for example, can obscure some areas from view, delineating a "viewshed" that contains all visible points on a terrain surface from a given observation point (Lee and Stucky, 1998). Vegetation can also reduce visibility; for example, white-footed mice are able to detect forest habitat at greater distances in barren fields than in soybean fields (Zollner and Lima, 1997). Terrain and vegetation will also affect how sound waves are propagated across a landscape (Reiners and Driese, 2001). Wind and water may convey chemical cues from a source, so wind direction and velocity, for example, may affect the ability of animals to detect signals from objects (Schooley and Wiens, 2003).

Many conceptual models for perception treat all points in the detection space equally; however, the processes of signal propagation, environmental attenuation, and constraints on attention suggest that this is not realistic. I propose a fourth property of a detection space that I call *perceptual weight*, which I define as the relative effect of an object, compared to other objects in the detection space, on behavioral decisions made by a particular animal as a function of its location in the animal's detection space. In other words, objects with a lower perceptual weight will have less effect on animal responses than other objects in the animal's detection space with higher perceptual weights. In this paper, I account for perceptual weight by making the effect of an object a function of its distance from the perceiving agent, relative to the distances of other objects from the agent.

With visual perception, an animal's *field of view* is defined by Gibson as the "solid angle of the ambient light that can be registered by its ocular system" (1986). The field of view limits the perceptual horizon, while decreasing strength of visual signals

increasing distance from the object to the observer limits perceptual range (eventually, the strength of the signals decline until they are below the threshold needed to excite visual receptors in the eye). Together, we should expect these limitations to form a detection space that is, in two dimensions, shaped roughly like a sector of a circle (Figure 2). However, environmental attenuation, perspective (Gibson, 1986), constraints on attention (Duncan, 1984; Yantis, 1992), integration of perceptions over recent movements of the eyes, head, and body (Gibson, 1986) indicate that this is not necessarily the only shape to consider in a model. A detection space consisting of a sector of a circle with its center at the location of the animal (Figure 2) excludes the possibility that knowledge of objects behind the animal can be used in decision making, which may be unrealistic because these objects may have been viewed from locations that the animal has recently occupied and it can turn its head or body to view objects behind it if it decides to do so. From a modeling point of view, this can lead to situations in which an agent (representing an animal) may reach the end of a *cul de sac*, for example, and have no information that it can use to reverse its direction to back-track out of it (see section 4.1). In this paper, I assume that perceptual range is greater in the direction of the agent's previous move angle which corresponds to the angle the agent is facing. I use an elliptical detection space with the agent location at one of the foci because this will include some information about the environment behind the animal, the degree of anisotropy can be controlled by changing distance between the foci, and the detection space reduces to the isotropic case when the distance between the foci is zero (Figure 2).

# 3 Model Formulation

I present a model for perception in agent-based ecological models, which I refer to as a *distance-weighted anisotropic detector model* (or *detector* for brevity), that quantifies the relation between an agent location and a set of objects of the same type. The model is motivated by visual perception of its surroundings by an agent and is guided

by the conceptual and modeling work described above. I assume that any object outside of the elliptical detection space cannot be perceived by the agent, is ignored by the agent, or that its influence on movement is so small that it is negligible. Besides the biological justifications, a detection space has practical computational benefits. With a detection space an agent need only take into account a subset of the objects in the landscape each time it makes a movement or other response. The computational investment needed to generate a single move is related to the number of objects the detection space contains. Without a detection space, on the other hand, the agent would have to consider every object in the landscape each time it moves, so the computational investment is related to the number of objects in the entire landscape.

Typically, spatial information is stored as a raster-based (e.g. grid cell) or vector-based (point, line, and polygon) representation, which correspond to fields and objects, respectively (Bian, 2003). For convenience, and because they are handled in the same way by the detector, I will consider a grid cell in a raster-based representation an object, just as I do each point, line or polygon in a vector-based representation. Conceptually, however, there is no advantage in regarding grid cells as objects since they do not correspond to a real-world entity (Bian, 2000, 2003). Each of these objects will have a location and belong to a category, and may also have a size and continuous value associated with it. Objects are weighted in their effect based on their distance from the agent in relation to other objects of the same type according to the idea of perceptual weight. The influence of all objects of a given type are combined to produce a distance-weighted mean vector (DWMV) with two components that can be passed into the response function of an agent-based model. The angle component of the DWMV provides information on the central weighted direction to objects of a given type, and the length component of the DWMV provides information on their relative distances and whether they are concentrated or dispersed within the detection space.

## 3.1 Ellipse Equations

First, I describe the equation for the ellipse. Let $C = (x_C, y_C)'$ be the center of an ellipse with foci $F_1 = (x_{F1}, y_{F1})'$ and $F_2 = (x_{F2}, y_{F2})'$. In this model, I consider $F_1$ to be the location of the agent that is observing its environment. We let $\alpha > 0$ be the length of the semi-major axis of the ellipse. Let $\delta_F$ be the distance and $\phi_F$ be the angle between $F_1$ and $F_2$, where $0 \leq \delta_F < 2\alpha$. The angle $\phi_F$ is considered to be the direction toward which the detection space is oriented; for example, it might be the angle the agent moved at the previous time step, or a biased direction movement. In implementation of the detector, the derived properties of the detector ($F_2$, $C$, and $\beta$) can be determined from the states and parameters of the detector and hence do not need to be explicitly represented. The focus $F_2$ can be determined from $x_{F2} = x_{F1} + \delta_F \cos(\phi)$ and $y_{F2} = y_{F1} + \delta_F \sin(\phi)$. The center of the ellipse can be calculated by $x_C = \frac{1}{2}(x_{F1} + x_{F2})$ and $y_C = \frac{1}{2}(y_{F1} + y_{F2})$. The length of the semi-minor axis of the ellipse is $\beta = \sqrt{\alpha^2 - 0.25\delta_F^2}$. The focus $F_1$ and the angle $\phi_F$ are considered states of the detector. When used in a movement simulation, the states of the detector may be updated from one time step to another. The distance between foci ($\delta_F$), the semi-major axis length ($\alpha$), and a distance-weighting parameter ($\lambda$, see below) are considered parameters of the detector. We consider the parameters to be fixed, but the model could be extended to allow them to change as with conditions internal or external conditions to the agent.

In general, let $\text{dist}(a, b)$ be the Euclidean distance from $a$ to $b$ and $\text{ang}(a, b)$ be the angle from point $a$ to point $b$ in radians. The distance from $C$ to some point $p$ on the ellipse (that is, $\text{dist}(C, p)$ is

$$\text{dist}(C, p) = \alpha\beta \left[\beta^2 \cos^2(\text{ang}(C, p) - \phi_F) + \alpha^2 \sin^2(\text{ang}(C, p) - \phi_F)\right]^{-1/2} \qquad (1)$$

which can be used to delineate the boundary of the detection space. Note that if $\delta_F = 0$, then $\alpha = \beta$, and the perceptual range is isotropic.

## 3.2 Weight Calculations

In this detector, each object within the detection space is assigned a perceptual weight based on up to five factors: (1) whether the object falls within the detection space or potentially a viewshed or other region, (2) the type, such as a set of land cover types, to which the object belongs , (3) the distance from the animal location to the center of or nearest point on the object, (4) the size of the object, and (5) a continuous attribute, such as elevation or temperature, associated with the object. Depending on the representation of the objects in the simulated environment, some or all of these factors may be used.

Let $i$ and $j$ index objects and $q_i$ be the location of the $i^{th}$ object. For reasons presented above, objects outside of the boundary of the detection space are given no weight; that is, they are given a weight of 0 or simply excluded from all calculations. Thus, we have the following indicator function:

$$\omega_i = \begin{cases} 0 & \text{, if the object is outside of the detection space} \\ 1 & \text{, otherwise.} \end{cases} \tag{2}$$

Note that this indicator function can be extended to exclude objects outside of a viewshed, soundshed, or other region. Equation (2) serves to exclude objects that are not in the detection space for a given detector. An object is in the detection space if $\text{dist}(F_1, q_i) + \text{dist}(F_2, q_i) \leq 2\alpha$.

Each object may be assigned to a type $z$ based on its attributes. A given detector will have the task of calculating the DWMV to objects belonging to type $z$. Thus, I include the following indicator function in our weighting:

$$\nu_i = \begin{cases} 1 & \text{, if object i belongs to category } z \\ 0 & \text{, otherwise.} \end{cases} \tag{3}$$

Equation (3) serves to exclude types of objects that are not perceived by a given detector.

Objects are weighted based on how far they are from the animal based on an inverse-distance weighting function commonly used in spatial analysis (Fortin and

Dale, 2005). Let $\rho_i$ quantify the distance relation between the animal location ($F_1$) and the object location $q_i$. The value of $\rho_i$ is given by:

$$\rho_i(q_i|F_1;\lambda) = [1 + \text{dist}(F_1, q_i)]^{-\lambda}. \tag{4}$$

The distance-weighting parameter $\lambda$, where $-\infty < \lambda < +\infty$, controls the distance effect. If $\lambda = 0$, then $\rho_i = 1$, and the model is reduce to the case where there is no distance-based perceptual weight (Figure 3). However, if $\lambda > 0$ objects near the agent are weighted more, and if $\lambda < 0$ objects further from the agent are weighted more.

Each object $i$ may have a size, $v_i$, associated with it. The size of the object is conceptually related to the number of visual receptors stimulated when an animal observes the object or the number of objects, so we multiply by size in the distance weighted mean vector equation (below). However, in a raster landscape representation, the size of all objects are equal, and because the weights are normalized, the size can be ignored. Thus, we can scale the weight by the size of the object in the following way:

$$\eta_i = \begin{cases} v_i & \text{, to take the size associated with each object into account} \\ 1 & \text{, to disregard size, or if all objects are equal in size.} \end{cases} \tag{5}$$

Finally, each object $i$ may also have a continuous attribute, $u_i$, which is accounted for by:

$$\iota_i = \begin{cases} u_i & \text{, to take a continuous attribute associated with each object into account} \\ 1 & \text{, to disregard the continuous attribute} \end{cases} \tag{6}$$

The continuous attribute comes into the final calculation of the components of the distance weighted mean vector.

## 3.3 Distance-Weighted Mean Vector

A mean vector is a resultant vector from a sum of unit length vectors and scaled by dividing by the number of unit length vectors (Batschelet, 1981). Hence, each unit

vector is weighted by 1 over the number of unit length vectors and the sum of the weights is equal to one. If many unit vectors are arranged at uniformly distributed angles the length of the mean vector will be near zero. A zero length mean vector will also be produced if for every unit vector, there is another unit vector in the opposite direction. As the angles of the unit vectors become more clustered in one direction, the length of the mean vector increases. If all the unit vectors are at the same angle, the length of the mean vector will be one. When the angles are non-uniformly distributed, the angle of the mean vector will be oriented toward the center of mass of the unit vector angles (Batschelet, 1981). In the DWMV, the unit vectors are the angles to the objects, and the weights are based on the size of and distance to the objects. Thus, more heavily weighted unit vectors will have a larger contribution to the resultant mean vector. Like a mean vector, the distance-weighted mean vector will have a length between zero and one, unless continuous attributes of the objects are taken into account.

Each object $i$ is assigned a perception weight given by:

$$w_i = \frac{\omega_i \nu_i \eta_i \rho_i(q_i|F_1;\lambda)}{\sum_j \omega_j \eta_j \rho_j(q_j|F_1;\lambda)} \,. \tag{7}$$

If no objects in category $z$ are detected, then we set $w_i = 0$ for all $i$.

The mean vector is calculated by taking a weighted sum of the cosine

$$\Delta_x = \sum_i w_i \iota_i \cos(\text{ang}(F_1, q_i))$$

and the sine

$$\Delta_y = \sum_i w_i \iota_i \sin(\text{ang}(F_1, q_i))$$

of the of the angles to each object. Then, the length of the mean vector is given by $r = \left[\Delta_x^2 + \Delta_y^2\right]^{1/2}$ and the mean angle is given by $\theta = \text{atan2}(\Delta_y, \Delta_x)$ (Batschelet, 1981; Mardia and Jupp, 2000). Thus, information about objects belonging to categories $\bar{z}$ within the detection space are summarized as a distance weighted mean vector (DWMV) which has a length ($r$) and angle ($\theta$) component, or alternatively, an $\Delta_x$

and $\Delta_y$ component. The two vector components are passed into the response function of an agent-based model.

The weighted mean vector has a mean angle on $(-\pi, \pi]$. If no continuous attributes are taken into account, the mean vector has a length on $[0, 1]$; otherwise, the length of the mean vector depends on the values of $\bar{\iota}$.

The three parameters ($\alpha$, $\delta_F$, and $\lambda$) control the size and shape of the detection space. The length of the semi-major axis ($\alpha$) and the distance between foci ($\delta_F$) determine the shape of the detection space. The length of the major axis of the detection space is $2\alpha$. As $\delta_F$ increases from 0.0 to $2\alpha$, the detection space becomes more elongated and goes from circular, to elliptical, to linear. Therefore, $\delta_F$ determines if the detection space is isotropic or anisotropic. Perceptual range increases in all directions with increasing $\alpha$, perceptual breadth increases with increasing $\alpha$ and decreasing $\delta_F$, and perceptual horizon decreases with increasing $\delta_F$ and increasing distance from the agent.

The distance-weighting parameter ($\lambda$) determines how objects within the detection space are weighted by distance. When $\lambda = 0$, distance has no effect on the weight given to each object in the detection space (Figure 3). As $\lambda$ increases from 0.0 to $+\infty$, the weighting of objects within the detection space goes from weighting all objects in the detection space equally to increasingly weighting objects nearer to the animal location. As $\lambda$ increases from 0.0 to $-\infty$, the weighting of objects within the detection space goes from weighting all objects in the detection space equally to increasingly weighting objects farther from the animal location. Again, note that this formulation does not allow higher weighting of objects at intermediate distances within the detection space.

By altering the detector parameters, we can produce four basic types of detection spaces: (1) an anisotropic detection space with distance weighting of all objects, (2) an isotropic detection space with distance weighting of all objects, (3) an anisotropic detection space with equal weighting of all objects, and (4) an isotropic detection

space with equal weighting of all objects. Hence, the shape of the detection space can reduce to the isotropic detection space consistent with Lima and Zollner (1996) and an anisotropic detection space as proposed by Olden et al. (2004). This allows us to explore the consequences of the different types of detections spaces, and if the detector model is fitted to data, to identify the one that is most supported by observations.

# 4 Examples

## 4.1 Distance Weighted Mean Vector Calculations

An infinite number of arrangements of objects within a detection space is possible. Here, I provide some illustrative examples to highlight the effects of object arrangement and distance-weighting parameter ($\lambda$) on DWMV calculations. These examples, in conjunction with the explanation in the previous section, serve as building blocks to understand path-level consequences of detection space properties in the next section. In the examples, objects are grid cells that are assigned to category 1 (low-risk transition habitat; Wiens et al., 1993) and category 2 (high-risk transition habitat). The detector calculates the DWMV for the low-risk transition habitat grid cells (that is, $z = \{\text{category 1}\}$). All objects are equal in size and have no continuous attribute associated with them. The location of the object is taken to be the center of the grid cell.

For a first example, consider a single object or single tight cluster of objects. In this case mean vector calculations are similar with varying distances and angles to the object or cluster, and across values of $\lambda$. This is because objects are weighted relative to the other objects within the detection space, and if object properties and locations are very similar, the detector will yield similar DWMVs regardless of $\lambda$. For a single object or single tight cluster of objects, the angle of the DWMV is oriented toward the cluster of objects.

As a second example, if objects are regularly distributed in space, density of the objects has little effect on the mean vector calculated by an object. However, the dis-

tance between foci ($\delta_F$) and distance-weighting parameter $\lambda$ does affect the resulting DWMV (Figure 4). This is because for an anisotropic elliptical detection space the perceptual horizon, and hence the range of possible angles to objects, decreases with increasing distance from the agent (Figure 1). Because the angles to objects at greater distances are closer together, the DWMV is longer. The shape of the detection space determines the range of possible angles to objects at different distances.

When objects are more clustered in space, the DWMV will be longer (Figure 5). However, the effect of clustering is greater for nearer objects with $\lambda > 0.0$ than for distant objects when $\lambda < 0.0$. Again, this is due to the decreasing perceptual horizon with increasing distance from the agent to the object. Also, because the objects are arranged symmetrically about the major axis of the detection space, the resulting DWMV points in the direction of the major axis ($\phi_F$). In this case, if an agent moves in the direction of the DWMV, there is no random component to movement, and there are no other objects in the landscape, then there would not be a way to break this symmetry and the agent would continue to move between the clusters of objects.

When two objects or two clusters of objects are present in the detection space, the shape parameter becomes much more important for the resulting DWMV (Figure 6). As one might expect, the nearer object or cluster has a greater effect on the DWMV when $\lambda > 0.0$, the more distant object or cluster has a greater effect on the DWMV when $\lambda < 0.0$, the effect of each cluster is equal when $\lambda = 0.0$. When the objects are of different sizes, or the clusters have a different number of objects, the larger object or cluster will have a stronger influence on the resulting DWMV, but the effect depends on the distance to the cluster and the value of $\lambda$.

In a final example, imagine that an agent is moving toward the end of a linear *cul de sac* composed of low-risk transition habitat and surrounded by high-risk transition habitat. In this case, what might be perceived as a movement corridor by an agent turns out to be a dead end (Figure 7). When $\lambda > 0.0$ the agent pays attention mostly to its immediate surroundings (Figure 7a–c) which consists primarily of low-

risk habitat and so the resulting mean vector is short. It is not until it reaches the end of the *cul de sac* (Figure 7c) that the mean vector reverses direction and the agent may tend to backtrack out of it. However, if $\lambda \leq 0.0$ the mean vector is more directed toward the end of the *cul de sac* (Figure 7g,h), which may (depending on the agent's response function) result in more directed movement toward the dead end. However, the DWMV starts getting shorter as the agent approaches the end of the *cul de sac* (Figure 7h), and reverses direction when it reaches the end (Figure 7i) because there is no longer any low-risk transition habitat in the direction toward which the detection space is oriented. In this case (under the movement model described in the next section) the agent would more rapidly explore and backtrack out of this dead end *cul de sac.*

In summary, the effect of the objects on the DWMV in this detector model will depend on the shape of the detection space, how the objects are arranged within the detection space, and how they are weighted (controlled by the distance-weighting parameter $\lambda$). The perceptual horizon at different distances from the agent and the perceptual range at different angles from the agent are determined by the shape of the detection space.

## 4.2 Application to Movement Modeling

### 4.2.1 Methods

In this section, I demonstrate how to use the detector in a simple model of individual-based animal movement and illustrate the consequences of detector and landscape properties on simulated dispersal ability. The model is implemented in C++ and compiled with GNU GCC version 3.4.3. The results are visualized using the R statistical software package Linux version 2.2.0 and the lattice graphics package (R Development Core Team, 2003). In this model, I generate moves at discrete regular time steps with a fixed move distance and a continuous, von Mises distributed move angle. The von Mises distribution is a circular analogue to the normal distribution commonly

used for linear quantities (Mardia and Jupp, 2000). The distribution has two parameters: a mean angle ($\mu$), and a concentration parameter ($\kappa$). It is symmetric about the mean angle, which is the angle of highest density. The concentration parameter controls amount of dispersion in the distribution. When $\kappa = 0$ the distribution is uniform; hence, every angle is equally likely. As $\kappa$ increases the distribution becomes increasingly clustered about the mean angle. In this simple movement model, the mean angle of movement is the mean angle of the vector calculated by the detector plus a *mean response angle* (Tracey et al., 2005), which is a parameter of the movement model. The mean response angle is the mean angle the animal moves relative to the angle of the DWMV returned by the detector. The concentration of the von Mises distribution is the product of the length of the weighted mean vector and a second move model parameter called the *response factor*, which scales the length of a DWMV returned by the detector to control how influential it is on the mean angle and concentration parameter of the von Mises distribution. After the von Mises distribution parameters have been calculated, a move angle is drawn from the von Mises distribution using a rejection method (Lang, 1999; Mardia and Jupp, 2000). I used the ran2() algorithm seeded from the system clock as the underlying uniform pseudo-random number generator (Press et al., 1992). During each simulated move, the new agent location is calculated from its current location, the fixed move length, and the randomly drawn move angle. The detector state is updated by setting $F_1$ to the new agent location and $\phi_F$ to the move angle; thus, if the detection space is anisotropic ($\lambda > 0$) it is oriented in the direction of the previous move.

I ran a set of simulations to explore the effects of perceptual weight (via the distance-weighting parameter $\lambda$), anisotropy (through the distance between foci $\delta_F$), and landscape properties on simulated dispersal ability. In the landscape layer, objects are grid cells (as in the examples in the previous section) with cells assigned to category 1 ("low-risk" transition habitat) and category 2 ("high-risk" transition habitat). Conceptually, I am simulating dispersal between patches of suitable habi-

tat (not represented) through a landscape consisting of transition habitat which is less hazardous and transition habitat which is more hazardous, where both types are devoid of resources required for long-term survival. The low-risk transition habitat is attractive to the agent. Therefore, the risk the animal takes when moving through the landscape depends on the proportion of time it spends in low-risk versus high-risk transition habitat and the total path length. Each landscape was a 320 $\times$ 320 cell neutral landscape generated using an algorithm by Tischendorf (2001). The neutral landscape algorithm allows the proportion and the amount of clustering of low-risk grid cells to be set by the user. The proportion of low-risk cells is determined by the parameter $P_{cov}$, where $0.0 \leq P_{cov} \leq 1.0$. The clustering of low-risk transition habitat cells is controlled by the parameter $FRAG$, where $0.0 \leq FRAG \leq 1.0$ and clustering increases with decreasing $FRAG$ (Tischendorf, 2001).

Simulations were run over a range of parameters. The neutral landscape parameters used are $P_{cov}$ with values of 0.1, 0.2, 0.3, 0.4, 0.5, 0.6, 0.7, 0.8, and 0.9 and $FRAG$ with values of 0.01, 0.03, 0.05, 0.07, and 0.09. Values for $\lambda$ were 2.0, 1.5, 1.0, 0.5, 0.0, -0.5, -1.0, -1.5, and -2.0. The distance between the foci was expressed as a fraction of the major axis length ($\delta_F/2\alpha$) for which I used values of 0.0, 0.1, 0.2, 0.3, 0.4, 0.5, 0.6, 0.7, 0.8, and 0.9. The length of the semi-major axis ($\alpha$) is held constant at 4.0 and the move distance was held constant at 1.0. The response angle is set to 0.0, which produces "on average" movement toward the low-risk habitat. The response factor was set to 10.0, which results in concentration parameters ranging from 0.0 to 10.0. For each combinations of the parameters, 500 movement paths of 150 moves were generated. Therefore, the agent never reached or perceived the boundary of the landscape. For each simulated movement path, a new neutral landscape layer was created using the appropriate landscape parameters. The initial agent location for each path was at the center ($x_{init} = 160$, $y_{init} = 160$) of the landscape and the initial $\phi_F$ was randomly drawn from a uniform distribution over the interval of $-\pi$ to $\pi$.

The path-level behavior of the model is quantified in terms of the maximum net

displacement achieved during a path ($ND_{max}$), and the number of simulated locations in a path that fall within low-risk transition habitat grid cells ($H_{count}$). The maximum net displacement ($ND_{max}$) is simply the Euclidean distance from the agent's initial location to the most distant location on the simulated move path. I interpret $ND_{max}$ to be a measure of the permeability of the landscape to the agent and $H_{count}$ is a measure of the safety of the movement path. As $ND_{max}$ declines, we expect mortality to increase due to starvation since more movement is required to reach patches of suitable habitat and more time is spent in transition habitat. As $H_{count}$ declines, we expect mortality to increase due to increased use of the more hazardous parts of the landscape. For each combination of parameters, I recorded the minimum, maximum, mean, and variance of $ND_{max}$ and $H_{count}$ from the 500 simulated paths.

### 4.2.2 Results

When the detection space is isotropic (that is, $\delta_F = 0.0$) the fragmentation and proportion of coverage of the landscape and the distance-weighting parameter ($\lambda$) matter relatively little to mean maximum net displacement ($ND_{Max}$, Figure 8). However, when $\delta_F > 0$, $ND_{max}$ increases with increasing anisotropy, increasing proportion of low-risk transition habitat, and decreasing shape parameter. The variance in maximum net displacement shows a similar pattern to the mean for the range of parameters considered (not shown). The effect of $\lambda$ on mean $ND_{max}$ diminishes as $\lambda$ decreases. Increasing mean maximum net displacement results from straighter (less sinuous) movement paths (Figure 8 and 9). Fragmentation in the neutral landscape appears to work in interaction with other parameters to influence mean net maximum displacement (Figure 8) although this simple movement model under the given parameters does well in finding a path through patches of low-risk cells regardless of the degree of fragmentation (Figure 9).

The number of locations in the low-risk transition habitat can range from zero to the number of simulated locations (in our case 150). If we were to randomly assign locations to the landscape, the expected value of $H_{count}$ would be $150 \times P_{cov}$. When

$P_{cov} = 0.0$ there is no alternative but that mean $H_{count} = 0$ and when $P_{cov} = 1.0$ there is no alternative but that mean $H_{count} = 150$. At intermediate values of $P_{cov}$ observed mean $H_{count}$ can deviate from what is expected from random. In general, the detector model used within the simple movement model described above, with the given parameters, performs remarkably well in generating movements that are attracted to the low-risk transition habitat regardless of the degree of fragmentation (Figure 9) performing much better than expected at random (Figure 10).

Increasing anisotropy and decreasing distance-weighting parameter ($\lambda$, that is, more weight on more distant objects) reduces the mean number of locations in low-risk habitat (Figure 10), with anisotropy having the greater effect. The distance-weighting parameter has little effect when the detection space is isotropic ($\delta_F = 0$), and its effect is reduced for certain combinations of landscape fragmentation ($FRAG$) and anisotropy. There is an interaction between $FRAG$ and $\delta_F$ that is most evident when comparing the subplots in Figure 10 on the diagonal from the lower-left ($FRAG = 0.01$, $\delta_F = 0.0$) upward (to $FRAG = 0.07$, $\delta_F = 0.9$). For these plots, mean $H_{count}$ is lowest (Figure 10) and the variance is the highest. Hence, in this model there are some degrees of anisotropy that perform poorly at particular intermediate levels of fragmentation.

There is a tradeoff between maximum net displacement and the number of locations that fall within the low-risk transition habitat (Figure 11). As $\delta_F$ increases the detection space becomes more anisotropic. With increasing anisotropy, mean net maximum displacement (mean $ND_{max}$) increases and mean number of locations in low-risk transition habitat ($H_{count}$) decreases (not considering the anisotropy-fragmentation interaction described above). Distance weighting shows a similar, but weaker, effect where mean $ND_{max}$ increases and mean $H_{count}$ decreases with decreasing $\lambda$.

# 5 Discussion

Few previous modeling studies have explored the consequences of detection space shape and other properties in movement modeling. In this paper, I have proposed a distance-weighted anisotropic detector model with three main properties: (1) an elliptical detection space, (2) weighting the influence of objects based on distance from the agent, and (3) summary of the relation between the agent and objects of a given type as a distance-weighted mean vector (DWMV). The DWMV provides information on the angles to objects and their dispersion within the detection space. Further, the model can reduce to an isotropic case and/or to an equal-weighted case. I have illustrated behavior of the detector model, and illustrated its use and behavior in an agent-based movement model.

The concepts and models I have presented have several implications for animal movement and modeling animal movement. One important consideration is the shape of the detection space. I have argued that at an instant in time, there is a boundary that encloses objects in the environment from which signals can be detected. A reasonable simplification of the shape of this space for vision in the absence of environmental attenuation should be "fan shaped," or the sector of a circle. However, the animal will also posses knowledge of its local environment from recent eye and head movements, and recent displacements in its environment – all of which will affect the shape of the detection space. I have used an ellipse to approximate this space, but other shapes should be considered.

The shape and size of the detection space will determine which objects are included and excluded when making movement decisions by both real animals and in agent-based models. The shape of the detection space constrains the perceptual horizon at different distances, and hence the angles to objects to which an animal will move in response. The shape will also determine the length of an arc that intersects the detection space at a given distance. This determines the representation of each distance within the detection space which will influence distance-weighted calcula-

tions. A sector of a circle whose center is at the animal location will have the same perceptual horizon at every distance within the detection space. It is also possible to construct detection spaces that have constant arc lengths at each distance for some range of distances. Other than a line, which is not a useful detection space, there is no detection space in two dimensions that preserves both perceptual horizon and arc length over a range of distances from the observer.

The models I have presented predict that increased anisotropy of the detection space tends to produce increased directional persistence when moving in response to attractive objects. In fact, this may be an explanation for directional persistence (or serial autocorrelation in move angle) observed in many animal movement paths. In the models, most of the area of a highly anisotropic detection space is ahead of the animal (oriented toward its previous direction of movement), so if low-risk transition habitat was present in this area the agent would tend to move toward it. This tends to create autocorrelation in the direction of movement, but does not preclude a change of movement direction if no low-risk habitat is ahead of the animal. When the shape parameter is small (the smallest values I considered as $\lambda = -2.0$), distant objects are weighted more than nearby ones. If an agent perceives a distant object and moves toward it, the object will become less weighted if there are other attractive objects in the detection space (a negative-feedback). This can result in a behavior where the agent can "hop-scotch" from one attractive object (or cluster of attractive objects) to another while simultaneously tending to move in a directionally persistent manner. This interpretation is consistent with the results that mean maximum net displacement increases with increasing anisotropy and increased weight on more distant objects.

The model I have presented is flexible enough to produce other behaviors. For example, it can produce "object orientation" consistent with the description given by Jander (1975). If nearby objects are weighted more heavily ($\lambda$ is large), when an agent detects and orients toward an attractive object, the weight placed on this

object will increase as the agent approaches it, resulting in stronger attraction (a positive feed-back). In this case, the animal may be drawn to an attractive object (or cluster of such objects) and remain in the same vicinity for many moves. In the simple movement model used in this paper, low-risk transition habitat was attractive because the response angle was 0.0 radians. Once the object is detected and the agent moves toward it, the detection space is re-oriented toward the object, and hence the orientation of the detection space is modified by environmental stimuli as suggested by Olden et al. (2004). If the response angle was $\pi$ radians, then the low-risk transition habitat would have been repulsive and the agent would have avoided it. In this case, when $\lambda$ is large, the strength of this avoidance would increase as the agent approaches the object, provided that there are other such objects within the detection space. However, if $\lambda$ was small the strength of repulsion would diminish as the agent approached the object under the same conditions.

The results of the simulations also predict a tradeoff between mean maximum net displacement and the number of locations in low-risk habitat. In the model, mean $ND_{max}$ increased and $H_{count}$ decreased with increasing anisotropy ($\delta_F$) and decreasing distance-weighting parameter ($\lambda$). This tradeoff may be a real one faced by animals dispersing between patches of suitable habitat. For example, animals may have to chose between moving rapidly but more recklessly through transition habitat, or moving more slowly and cautiously. Zollner and Lima addressed tradeoffs associated with dispersal behavior (2005), but these tradeoffs were linked to dispersal speed and built into the model. In the models I have presented, this tradeoff is a consequence of anisotropy or perceptual weight of the detection space. Increasing the dispersal path length (related to decreasing $ND_{max}$) will increase the cost of dispersal and will increase risk because the animal will spend more time in transitional habitat (whether it is high-risk or low-risk). Spending more time in low-risk habitat (related to increasing $H_{count}$) will result in increased safety. This provides a link between properties of the detection space and survival of the individual while dispersing. Since attention,

body orientation, head and eye movements, and fine-scale exploratory movements are under behavioral control, the animal has some control over the size and shape of its detection space, and it may make adjustments depending on its objectives and the environment. The best perceptual strategy will depend on the structure of the environment, mortality in each type of transition habitat, environmental constraints on perception, perceptual capabilities of the animal, the arrangement of patches of suitable habitat, and possibly other factors.

The predictions I have described above are available for empirical study; however, the detector model is proposed primarily as a component of an agent-based model. In an agent-based model, an agent can have an array of such detectors for each type of object in the environment that we chose to allow it to perceive. For categorical raster-based or vector-based spatial data, we use one detector for each category. For continuous raster-based and vector-based data (e.g., a set of point objects with a continuous attribute), we use one detector for each type of continuous variation. A collection of such detectors forms a perception component of an agent-based model. In this case, the problem is designing a response function for the agent that can incorporate information from an array of detectors to yield a movement.

It will benefit us in our efforts to improve agent-based models to develop a solid theoretical foundation for perception and clear, consistent terminology. Further, we must formulate models for perception and evaluate them. I have proposed one such model, and it is my hope that it is explored, tested, and eventually replaced with better ones. Detection spaces of different shapes and different object weighting schemes can be explored. In these models, I assume that the environment remains fixed during the simulated movement path, but the model I have presented can be extended to change with the agent's internal state and external environment. Further, animal's may possibly employ "composite perception" strategies. For example, an animal might look far ahead to select a heading, and then focus on its immediate surroundings as it negotiates its way through its environment in that general direction. Clearly,

the study and modeling of perception is fertile ground and there is much work to be done.

# References


Batschelet, E. 1981. Circular Statistics in Biology. Academic, New York.

Berg, H. C. 1993. Random Walks in Biology. Princeton University Press, Princeton.

Bian, L. 2000. Component modeling for the spatial representation of wildlife movements. Journal of Environmental Management **59**:235–245.

Bian, L. 2003. The representation of the environment in the context of individual-based modeling. Ecological Modelling **159**:279–296.

Crooks, K. R., and M. Sanjayan, editors. 2006. Connectivity Conservation. Cambridge University Press, Cambridge.

DeAngelis, D. L., and L. J. Gross, editors. 1992. Individual-Based Models and Approaches in Ecology. Chapman and Hall, New York.

d'Inverno, M., and M. Luck, editors. 2001. Understanding Agent Systems. Springer, New York.

Duncan, J. 1984. Selective attention and the organization of visual information. Journal of Experimental Psychology. General **113**:501–517.

Enquist, M., and S. Ghirlanda. 2005. Neural Networks and Animal Behavior. Princeton Univesity Press, Princeton.

Forman, R. T. T. 1997. Land Mosaics: The ecology of landscapes and regions. Cambridge, New York.

Fortin, M., and M. Dale. 2005. Spatial Analysis: A Guide for Ecologists. Cambridge, New York.

Gibson, J. J. 1986. The Ecological Approach to Visual Perception. Lawrence Erlbaum Associates, Hillsdale.

Gimblett, H. R., editor. 2002. Integrating Geographic Information Systems and Agent-based Modeling Techniques for Simulating Social and Ecological Processes. Oxford University Press, Oxford.

Grimm, V., E. Revilla, U. Berger, F. Jeltsch, W. M. Mooij, S. F. Railsback, H. Thulke, J. Weiner, T. Weigand, and D. L. DeAngelis. 2005. Pattern-oriented modeling of agent-based complex systems: lessions from ecology. Sciece **310**:987–991.

Holland, J. H., editor. 1992. Adaptation in Natural and Artificial Systems. MIT Press, Cambridge, Mass.

Huston, M., D. DeAngelis, and W. Post. 1988. New computer models unify ecological theory. BioScience **38**:682–691.

Ims, R. A., 1995. Movement Patterns Related to Spatial Structures. *in* L. Hansson, L. Fahrig, and G. Merriam, editors. Mosaic Landscapes and Ecological Processes. Chapman and Hall, London.

Jander, R. 1975. Ecological aspects of spatial orientation. Annual Review of Ecology and Systematics **6**:171–188.

Jiang, B., and H. R. Gimblett, 2002. An Agent-Based Approach to Environmental and Urban Systems within Geographic Information Systems. *in* H. R. Gimblett, editor. Integrating Geographic Information Systems and Agent-based Modeling Techniques for Simulating Social and Ecological Processes. Oxford University Press, Oxford.

Judson, O. P. 1994. The rise of the individual-based model in ecology. Trends in Ecology and Evolution **9**:9–14.

Lang, K. 1999. Numerical Analysis for Statisticians. Springer, New York.

Lee, J., and D. Stucky. 1998. On applying viewshed analysis for determining least-cost

paths on Digital Elevation Models. International Journal of Geographic Information Science **12**:891–905.

Lima, S. L., and P. A. Zollner. 1996. Towards a behavioral ecology of ecological landscapes. Trends in Ecology and Evolution **11**:131–135.

Mardia, K. V., and P. E. Jupp. 2000. Directional Statistics. Wiley, New York.

Olden, J. D., R. L. Schooley, J. B. Monroe, and N. L. Poff. 2004. Context-dependent perceptual ranges and their relevance to animal movements in landscapes. Journal of Animal Ecology **73**:1190–1194.

Press, W. H., S. A. Teukolsky, W. T. Vetterling, and B. P. Flannery. 1992. Numerical Recipes in C. 2 edition. Cambridge.

R Development Core Team, 2003. R: A language and environment for statistical computing. R Foundation for Statistical Computing, Vienna, Austria. URL `http://www.R-project.org`.

Reiners, W. A., and K. L. Driese. 2001. The propagation of ecological influences through heterogeneous environmental space. BioScience **51**:939–950.

Schooley, R. L., and J. A. Wiens. 2003. Finding habitat patches and directional connectivity. Oikos **102**:559–570.

Serway, R. A. 1990. Physics for Scientists and Engineers. Sunders College Publishing, Philadelphia.

Soulé, M. E., and J. Terborgh. 1999. Continental Conservation. Island Press, Washington.

Strand, E., G. Huse, and J. Giske. 2002. Artificial evolution of life history and behavior. The American Naturalist **159**:624–644.

Taylor, P. D., L. Fahrig, K. Henein, and G. Merriam. 1993. Connectivity is a vital element of landscape structure. Oikos **68**:571–573.

Tischendorf, L. 2001. Can landscape indices predict ecological processes consistently? Landscape Ecology **16**:235–254.

Tracey, J. A., J. Zhu, and K. Crooks. 2005. A set of nonlinear regression models for animal movement in response to a single landscape feature. Journal of Agricultural, Biological, and Environmental Statistics **10**:1–18.

Van Vuren, D., 1998. Mammilian Dispersal and Reserve Design. *in* T. Caro, editor. Behavioral Ecology and Conservation Biology. Oxford, New York.

Weigand, T., F. Jeltsch, I. Hanski, and V. Grimm. 2003. Using pattern-oriented modeling for revealing hidden information: a key for reconciling ecological theory and application. Oikos **100**:209–222.

Wiens, J. A., N. C. Stenseth, B. Van Horne, and R. A. Ims. 1993. Ecological mechanisms and landscape ecology. Oikos **66**:369–380.

Yantis, S. 1992. Multielement visual tracking: attention and perceptual organization. Cognitive Psychology **24**:295–340.

Zollner, P. A., and S. L. Lima. 1997. Landscape-level perceptual abilities in white-footed mice: perceptual range and the detection of forested habitat. Oikos **80**:51–60.

Zollner, P. A., and S. L. Lima. 1999*a*. Illumination and the perception of remote habitat patches by white-footed mice. Animal Behaviour **58**:489–500.

Zollner, P. A., and S. L. Lima. 1999*b*. Search strategies for landscape-level interpatch movements. Ecology **80**:1019–1030.

Zollner, P. A., and S. L. Lima. 2005. Behavioral tradeoffs when dispersing across a patchy landscape. Oikos **108**:219–230.

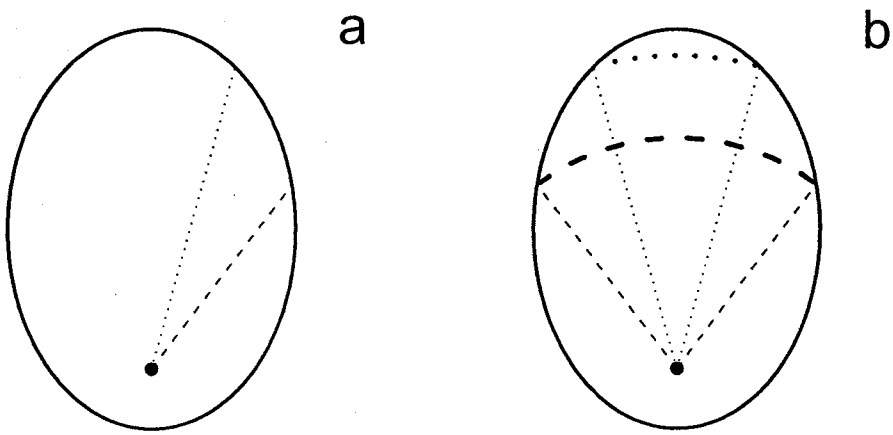


Figure 1: Perceptual range (a) and perceptual horizon (b). I define perceptual range as the distance from the agent (or animal) location at a given angle to the boundary of its detection space, and perceptual horizon as the angular range of the detection space at a given distance from the agent. In both subplots, the location of the animal (or agent) is shown as a solid point and the boundary of the ellipse as a solid line. With an elliptical detection space, perceptual range depends on the angle from the animal (or agent) to the object (subplot a). The perceptual range for a smaller angle from the major axis of the ellipse is shown as a dotted line, and the perceptual range for a larger angle from the major axis of the ellipse is shown as a dashed line. Perceptual horizon for an elliptical detection space depends on the distance from the animal (subplot b). In this example, the perceptual horizon (dotted lines) is smaller at a greater distance than at a smaller distance (dashed lines).

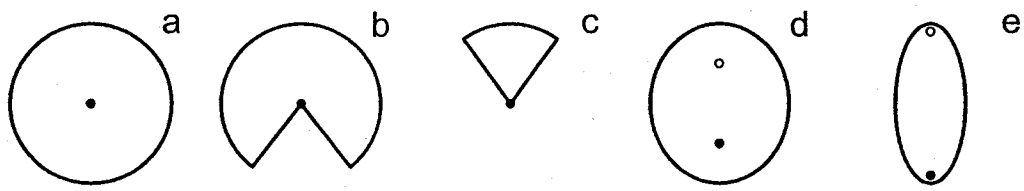


Figure 2: An isotropic detection space (a) and two types of anisotropic detection spaces (b, c and d, e; following (2004)). In all subplots the animal (agent) location is show as a filled point. Subplot a shows the "traditional" circular isotropic detection space. An anisotropic detection space can be formed from the isotropic case by taking a sector of the circle (subplots b – c) or treating the circle as the special case of an ellipse and increasing the distance between the foci (subplots d – e). Using the "sector approach" we can vary the perceptual horizon from larger (subplot b) to smaller (subplot c). Within the sector of the circle the perceptual range will not change with the angle from the agent and perceptual horizon will not change with distance from the agent. If the angle forming the sector of the circle is $2\pi$ the result is an isotropic detection space. In subplots d and e, the animal location is the first focus of the ellipse, which is shown as a filled point. The second focus is shown as an open point. The degree of anisotropy is determined by the distance between the foci (subplot d and e). If the distance between foci is 0, the results is an isotropic detection space. For an elliptical detection space, perceptual range will change with angle from the agent and perceptual horizon will change with distance from the agent.

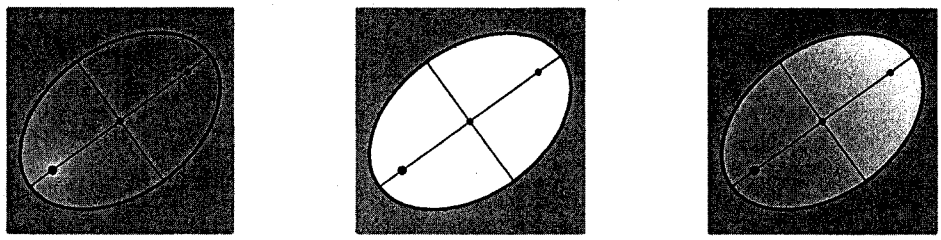

Figure 3: An example of an ellipse and calculations associated with an elliptical detection space. The ellipse delineating the detection space and the major and minor axes of the ellipse are shown as black lines. The animal location ($F_1$) is shown as a large point, and the center and second focus of the ellipse ($C$ and $F_2$, respectively) are shown as smaller points. The lighter areas are weighted higher. In the left subplot, $\lambda = 1.0$. In the center subplot, $\lambda = 0.0$. In the right subplot, $\lambda = -1.0$. Notice that when $\lambda = -1.0$ (right) , much more of the area within the detection space is given a higher weight compared to when $\lambda = 1.0$ (left).

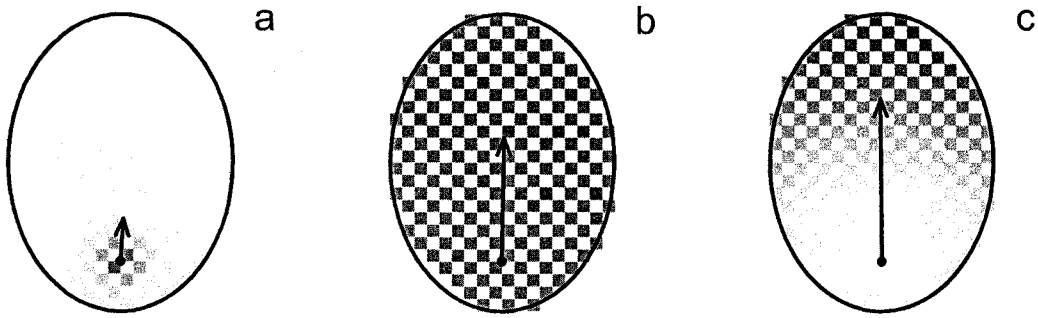


Figure 4: The effect of the distance-weighting parameter ($\lambda$) on the distance-weighted mean vector in an environment filled with regularly distributed objects. In each subplot, the objects are grid cells. The cells are shaded according to distance weighting, where darker cells are weighted more. The agent location is shown as a filled point and the distance-weighted mean vector (DWMV) is shown as an arrow (scaled by a constant for illustration). In subplot a, $\lambda = 2$, so nearby cells are weighted more. In subplot b, $\lambda = 0$, so all cells are weighted equally. In subplot c, $\lambda = -2$, so distant cells are weighted more. As distance from the agent increases, perceptual horizon decreases. When more distant objects are more heavily weighted (subplot c) the length of the DWMV increases because there is less variation in the angles to the more heavily weighted objects.

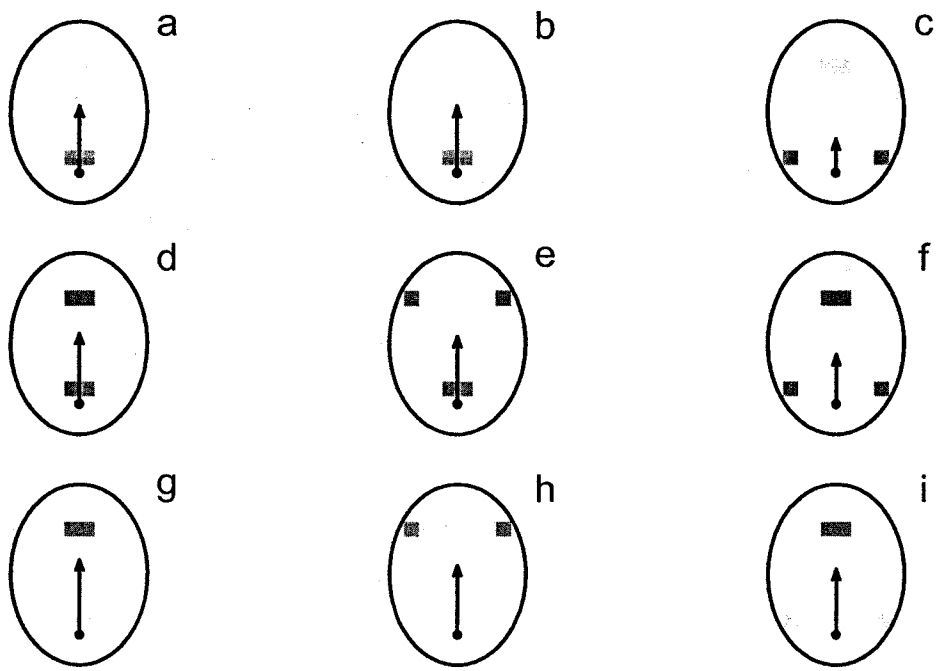


Figure 5: The effect of object clustering on the distance-weighted mean vector (DWMV). The agent location is shown as a filled point, the DWMV as an arrow, and the elliptical detection space as a black line. The objects are grid cells shaded according to how much they are weighted. Darker grid cells are weighted more. The top row of subplots (a – c) corresponds to a distance-weighting parameter of $\lambda = 2.0$ which weights nearby objects more heavily. The middle row of subplots (d – f) corresponds to $\lambda = 0.0$ which weights all objects equally. The bottom row of subplots (g – i) corresponds to $\lambda = -2.0$ which weights distant objects more heavily. The left column shows an arrangement of two clusters of objects at near and far distances. In the middle column the distant cluster is separated into two smaller clusters. In the right column the nearby cluster is separated into two smaller clusters. The effect of clustering is greater for nearby objects because of the greater perceptual horizon at shorter distances. In addition, the effects of changes in clustering at near and far distances depends on the distance-weighting parameter.

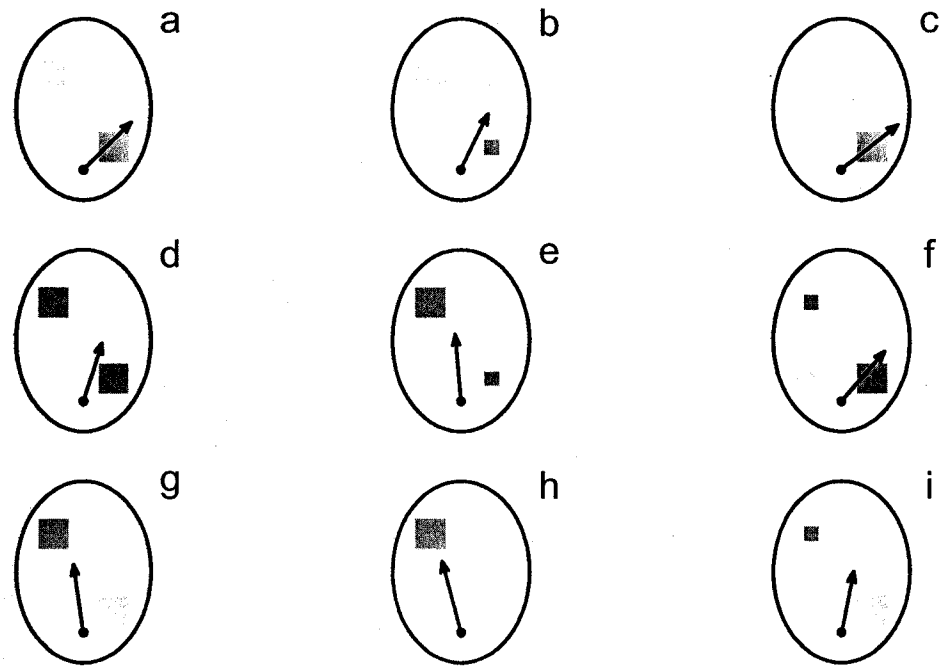


Figure 6: The effect of object cluster size, angle, and distance on the angle of the distance-weighted mean vector (DWMV). The agent location is shown as a filled point, the DWMV as an arrow, and the elliptical detection space as a black line. The objects are grid cells shaded according to how much they are weighted. Darker grid cells are weighted more. The top row of subplots (a – c) corresponds to a distance-weighting parameter of $\lambda = 2.0$ which weights nearby objects more heavily. The middle row of subplots (d – f) corresponds to $\lambda = 0.0$ which weights all objects equally. The bottom row of subplots (g – i) corresponds to $\lambda = -2.0$ which weights distant objects more heavily. The left column shows an arrangement of equal-sized clusters of objects with the nearer cluster to the right of the agent and the more distant cluster to the left of the agent. The middle column shows the same arrangement as the left column but the number of objects in the nearer cluster is reduced. The right column shows the same arrangement as the left column but the number of objects in the distant cluster is reduced. The angle of the DWMV is a weighted mean angle to all of the objects in the detection space. When the number of objects in a cluster is reduced, that cluster has less effect on the angle of the DWMV. The effect in changing the number of objects nearby or distant from the agent on the angle of the DWMV also depends on the distance-weighting parameter.

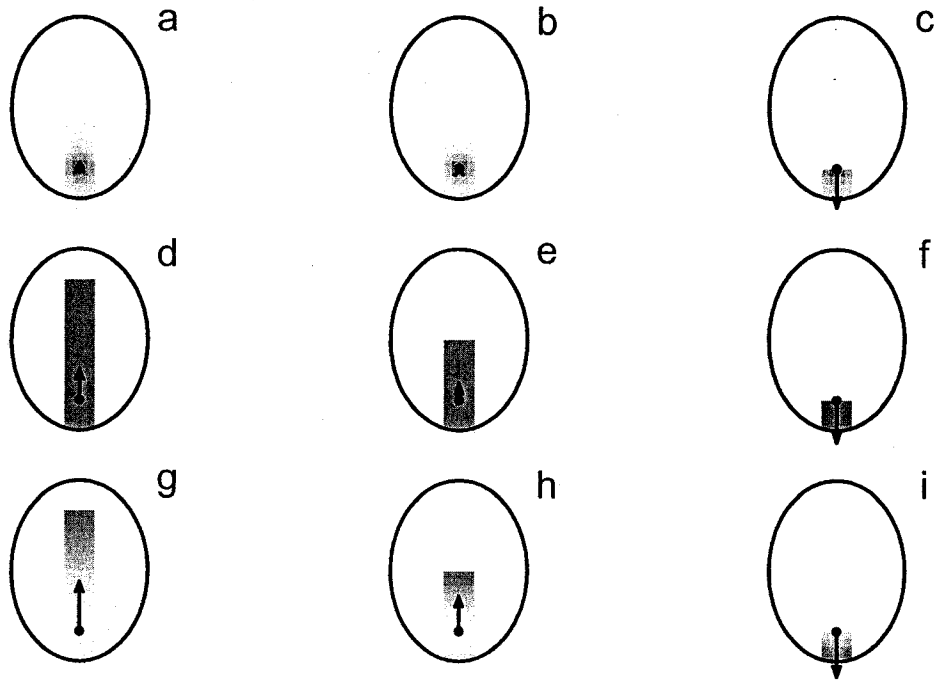


Figure 7: The distance-weighted mean vector (DWMV) as an agent travels to the end of a *cul de sac*. The agent location is shown as a filled point, the DWMV as an arrow, and the elliptical detection space as a black line. The objects are grid cells shaded according to how much they are weighted. Darker grid cells are weighted more. The top row of subplots (a – c) corresponds to a distance-weighting parameter of $\lambda = 2.0$ which weights nearby objects more heavily. The middle row of subplots (d – f) corresponds to $\lambda = 0.0$ which weights all objects equally. The bottom row of subplots (g – i) corresponds to $\lambda = -2.0$ which weights distant objects more heavily. As we go from the left most to the center to the right column, the agent gets progressively closer to the end of the *cul de sac*. In the right column, the DWMV reverses direction at the end of the *cul de sac*. When $\lambda$ is larger, the agent weights nearby objects more heavily, so the DWMV is short and does not change much until the agent reaches the very end of the *cul de sac*. If a short DWMV translates to a weak influence on move angle, then the agent may take a more sinuous path through the *cul de sac*, and will take a longer time to explore and backtrack out of it. On the other hand, when $\lambda < 0.0$, more distant objects are weighted more and the resulting DWMV is longer. If a longer DWMV translates into a strong influence on move angle, the agent will quickly move to the end of the *cul de sac* and then backtrack out of it. This will tend to reduce the time it takes for the agent to explore the *cul de sac*.

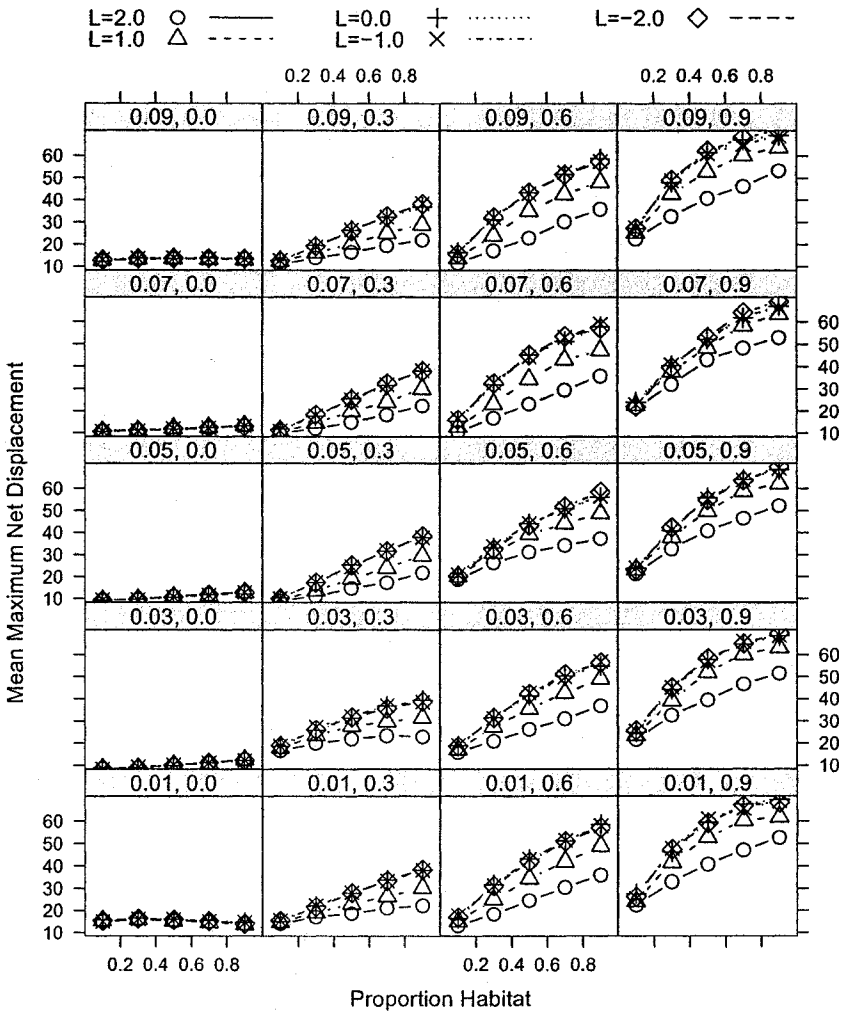


Figure 8: Effect of landscape and detector properties on mean maximum net displacement. Rows correspond to a value of $FRAG$ and columns correspond to a value of $\delta_F/2\alpha$, which is a measure of anisotropy. These values are indicated in the gray bar above each panel (left value is $FRAG$ and the right value is $\delta_F/2\alpha$). Hence, each panel in this Trellis plot corresponds to a particular combination of $FRAG$ and $\delta_F/2\alpha$. Each line in each panel corresponds to a value of $\lambda$ and a key is given at the top of the figure (L refers to $\lambda$). The x-axis in each panel is the value of $P_{cov}$, the proportion of low-risk habitat in the neutral landscape, and the y-axis in each panel is the mean maximum net displacement. See the text for a description of the results.

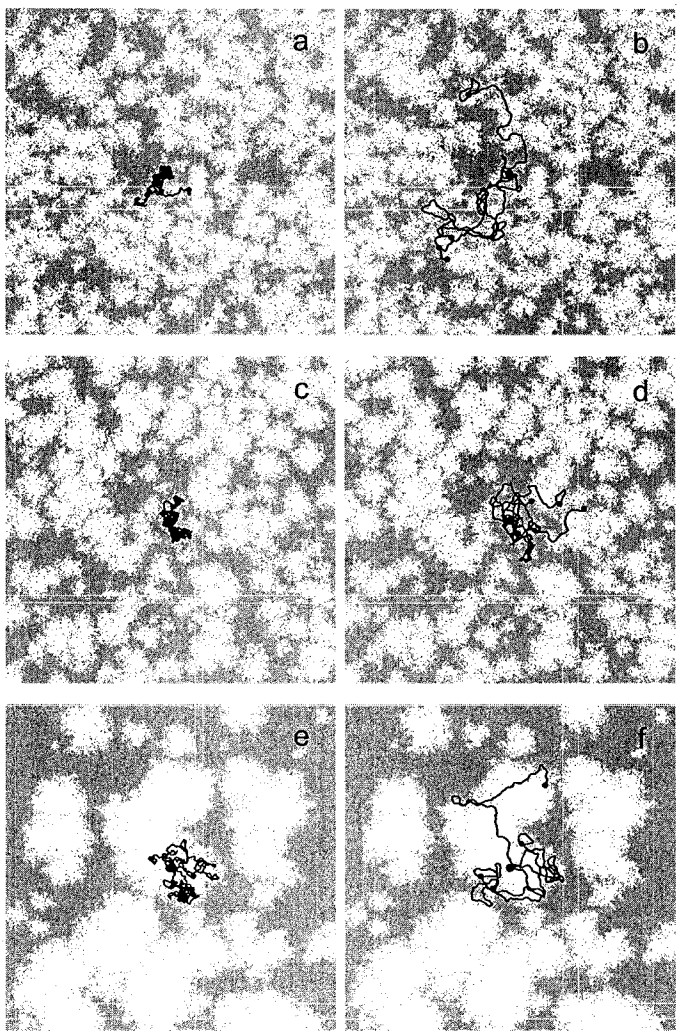


Figure 9: Simulated paths on three different neutral landscapes with two different degrees of anisotropy. Each neutral landscape has 50 percent "low-risk transition habitat" (in white, $P_{cov} = 0.5$). In sub-figures a-b, $FRAG = 0.05$, in c-d $FRAG = 0.03$, and in e-f $FRAG = 0.01$. As $FRAG$ increases, clustering of low-risk transition habitat decreases. In the left column of figures $\delta_F = 2.0$ (lower anisotropy) and in the right column $\delta_F = 6.0$ (higher anisotropy). For all figures, $\lambda = 0.0$, which means all low-risk transition habitat cells are weighted equally, and all other parameters are as described in section 4.2.1. Increased anisotropy of the detection space (b, d, and f) results in greater correlation between move angles in adjacent time steps.

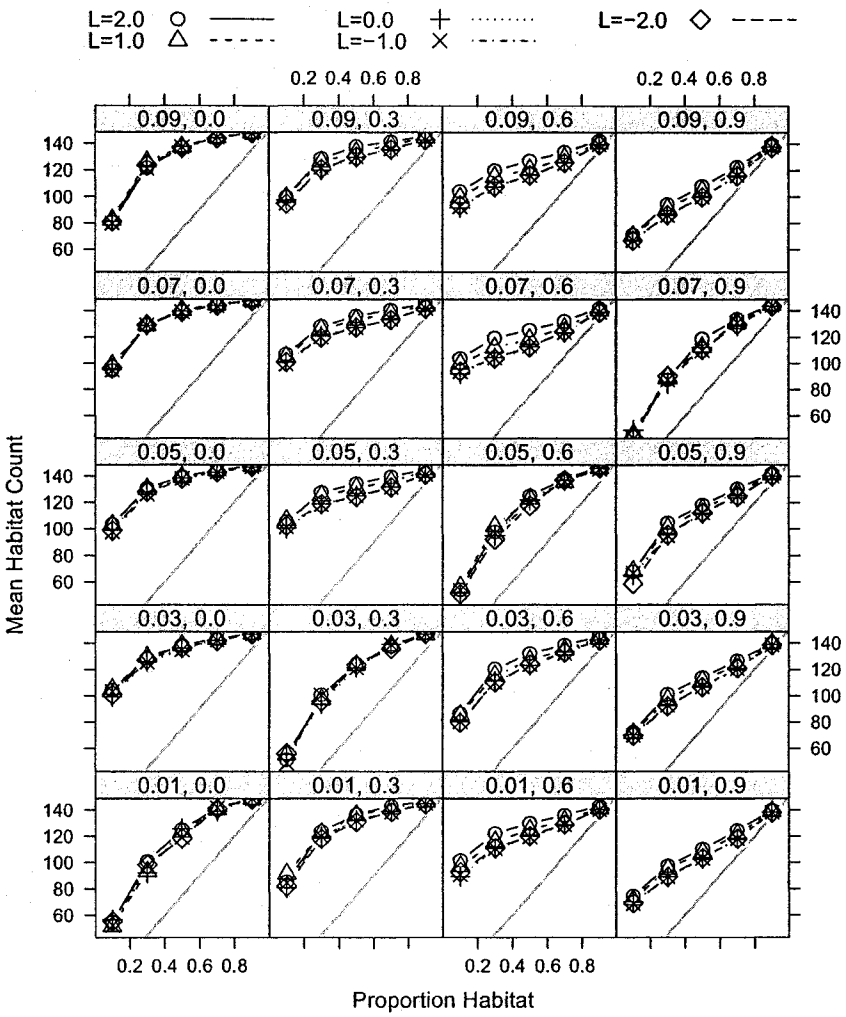


Figure 10: Effect of landscape and detector properties on mean low-risk transition habitat use. Rows correspond to a value of $FRAG$ and columns correspond to a value of $\delta_F/2\alpha$. Hence, each panel in this Trellis plot corresponds to a particular combination of $FRAG$ and $\delta_F/2\alpha$. These values are indicated in the gray bar above each panel (left value is $FRAG$ and the right value is $\delta_F/2\alpha$). Each line in each panel corresponds to a value of $\lambda$ and a key is given at the top of the figure (L refers to $\lambda$). The x-axis in each panel is the value of $P_{cov}$, the proportion of low-risk habitat in the neutral landscape, and the y-axis in each panel is the mean number of locations in low-risk transition habitat. The gray line shows the expected mean low-risk transition habitat use if agent locations are assigned randomly on the landscape. See the text for a description of the results.

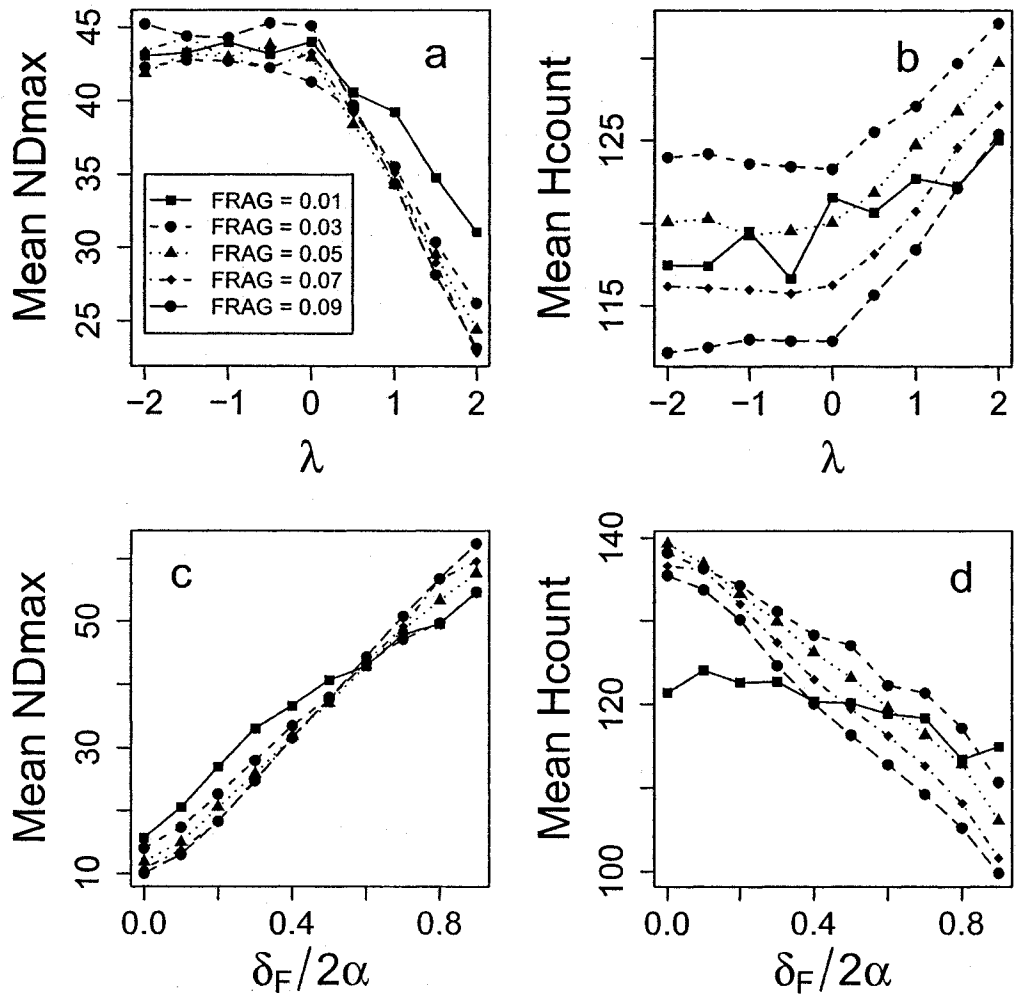


Figure 11: Tradeoff between mean $ND_{max}$ and mean $H_{count}$ with anisotropy and distance weighting. The top subplots a and b correspond to the effect of the distance-weighting parameter $\lambda$. In these figures $P_{cov} = 0.5$ and $\delta_F/2\alpha = 0.6$. The bottom subplots c and d correspond to the effects of anisotropy ($\delta_F/2\alpha$). In these figures $P_{cov} = 0.5$ and $\lambda = 0.0$. Each line in the plots correspond to a different value of $FRAG$, and a key is given in subplot a. In subplot a, net displacement decreases with increasing $\lambda$. In subplot b, use of low-risk habitat increases with increasing $\lambda$. In subplot c, net displacement increases with increasing anisotropy. In subplot d, use of low-risk habitat decreases within increasing anisotropy of the detection space. In some cases (depending on other model parameters), the best distance weighting and degree of anisotropy will depend on the degree of habitat fragmentation in the neutral landscape.

# Agent-based models for animal movement in landscapes

Jeff A. Tracey Jun Zhu Paul Beier Kevin Crooks

## 1 Introduction

Animal movement is an individual-level process with individual, population, and community-level consequences. Movement is based on animal decisions in response to stimuli from the local environment and internal state (including memory), and constrained by perceptual, cognitive, and physical capabilities of an individual (Bell, 1990). A movement decision, in turn, determines which local environment of those available to it the animal will experience next. This new location will present the animal with new information about the landscape it inhabits, threats, and resources that it may require to maintain its internal state. A sequence of movement decisions over the lifetime of the animal determines, in part, its success in survival and reproduction. Movement decisions of many animals leads to the redistribution of organisms in space, exchange of genetic material, transfer of pathogens from one area to another, recolonization of vacant suitable habitat, discovery of new resource patches in dynamic landscapes, demographic rescue in small populations, and predator-prey interactions (Wiens et al., 1993; Ims, 1995; Caro, 1999; Zollner and Lima, 1999).

Human-caused landscape change removes natural habitat, fragments remaining habitat, and introduces new types of landscape features that animals respond to at an individual level. Often, these changes are hazardous to wildlife and may elicit individual-level behavioral responses that alter individual survival, reproduction, and movement across a landscape. Connectivity, which has been defined as "the degree to which the landscape facilitates or impedes movement among resources patches"

(Taylor et al., 1993), is believed to ameliorate these effects when maintained at appropriate levels (Crooks and Sanjayan, 2006). Wildlife movement corridors have been advocated as a means of maintaining functional connectivity among core areas or resource patches in a reserve system (Beier and Noss, 1998; Soulé and Terborgh, 1999). How animals use corridors depends on how animals move through a landscape and respond to local spatial variation (Beier and Noss, 1998; Haddad, 1999). Thus, movement behavior of individuals in response to landscapes has important consequences for wildlife conservation.

In order to prevent local extinction of wildlife populations, we require tools for making useful predictions of individual and population responses to landscape change (Pettifor et al., 2000). We can use such predictions to evaluate alternative choices for reserve design, land use planning, and other decisions that ultimately direct landscape change. Ecological modeling provides a means to apply knowledge to landscapes that we cannot study empirically, such as future landscapes that do not yet exist. Individual-based modeling is a type of agent-based modeling in which software agents represent individual organisms (Huston et al., 1988; DeAngelis and Gross, 1992; Grimm et al., 2005). It is a "bottom-up" approach in which explicit representation of mechanisms at lower levels of hierarchical organization interact to produce behaviors (emergent or otherwise) at higher levels (Railsback, 2001). Agent-based models can incorporate individual-level processes and allow agent behavior to emerge from them, rather than being imposed upon them (Railsback, 2001). As a consequence, agent-based models may be more useful for predicting responses to changing landscape and environmental conditions, and may produce more robust predictions at the individual or population level (Pettifor et al., 2000; Railsback, 2001). Individual-based models have been used to study and predict movement paths of animals across space by iteratively applying movement rules that permit responses to the local environment and possibly internal state (Gustafson and Gardner, 1996; Westervelt, 2002; Gardner and Gustafson, 2004; Kramer-Schadt et al., 2004; Morales et al., 2005).

Our objective is to construct individual-based movement models for use in evaluating functional landscape connectivity. Animal movement is an inherently individual-level process that often depends on an animal's internal state, history, and objectives. Individuals may potentially have different strategies for orienting in their environment. Further, animal movement is based in part on local interactions between an animal and its environment. Using an individual-based approach, we can directly account for individual differences and local interactions between an individual and its environment (Huston et al., 1988). Our current focus is on functional connectivity for low density, wide-ranging species such as mountain lions (*Puma concolor*) which are prone to human-caused mortality beyond the boundaries of protected areas due to the extent of their ranging, migration, or dispersal movements (Beier and Barrett, 1993; Woodroffe and Ginsberg, 1998, 2000). Thus, our models focus on dispersal and ranging movements and movement response to landscape variation, rather than movement in response to other organisms and details of internal physiological processes. For our intended applications, our models have several requirements.

The first requirement is that the agents in our models must be able to operate in a spatially complex environment. When evaluating functional connectivity, we may be interested in simultaneous response to land cover, roads, terrain, and other landscape features. Thus, the agent-based models we develop must be able to respond to a wide range of environmental contexts. In order to operate in such an environment, the models required several essential features. First, the agent must have some ability to collect information from the landscape surrounding its location. Second, this information and information on internal state must be reduced to a single movement response consisting of a continuous move angle and move distance. In the absence of external information to guide movement decisions, the agents base decisions on "default" rules of movement that depend on internal states or recent move history.

The second requirement is that we have the capability to evaluate models with data. These models are intended to guide conservation decisions, so we require the

model predictions to be informative about real target species moving in real or potential future landscapes. Individual-based models have been criticized on the basis of a lack of empirical support, and many suggestions have been made to remedy this situation (Bart, 1995; Weigand et al., 2003; Grimm et al., 2005). With respect to movement, the usefulness of individual-based models may be limited by our understanding of individual-level perception and movement responses (Zollner and Lima, 1999; Tracey, 2006). But there are several advantages to an individual-based approach. Individual-based models are often more directly related to field data (Huston et al., 1988), as is the relation between our movement models and data collected by radio or global positioning system (GPS) telemetry. Further, individual-based movement models can produce patterns at different scales or hierarchical levels such as the move level, daily path level, seasonal path level, seasonal utilization distribution, habitat utilization, and others (Kramer-Schadt et al., 2004; Morales et al., 2005). These patterns can be used to evaluate alternative models using a pattern-oriented approach (Weigand et al., 2003; Grimm et al., 2005). We took advantage of these benefits by proposing a range of alternative models, designing the models so that they can be fit to observed data by a likelihood-based approach, and evaluating the models within information-theoretic and pattern-oriented modeling frameworks.

Third, we must be able to implement a range of alternative models and alter and extend existing models based on what we learn from them. Individual-based models are closely related to their computer implementation and are typically more difficult to implement and communicate than traditional ecological models (Lorek and Sonnenschein, 1999; Pettifor et al., 2000; Railsback, 2001). Because of the effort involved in designing and coding agent-based models, re-usability of code or model components and the ability to alter programs to implement different kinds of agent behaviors is desirable. We want the models to be easily modified to accommodate new model structures. This consists of exchanging some of the model components controlling agent behavior with new components, with minimal re-writing of the code.

In addition, we want the models to be extensible; that is, to be able to add other processes in the future such as response to conspecifics, spatial learning, or internal physiological processes. Finally, some of the parts of the software implementation might be useful in completely unrelated applications, so we want them to be a stand-alone software component.

Our specific goals in this paper are two-fold. First, we will describe the agent-based movement models we have constructed and address several important aspects of modeling animal movement. We will provide details on model formulation and implementation, demonstrate how they can be evaluated with data, and show how fitted models behave in simulations. Second, we will explain how we address issues of empirical support and implementation in agent-based modeling. In order to implement a wide range of alternative models, we utilize a modular or loosely component-based software design (Bian, 2000), and maximized the range of possible configurations each component can assume. This allows a range of alternative models to be configured at run time. We specify a likelihood function for each alternative model, which allows us to fit model parameters by optimizing the likelihood function and apply likelihood-based statistical methods. It became apparent to us during this research that the two issues of implementation and empirical support are related, since the ability to instantiate a range of alternative models within a program also facilitates statistical procedures such as model selection.

# 2 Model formulations and software implementation

## 2.1 Model Overview

The models we designed are composed of three major components that represent the spatial environment, movement agents, and interactions between agents and their environment (Maley and Caswell, 1993; Figure 1). The spatial component contains integer grid objects for representing categorical spatial data and floating-point grid

objects for representing continuous spatial data (Figure 1). The move agent component, which is the focus of this paper, is constructed from a perception component, information processing network, move effector, and genetic algorithm (Figure 1). The agent component also contains data on the agent state, an interface for interacting with the agent component, and functions to set up and coordinate the activities of the smaller components. The perception component consists of an array of detector objects. Each detector collects and summarizes information on a particular type of spatial information (Tracey, 2006). The agent state and the outputs from the perception component constitute *motivational variables* which are passed into the agent's *response function*, also called a *behavioral map* (Enquist and Ghirlanda, 2005). In our models, the response function consists of an *information processing network* and a *move effector*. We have implemented two types of networks: *fully-connected, feed-forward neural networks* (FF-ANNs) and a second type network of our own design that we call *structured networks* (SNs). The FF-ANN and SN information processing networks, due to the component design, can be "swapped out" during construction of an agent object. These networks map the motivational variables to move effector inputs. The move effector component allows one or more move response states. It converts the effector inputs into parameters for the move angle and move distance distribution for each response state, and parameters for selecting a response. Selection of a response state is done using either a finite mixture model (FMM), or a hidden Markov model (HMM). The move effector draws a movement move angle and distance from the appropriate distribution (using pseudo-random number generators, Figure 1) or calculates a likelihood for a set of observed movement responses (using probability density functions, Figure 1); hence, the effector is the "stochastic part" of the models. A genetic algorithm (GA) is a stochastic search algorithm inspired by the mechanisms of evolution by natural selection (Mitchell, 1996). We use the genetic algorithm component to fit the agent's movement model to observed data; however, it can also be used to model learning and behavioral adaptation (Holland, 1992; Strand

et al., 2002; Enquist and Ghirlanda, 2005). Finally, the interaction component relays data between the spatial component and agent component of the model. Its main purpose is to facilitate perception of the local environment by an agent.

From the major components, we constructed two programs in C++. The first is used to fit models to observed data yielding a set of model parameters for a given model and data set, and the second is used to simulate movement from a parameterized model to produce simulated data. The design of the agent component and its sub-components facilitates both model fitting and simulation by altering the flow of information within the agent and between the agent and a data set (Figure 1) and using the move effector to either iteratively draw move angles and distances from the appropriate distributions (for simulation) or to calculate log-likelihood values for a parameter set given a model and observed data (for model fitting). Whether in fitting mode or simulation mode, the flow of information within the agent is always from perception to information processing network to effector, but information flows from the agent state to the effector when in fitting mode, and in the reverse direction when in simulation mode (Figure 1). The GA component is only used in the fitting program, but could easily be used to simulate adaptive movement behavior. In the following sections, we will describe the spatial component, move agent component, and interaction components in greater detail.

## 2.2 Spatial component

In most agent-based ecological models, the process of object recognition is too "low-level" to be represented in detail. We often assume that the agent can recognize objects that we chose to include in the *spatial component* of the model; thus, we make decisions about agent perception and object recognition. In our implementation, continuous spatial data is represented by a grid-based model with a floating-point value in each cell, and categorical spatial data is represented by a grid-based model with an integer value in each cell. Each type of grid is implemented in a separate grid

class that contains a 2-dimensional array for the grid data, spatial attributes of the grid, and member functions that provide an interface and additional functionality such as raster file input/output, spatial calculations, and neutral landscape generation. The software design can be extended to accommodate vector-based spatial data.

## 2.3 Move agent component

In this sub-section, we will describe the agent state and perception, the move effector, how the information processing network maps the motivational variables to effector inputs, and the genetic algorithm component.

### 2.3.1 Agent state

We let $\mathbf{s}_t$ be the vector of agent state variables, where $t$ indexes the observation when in fitting mode, or the time step when in simulation mode. The agent state may include the initial location ($x_0$, $y_0$), the current location ($x_t$, $y_t$), previous move angle ($a_{t-1}$), previous move distance ($l_{t-1}$), and the previous move effector response state ($r_{t-1}$). These state variables provide information needed by the default rules of movement to set detector states (Tracey, 2006) and for response state transitions in the move effector. When fitting data, the agent state is set from observed data, except for the previous move effector response state, which is "hidden." When simulating movement, the agent state is updated from the previous agent state and the response state, move angle, and move distance generated by the move effector.

### 2.3.2 Perception component

The perception component of the model collects and summarizes information from spatial data structures that describe the agent's local environment. The perception component is an array of detector objects, where the detector class implements a *distance-weighted anisotropic detector model* (Tracey, 2006). In this perception model, agents detect objects within an elliptical detection space, weights the effect of each object within the detection space based on distance from the agent, and sum-

marizes the information. Since perception is an interface between a real animal and its environment, it is natural to expect that part of the interface of the agent component serves to pass data directly into the perception component. Each detector in the perception component corresponds to either a single field (such as elevation or temperature) represented as a grid of floating point values or a single type of object (for example urban land cover, a particular category of road) represented as a set of categories in an integer grid. Thus, the maximum number of detectors an agent may have is limited by the spatial data used in the model, but an agent may have fewer detectors and thus ignore some spatial information.

Each detector has three parameters (see Tracey, 2006 for more detail): the semi-major axis length ($\gamma_{h,n,g}$), the distance between foci ($\delta_{h,n,g}$), and the distance-weighting parameter ($\lambda_{h,n,g}$), where $h$ indexes the detector, $n$ indexes the member of the GA population containing the $n^{th}$ set of parameters, and $g$ indexes the generation of the GA population. The three parameters are contained in the segment of the $n^{th}$ member of the GA population designated as $\theta_{Det,h,n,g} = (\gamma_{h,n,g}, \delta_{d,n,g}, \lambda_{h,n,g})$, where $\theta_{Det,n,g}$ contains the parameters for all of the detectors in the model, which may be fitted to data. When in simulation mode, the GA is not used and the indexes $n$ and $g$ can be dropped. In the software implementation, each detector may have its own set of parameters, or all detectors may have the same parameters. If all detectors have the same parameters, the index $h$ can be dropped from the notation. Further, we can set $\delta_{...} = 0$, forcing the detection spaces to be isotropic (circular).

Each detector performs some data reduction functions by selecting only those objects or grid cells that belong to a particular type and fall within its detection space, and by summarizing all of the information for the objects or grid cells it detects within its detection space as a distance weighted mean vector (DWMV, Tracey, 2006). Let $L$ designate the spatial data used in the model. Let $D_h$ be the detector function for the $h^{th}$ detector. The outputs of detector $h$ at time $t$ are ($\Delta x_{h,t}$, $\Delta y_{h,t}$, ang($\Delta x_{h,t}, \Delta y_{h,t}$), dist($\Delta x_{h,t}, \Delta y_{h,t}$)) = $D_h(L|\mathbf{s}_t, \theta_{h,n,g})$, where $\Delta x_{h,t}$ is the x-axis component, $\Delta y_{h,t}$ is

the y-axis component, ang($\Delta x_{h,t}, \Delta y_{h,t}$) is the angle, and dist($\Delta x_{h,t}, \Delta y_{h,t}$) length of the DWMV (Tracey, 2006). Some of these outputs are passed into the information processing network. We let $\mathbf{d}_t$ be the vector of all detector outputs passed into the information processing network at time $t$.

### 2.3.3 Move effector

The move effector allows one or more move responses under the same inputs, and accounts for uncertainty in the movement responses. Hence, it models a choice between one or more possible movement response states and allows variation in move angle and distance within each state. The move effector may be configured to allow only one movement response under a given set of conditions. Alternatively, it may be important to allow the agent to select one of several possible movement responses. For example, a move agent may approach the boundary of urban land cover, but may not want to move into the urban area. It may chose to move away from the urban area. Alternatively, it may attempt to move around the urban area by moving parallel to the urban boundary in either a left or right direction. In this example, there are three possible responses an agent might make when encountering an urban area. For this reason, we postulated that it may be important in some cases to allow the agent to have more than one possible response under the same conditions. In this case, the effector models the selection of one response state from among a set of $R$ available responses using either a finite mixture model (FMM) or hidden Markov model (HMM). In the HMM, selection of a movement response state in the current time step depends on the response state selected at the previous time step and current conditions. The FMM is a reduced case of the HMM in which the selection of the response state in the current time step depends only on current conditions.

The effector uses the network outputs $\mathbf{u}_t$, $\mathbf{v}_t$, and $\mathbf{w}_t$ as inputs and parameters $\theta_{Eff,n,g} = (\alpha_1, \beta_1, \cdots, \alpha_R, \beta_R)$ from the $n^{th}$ GA chromosome at the $g^{th}$ generation (see below) to calculate either a log-likelihood value ($\ell(\mathbf{s}_t, L|\theta_{n,g})$) when in data fitting mode or a simulated move angle and distance ($a_t$, $l_t$) when in simulation mode. We

simplify our models by having fixed move distance parameters ($\alpha_r > 0$ and $\beta_r > 0$) for each of the $r \in 1, \cdots, R$ responses.

**Move angle and distance distributions** Move angles are assumed to come from a von Mises distribution and move distances are assumed to come from a gamma distribution. These distributions were used by Siniff and Jensen (1969) in one of the earliest individual-based movement simulations in ecology, and subsequently in other animal movement models that simulate continuous move angle and distance. We assume independence in move angle and distance, conditional on the move effector state.

The von Mises distribution is a circular analogue to the normal distribution; it has two parameters, a mean angle $\mu_r$ (from $-\pi$ to $\pi$) and a concentration parameter $\kappa_r \geq 0$ (Batschelet, 1981; Mardia and Jupp, 2000). The mean angle is the angle of maximum probability density and the concentration parameter controls the dispersion of the distribution about the mean angle. The distribution is symmetric about the mean angle $\mu_r$. When the concentration parameter $\kappa_r = 0$, the distribution is uniform on $(-\pi, \pi]$. As $\kappa_r$ increases, the distribution becomes more concentrated about the mean angle. In the effector, von Mises parameters are computed as $\mu_r = \text{atan2}(w_{y,r}, w_{x,r})$ and $\kappa_r = \sqrt{w_{x,r}^2 + w_{y,r}^2}$. Von Mises random variables we generated using the ran2() algorithm (Press et al., 1992) and a rejection method described by Mardia and Jupp 2000.

Gamma random variables are positive and the gamma distribution has a flexible shape that is similar to many empirical move length distributions. The distribution has a shape parameter $\alpha_r$ and an inverse scale parameter $\beta_r$ (Rice, 1995). The gamma distribution parameters are "evolved" directly for each response in the GA when fitting models to data, and are fixed when simulating movement. Gamma random variables we generated using the ran2() algorithm (Press et al., 1992) and an algorithm by Ahrens and Dieter (1974) when $\alpha_r < 1.0$ and the GKM3 algorithm by Cheng and Feast (1979) when $\alpha_r \geq 1.0$.

**Response state transitions** We model selection from a set of alternative responses is using a hidden Markov model (HMM) approach (McLachlan and Peel, 2000). The HMM approach allows us to model dependence of the current response state $r_t$ at the current time $t$ on the previous response state $r_{t-1}$ at the previous time $t-1$ (McLachlan and Peel, 2000). In the HMM, we replace the mixing proportions with $\phi_{r(t)} = \sum_{r(t-1)} \phi_{r(t-1),r(t)}\phi_{r(t-1)}$.

We can incorporate the transition probabilities from the $r(t-1)^{th}$ state to the $r(t)^{th}$ state by computing elements of the state transition matrix $\Phi_t$ as follows:

$$\phi_{r(t-1),r(t)} = \begin{cases} \rho_{r(t)} + \phi_{r(t-1)}(1-\rho_{r(t)}) & ; r_t = r_{t-1}, \\ \phi_{r(t-1)}(1-\rho_{r(t)}) & ; r_t \neq r_{t-1}. \end{cases}$$

Here, $\rho_t = (\rho_{1(t)}, \cdots, \rho_{R(t)})'$ are additional parameters where $0 \leq \rho_{r(t)} \leq 1$. We calculate the parameters from the network outputs by $\rho_{r(t)} = [1+\exp(-v_r)]^{-1}$. If all $\rho_{r(t)}$ go to 0, the HMM model reduces to the simpler FMM. In this case, the response state at the current time step is independent of the previous response state. When $r(t-1) = r(t)$, the probability of the $r^{th}$ response is increased by $\phi_{r(t-1)}(1-\rho_{r(t)})$. When $r(t-1) \neq r(t)$ the probability of the $r^{th}$ response is decreased by $\rho_{r(t)}\phi_{r(t-1)}$.

Since the HMM may increase the probability of selecting a response if it has been chosen before, our formulation may promote "stability of behavior" (Enquist and Ghirlanda, 2005, p. 106). Referring back to the urban response example above, under the FMM mode an animal might chose to respond to the urban edge by moving parallel to it in the left direction in one time step, then move parallel to it in the right direction in the next time step, and so on, which would lead to a lack of progress in circumventing the urban area. However, under the HMM mode, once the move agent decided to go around the urban area by following the boundary in the left direction, it would have a higher probability of making the same decision in the next time step.

### 2.3.4 Information processing networks

The information processing networks take detector outputs $\mathbf{d}_t$ and agent state variables $\mathbf{s}_t$ as inputs (Table 1) and produce vectors of outputs $\mathbf{u}_t, \mathbf{v}_t$, and $\mathbf{w}_t$ (Table 2).

The outputs $\mathbf{u}_t$ are used to calculate mixing proportions, $\mathbf{v}_t$ are used to calculate state transitions, and $\mathbf{w}_t$ are used to calculate von Mises distribution parameters in the move effector component. Therefore, both $\mathbf{u}_t$ and $\mathbf{v}_t$ will be empty if there is only one response state in the move effector, and $\mathbf{v}_t$ will be empty if there is more than one response state in the move effector if the effector implements an FMM (Table 2). The segment of the $n^{th}$ GA chromosome containing the network parameters is designated as $\theta_{Net,n,g}$. We designate the network mapping of inputs to outputs as $(\mathbf{u}_t, \mathbf{v}_t, \mathbf{w}_t) = M(\mathbf{s}_t, \mathbf{d}_t | \theta_{Net,n,g})$.

As introduced above, we use two general types of networks: a feed-forward neural networks (FF-ANNs) and structured networks (SNs). Each type of network is implemented as its own component that can be "swapped" with each other within the agent component. This arrangement affords us the opportunity to try different types of networks and create new types of response functions that can be easily "plugged into" the agent class. Each network can be configured to accept a range of inputs and produce outputs required for the move effector.

**Feed-forward neural networks** Artificial neural networks (ANNs) are computational systems with a structure that is motivated by biological neural networks in animals (Hassoun, 1995; Reed and Marks, 1999). ANNs consist of nodes, analogous to neurons, that are often arranged into input, hidden, and output layers (Hassoun, 1995; Reed and Marks, 1999; Figure 2). The nodes are linked to each other by directed connections. Associated with each connection between a pair of nodes is a weight ($\omega_{ji}$'s or $\omega_{kj}$'s below) that scales the "from" node output as it is passed into the "to" node (Hassoun, 1995; Reed and Marks, 1999; Figure 2). Our models use fully-connected feed-forward neural networks that have an input, hidden, and output layer. The term *feed-forward* refers to the "forward direction" of the connections in the network from input to hidden to output layers (Figure 2). Let $i$ index the input nodes, $j$ index the hidden nodes, $k$ index the output nodes of the network. Let $z_i$ be an element of $(\mathbf{s}_t, \mathbf{d}_t)$ and the $i^{th}$ input into the network. The output of the $j^{th}$ hidden

node is $z_j = [1 + \exp(-\omega_{j0} - \sum_i \omega_{ji} z_i)]^{-1}$. In this equation, the summation in the exponential emulates the integration of inputs from other neurons, and the logistic function acts as a nonlinear "threshold gate" that mimics "all-or-nothing" firing of the neuron (Campbell, 1993; Reed and Marks, 1999). The $k^{th}$ element in the vector of network outputs is $z_k = \omega_{k0} + \sum_j \omega_{kj} v_j$, where $z_k$ is an element of the outputs $(\mathbf{u}_t, \mathbf{v}_t, \mathbf{w}_t)$. The sum in the output node is not passed through a threshold function. Instead, the effector applies the appropriate functions to convert the network outputs to parameters for the move angle and distance distributions.

Neural networks have many advantages. One advantage of neural networks is their ability to "learn" by example (Hassoun, 1995; Reed and Marks, 1999). With a training data set consisting of inputs and outputs, the weights of the network ($\theta_{Net,n,g} = \omega$) can be adjusted to improve the input-to-output mapping by the network (Reed and Marks, 1999). Neural networks can also effectively combine many different kinds of inputs (Enquist and Ghirlanda, 2005). Another advantage of neural networks is their "universal approximation" capability (Hassoun, 1995; Reed and Marks, 1999). An ANN with one hidden layer is often sufficient to approximate a continuous function (Reed and Marks, 1999). Thus, neural networks are very useful for modeling complex systems for which we have input and output data, but that are poorly understood (Reed and Marks, 1999).

Network architecture influences the movement capabilities of the model. The input and hidden layers typically have a *bias node*, which simply contains a value of 1 rather than an input (Figure 2). The activation threshold in a node its set by the weight associated with its connection to the bias node (Reed and Marks, 1999). When a neural network is used to generate parameters for the von Mises distribution, as we do, the bias node creates the potential for (appropriately) *directionally biased* (DB; Marsh and Jones, 1988; Turchin, 1998) movement. In some models, we pass the previous move vector in $\mathbf{s}_{t-1}$ into the network which results in a *recurrent* network (an exception to the feed-forward architecture) which is capable of producing a *correlated*

*random walk* (CRW; Kareiva and Shigesada, 1983; Turchin, 1998). In conjunction with the directional bias effect of the bias node, the recurrent network is capable of producing a *directionally-biased correlated random walk* (BCRW) behavior in the models. Under BCRW movement, the agent has a tendency to move both in the direction of the previous move and in a particular compass direction.

In addition to the previous move vector, we can pass several types of inputs into the network, depending on the specific model formulation. If we pass the agent's spatial location or its displacement from its initial location into the network (Table 1) the agent has an ability to move in response to its location in space (we might call this "spatially structured behavior"). Depending on the data used to parameterize the model, this can result in a limited spatial memory that generates home range-like movement behavior (Morales et al., 2005). Furthermore, by passing time inputs into the network (Table 1) the agent can respond to the time of day or time of year, respectively. When $\mathbf{d}_t$, the detector outputs, are feed into the input nodes of the neural network the agent may respond to the landscape features detected by the perceptual component. This latter capability is critical to the application for which these models are designed.

In our implementation of the feed-forward neural network component, the numbers of inputs nodes, hidden nodes, and output nodes can be any positive integer. When used in the agent class, the numbers of inputs are dictated by the number of detectors and agent state variables used in a specific model. The number of output nodes is determined by the number of response states in the move effector. The number of hidden nodes is allowed to vary, and determining the number of hidden nodes is a part of the model selection process.

**Structured networks** There are two disadvantages of the feed-forward neural networks we describe above: they often have many parameters and the parameters do not have an obvious biological interpretation. Thus, we developed a second type of network called *structured networks* (SNs). These SNs have fewer parameters than a

comparable fully connected feed-forward ANN, and it is easier to interpret the meaning of the parameters at the expense of being less adaptable to observed movement behavior. SNs retain some of the network properties, but we impose some structure on the network by replacing some of the weights with functions. The SNs have only an input and output layer of nodes.

In an SN, we distinguish between "scalar inputs" consisting of a single value and "vector inputs" consisting of an x-component and a y-component input pair (Table 1). The scalar inputs are used to calculate the elements of $\mathbf{u}_t$ and $\mathbf{v}_t$ (used to calculate mixing proportions and transition probabilities, respectively, by the move effector) by multiplying each scalar input by a weight associated with the connection between the scalar input and the output node (Figure 3). Within each output node corresponding to $\mathbf{u}_t$ and $\mathbf{v}_t$ the weighted scalar inputs are summed to produce the output value for the node (Figure 3).

The vector inputs are used to calculate the elements of $\mathbf{w}_t$, which correspond to the von Mises move angle distribution parameters, and are also x-component and a y-component output pairs. Input vectors may be, for example, the cosine and sine of the previous angle of movement or a DWMV from a detector. The length of the input vector is interpreted to be correlated with the relative strength of the agent's response. The SN rotates these angles by a *response angle* (from $-\pi$ to $\pi$) and scales the length of the vectors by a *response weight* ($\geq 0$). The response angle is the agent's mean angle of movement in relation to the input vector for a given move response, while the length of the input vector times the response weight relates to the tendency to move in that direction. For example, if one detector calculates a DWMV to urban land cover within the detection space, we might rotate the angle of the DWMV by a response angle of $\pi$ radians (180 degrees) to produce a tendency to move away from urban areas. Further, we might scale the length of the vector by a large response weight which increases the strength of the avoidance response to urban land cover. Once we have rotated and scaled all of the input vectors, the

vectors are added together to yield a resultant vector. The angle of the resultant vector is the mean angle of the von Mises distribution for movement in response to all of the input vectors, and the length of the resultant vector is the concentration parameter of the von Mises distribution. If the move effector permits more than one response, the input vectors can be rotated and scaled in different ways to produce a different resultant vector for each response. For the outputs related to move angle parameters, we make the bias node optional, which allows us to remove directional bias from the model.

Let $z_{S,i}$ be the $i^{th}$ scalar input, and $z_{x,i}$ be the x-axis component and $z_{y,i}$ be the y-axis component of the $i^{th}$ input vector (Figure 3). Let $u_r$ be the $r^{th}$ output in $\mathbf{u}_t$, and $v_r$ be the $r^{th}$ output in $\mathbf{v}_t$. Finally, let $(w_{x,r}, w_{y,r})$ be the x-axis and y-axis components of the output vector in $\mathbf{w}_t$ that are used to calculate the von Mises distribution parameters for the $r^{th}$ response in the move effector. The output $u_r = \omega_{mix,r,0} + \sum_i z_{S,i}\omega_{mix,r,i}$, where $r = 2, \cdots, R$. The output $v_r = \omega_{trans,r,0} + \sum_i z_{S,i}\omega_{trans,r,i}$, where $r = 1, \cdots, R$. Finally, $(w_{x,r}, w_{y,r})'$, where $r = 1, \cdots, R$, is given by:

$$\begin{vmatrix} w_{x,r} \\ w_{y,r} \end{vmatrix} = \sum_i \left( \begin{vmatrix} \omega_{V,i,r}\cos(\nu_{V,i,r}) & -\omega_{V,i,r}\sin(\nu_{V,i,r}) \\ \omega_{V,i,r}\sin(\nu_{V,i,r}) & \omega_{V,i,r}\cos(\nu_{V,i,r}) \end{vmatrix} \times \begin{vmatrix} z_{x,i} \\ z_{y,i} \end{vmatrix} \right)$$

which rotates, scales, and sums the input vectors to produce the output vector for response $r$. For SN networks, the parameters evolved by the GA are $\theta_{Net,n,g} = (\omega_{mix}, \omega_{trans}, \omega_V, \nu_V)$.

### 2.3.5 Genetic algorithm component

Genetic algorithms belong to the domain of evolutionary computing (EC), which is characterized by "evolving" populations of solutions (Eiben and Smith, 2003). Genetic algorithms have been used in many applications to train weights in neural networks (Mitchell, 1996; Reed and Marks, 1999). GAs may be used with ANNs in agent-based modeling to fit ANN weights to a data set (set of training patterns), to model agent learning in response to its environment (Holland, 1992), or to model the evolution of agent behavior among generations (Strand et al., 2002; Morales et al.,

2005). Strand et al. (2002) proposed the ING (Individual-based Neural network Genetic algorithm) concept as a general approach to predict behavioral and life-history traits that are most fit in a particular environment given the physiology of a species.

Many algorithms, such as back-propagation, are available to train neural network weights (Reed and Marks, 1999). These methods have many advantages; however, they are more prone to being trapped by local minima and less useful for recurrent networks than random search procedures like GAs (Hassoun, 1995; Reed and Marks, 1999; Enquist and Ghirlanda, 2005). Genetic algorithms are useful for other model formulations, because we can use them to model learning within agents and evolution among generations of agents. Furthermore, back-propagation is an unrealistic representation of both evolution and learning (Enquist and Ghirlanda, 2005), whereas "trial-by-error" approach of genetic algorithms is a more realistic representation of learning and evolution (Holland, 1992; Strand et al., 2002; Enquist and Ghirlanda, 2005).

In a genetic algorithm, a solution is encoded as an array of bits, integers, floating point numbers, or other data type, depending on the nature of the problem. Each array representing a solution is referred to as a "chromosome" (Mitchell, 1996). In our model, a chromosome is designated by $\theta_{n,g} = (\theta_{Det,n,g}, \theta_{Net,n,g}, \theta_{Eff,n,g})$, where $n = 1, \cdots, N$ is an index identifying the $n^{th}$ chromosome in the population, and $g = 0, \cdots, G$ is the generation. Thus, each chromosome is an array of double-precision, floating-point numbers containing the parameters of the agent's movement model. At generation $g$, the entire set of solutions is:

$$\Theta_g = \begin{vmatrix} \theta_{1,g} \\ \vdots \\ \theta_{N,g} \end{vmatrix}.$$

At $g = 0$, the parameter values are assigned by taking random draws from a normal distribution. At each following generation, fitness is calculated for each chromosome, and the population of chromosomes for the next generation is created from the current generation (Figure 4). We calculate the fitness of a chro-

mosome from its corresponding log-likelihood. Let $\ell_g = (\ell_{1,g}, \cdots, \ell_{N,g})$ be a vector of log-likelihood values for each chromosome in the GA population at generation $g$. We calculated a vector of fitnesses for each chromosome $\mathbf{F}_g = (F_{1,g}, \cdots, F_{N,g})$ as $\mathbf{F}_g = [\ell_g - \min(\ell_g)]/[\max(\ell_g) - \min(\ell_g)] + 0.001$. In our algorithm, we use a selection procedure called "elitism" (Mitchell, 1996) which takes the best $N_{elite}$ chromosomes in the current generation and adds them to the next generation without modification (Figure 4). Elitism guarantees that we retain the best solutions from one generation to the next. Thus, highest fitness in the population will never decrease. The remaining $N - N_{elite}$ members of the next generation are created by a process of selection, recombination (or cross over), and mutation (Figure 4). We create two new chromosomes by first selecting two "parent" chromosomes from the current generation. Our program implements three selection methods: fitness-proportional, Boltzmann, and tournament selection (Mitchell, 1996). In this paper we used tournament selection when fitting the models. In tournament selection, two chromosomes are selected at random with equal probability. The higher-fitness chromosome is selected to be the first parent with probability $p_{tournament}$; otherwise, the lower-fitness chromosome is selected to be the first parent. This process is repeated to select the second parent. Next, a recombination operator is applied to the parent chromosomes with probability $p_{cross}$ to produce two "offspring" chromosomes; other wise, the offspring are copied directly from the parents.

Recombination operators were inspired by cross over between chromosomes during meiosis. Again, our program implements three recombination operators: one-point cross over, two-point cross over, and parameterized uniform cross over (Mitchell, 1996). In this paper we used parameterized uniform cross over when fitting the models. If the recombination operator is applied, "alleles" at a given locus in the chromosomes are exchanged with probability $p_{unif}$; otherwise, they are not exchanged. Next, a mutation operator is applied to each locus in the two "offspring" chromosomes. With probability $p_{mut}$, a normal random variable with mean 0 and variance $\sigma$ is drawn

and added to the current value at the locus. This procedure is applied to each locus in the two offspring chromosomes. After mutation, the two offspring chromosomes are added to the population for the next generation. The selection-recombination-mutation process is repeated until all $N - N_{elite}$ members of the next generation are created.

This process is repeated for a maximum number of generations, or until some other stopping condition is met. We allowed model parameters to evolve for $G = 50,000$ generations, or until 500 ($= G_{\Delta}$) generations passed without decrease in the lowest negative log-likelihood. The parameters controlling the operation of the GA are called *algorithm parameters* (Eiben and Smith, 2003). The parameters we used are given in Table 3, and were selected by trail-and-error experimentation. Alternatively, algorithm parameters can also be evolved (Eiben and Smith, 2003). We must qualify our results by stating that we cannot guarantee that the solutions we arrive at using this procedure are maximum likelihood estimates (MLEs), but we hope to achieve solutions that are near MLEs.

## 2.4 Interaction component

The interaction component of the model relays data from the grid objects to the agent object through the interface of each class. The interaction component acquires a minimum bounding box for the detection space of each detector in an agent's perception component. Next, it determines the rows and columns in each grid object that contains data that must be relayed to the detectors through the agent interface. Then it passes the information for each grid cell to the agent, including the grid object's identification number, the cell attribute, and the center coordinates of the grid cell. This information must be collected by the perception component for every observation during model fitting, or during every move during simulation.

# 3 Examples

## 3.1 Red diamond rattlesnake movement

In this first example we fit a simple neural network to data for movement of a red diamond rattlesnake (*Crotalus ruber*, animal M04) in response to an urban boundary (Tracey, 2000; Tracey et al., 2005). The snake lived in a small fragment of habitat 42 hectares in size in the City of Chula Vista, California. The habitat fragment was completely surrounded by paved roads and housing developments, and no observations suggested that the rattlesnake ever crossed these features (Tracey, 2000). The rattlesnake was tracked during seasons with high movement activity (spring and summer) of 1999 and 2000 by VHF radio telemetry using a small transmitter that was surgically implanted in its peritoneal cavity (Tracey, 2000). The snake was located at 2 or 3 day intervals using a receiver with a directional antenna. Spatial coordinates for each snake location was acquired using a GPS receiver and differential correction techniques to increase accuracy to within a two meters. The boundary of the habitat fragment, which occurred at the edge of roads or urban developments, was digitized from high-resolution aerial imagery (US Geological Survey DOQQs; Tracey et al., 2005). We computed the distance and angle from each rattlesnake location to the nearest point on the habitat patch boundary, the angle the rattlesnake moved, and the response angle for each observation. Data for relocation intervals during which the animal did not move were excluded from this analysis, leaving a total of 49 observed moves.

This example is useful because we can visualize the function fitted to the data, which is much more difficult for models with larger neural networks and many network inputs and outputs. In the model used in this example, rather than using the detectors, we simply passed the distance from the rattlesnake location to the nearest point on the urban boundary into the neural network. Thus, the network had one input node, plus a bias node, in the input layer. The response variable was the response angle (angle of movement minus the angle from the rattlesnake location to the

nearest point on the urban boundary). The neural network output the mean angle ($\mu$) and concentration parameter ($\kappa$) of a single von Mises distribution; therefore, the network had two output nodes. The network also had two nodes, plus a bias node, in the hidden layer. Therefore, the network had a total of ten weights.

The function fit to the data is shown in Figure 5 (the negative log-likelihood is 81.29). The figure shows the von Mises distribution for the response angle (in radians) as a function of distance to the urban boundary (in kilometers). The response angle indicates whether the movement response is one of attraction or avoidance. For example, if the mean response angle ($\mu$) is 0.0 radians, the animal would tend to move toward the urban boundary. However, as this rattlesnake approached the urban boundary (within approximately 80 meters), the mean response angle was close to $\pm\pi$ radians (or equivalently, $\pm$ 180 degrees) which indicates a tendency to move away from the urban boundary. Furthermore, the concentration of the von Mises distribution increases dramatically as the rattlesnake approaches the urban boundary, which suggests that the strength of its move angle response increases since it is less likely to move in a response angle far from the mean. In summary, this neural network model captures much information about the rattlesnake's move angle response to urban development surrounding its habitat and suggests that human alteration of the landscape affected its behavior.

## 3.2 Mountain lion movement

### 3.2.1 Background

Mountain lion (*Puma concolor*) populations in coastal California have been impacted by human-caused habitat loss and fragmentation, mortality from vehicle accidents, and direct killing as a result of conflicts between lions and humans or livestock (Beier and Barrett, 1993). Mountain lions populations are under threat of local extinction in southern coastal areas due to habitat fragmentation (Beier, 1993; Crooks, 2002). Paul Beier and colleagues conducted a VHF radio-telemetry mountain lion study in

the Santa Ana Mountains of coastal southern California, southeast of the City of Los Angeles, from 1986 to 1993 (Beier and Barrett, 1993; Beier, 1995). We fit models to data for three dispersing mountain lions (a female, F17 and two males, M6 and M8) from this study to demonstrate application of our models. These animals were selected because they were dispersers, had the largest numbers of observed movements after the data was prepared for fitting, and had many encounters with urban areas. All animals dispersed from their natal home range while they were radio-tracked. We used data from "diel" sampling sessions during which animals were located at 15 minute intervals during eleven 12 to 24 hour long periods using radio telemetry field methods (Beier, 1995). Observations were omitted if an animal did not move during a 15 minute intervals. We also used the move angle and distance of the previous 15 minute time interval in the models, so if no such previous observation was available we also omitted an observation. This resulted in 100, 160, and 95 observations for F17, M6, and M8, respectively. Land cover was represented as categorical grid with 100 meter square cells. Each cell was assigned to one of eight categories (1 = urban, 2 = rural residential, 3 = agriculture, 4 = orchards and vineyards, 5 = freeways, 6 = parks and open space, 7 = habitat, and 8 = water). These data were derived from land cover data collected around 1995 by the San Diego Association of Governments (SanDAG) and the Southern California Association of Governments (SCAG). Because we had relatively few observations per animal (compared to the numbers often collected using newer GPS tracking devices), we fit relatively simple models to the data.

### 3.2.2 Alternative models

Our objective was to test our approach by fitting several models to the data for each mountain lion based on minimizing the negative log-likelihood function for each model, selecting the best models using an information-theoretic approach (Burnham and Anderson, 2002), and further evaluating the results using a limited pattern-oriented modeling approach (Weigand et al., 2003). We considered 41 alternative models for each mountain lion data set (Table 4). Five models, referred to as "default-

only" models, used structured networks with only correlated random walk default movement rules and no response to land cover (Table 4, models 1–5). For the default-only models, alternatives were based on the number of effector response states and whether the effector used an FMM or HMM. The remaining models may be collectively referred to as "response models" since they include some capability to respond to land cover. Sixteen of the response models, referred to as "SN-based" models, were base on structured networks, a CRW default movement rule, and response to one or more land cover types (Table 4, models 6–21). For the SN-based models, alternative models were based on the types of land cover to which the response was modeled, the number of effector responses, and whether the effector used an FMM or HMM. Twenty of the response models, referred to as "NN-based" models, were based on neural networks, with BCRW default movement rules, and response to one type of land cover (Table 4, models 22–41). For the NN-based models, alternative models were based on the types of land cover to which the response was modeled, the number of effector responses, whether the effector used an FMM or HMM, and the number of hidden nodes in the network. In all versions of the models, we set the detectors to be isotropic (that is, circular, because $\delta = 0$) and all detectors within a model to use the same parameters. These models by no means exercised the full range of models that we are capable of implementing in the programs we developed.

### 3.2.3 Results

### 3.2.4 Model fitting and selection

The lowest negative log-likelihood values achieved by the GA when fitting the models decreased approximately linearly with an increasing number of model parameters. When fitting a model to data using a GA, the log-likelihood rapidly increased during the first several thousand generations, and then improvement was gained more slowly in subsequent generations. This is the typical behavior of evolutionary algorithms (Eiben and Smith, 2003). Models were selected using an information-theoretic approach using Akaike's Information Criterion adjusted for bias when sample sizes are

small ($AIC_c$; Burnham and Anderson, 2002). The negative log-likelihood for the five models with the smallest $AIC_c$ values for each mountain lion are given in Table 5. For all animals, there were at least two landscape response (SN-based or NN-based) models that out performed the best default-only model based on $AIC_c$.

For the female mountain lion F17, the best model used a neural network with three hidden nodes and a move effector with one response (Table 4 and 5). This model included a single detector that collected information on land cover classified as vegetation, and produced an attractive response to this land cover type. The best model had a bias correlated random walk default rule of movement. The second best model used a structured network and a two-response, FMM move effector. This model had a single detector that collects information on land cover classified as urban or water, and produced an avoidance response to these land cover types. The remaining two SN-based models that included response to land cover had $AIC_c$ values that were not very different from the fifth-ranked default-only model.

For the male M6, the top two models had similar $AIC_c$ values (Table 4 and 5). Both were structured network models. One had a 3-response, FMM effector and the other had a 2-response, FMM effector. Both had a single detector that collected information on vegetation land cover, produced attractive movement responses to vegetation cover, and had a correlated random walk default rule of movement. The third-ranked model was an NN-based model with an $AIC_c$ that was $< 2$ away from the fourth-ranked default-only model. The NN-based model also had a 2-response, FMM effector and a detector that collected information on vegetation land cover.

The male M8 also had a top-ranked model that out-performed all others based on $AIC_c$ values (Table 4 and 5). It was an SN-based model with a two-response FMM-based move effector. Like the other male M6, the top model for M8 had a single detector that collected information on vegetation land cover, produced attractive movement responses to vegetation cover, and had a correlated random walk default rule of movement. The second ranked model had similar characteristics as the top-

ranked model, but had an HMM-based move effector. The third-ranked through fifth-ranked models consisted of two default-only models and a structured network model with $AIC_c$ values within 2.16 of each other.

Considering the five models with the lowest $AIC_c$ values for each mountain lion, for a total of fifteen "top-ranked models", ten of these models included land cover response, and the remaining five were default-only models. Seven of the ten land cover response models in the top ranking models for these animals included a single detector for response to vegetation, and all of the "best" models for each animal included this type of response. Only two neural network-based models were among the top-ranked models. This is most likely due to the number of observations we had available for each animal compared to the number of parameters in the FF-ANN models. Four out of five default-only models in the top-ranked models had three effector response states, and one had two response states. For the land cover response models among the top-ranked models, one had an effector with one response state, five had an effector with two response states, and four had an effector with three response states. Three of five default-only models had a HMM effector, while only one in ten response models had an HMM effector. This suggests that these default-only models compensated for a lack of landscape response capability by having more move response states and being more likely to have temporal autocorrelation in the response states.

### 3.2.5 Observed and simulated movement patterns

We compared simulated and observed patterns at two scales, the move level and nightly move path, in a limited pattern-oriented modeling approach to model evaluation (POM; Weigand et al., 2003; Grimm et al., 2005). We simulated 40 movements paths of 1500 move steps each using the best model for each mountain lion. Each simulated mountain lion started at the same initial location, just south of an important movement corridor called "Coal Canyon" which connects the larger Santa Ana Mountains to the Chino Hills area (Beier, 1993; Beier et al., 2006). After simulating the moves we visually compared simulated and observed move-level patterns of (a)

move angle, (b) turn angle, and (c) move distance. If the model has a capability for directional bias (as is the case for F17, due to the effect of the bias node in the neural network model that had the lowest $AIC_c$), then we expect the simulated move angle distribution to be similar to the observed move angle distribution. Otherwise, we expect the simulated move angle distribution to be fairly uniform. Turn angle, which is related to first-order temporal autocorrelation in move angles, is the difference between the move angle at the current time step and the move angle at the previous time step (Turchin, 1998). Hence, if an animal is moving according to a correlated random walk (which was included in all of the models we considered), we expect the distribution of turn angles to be non-uniform (Turchin, 1998).

We compared simulated and observed mean net displacement over the diel sessions. Each diel session occurred over a 12 or 24 hour period. Since mountain lions rarely moved during the day and zero length moves were omitted, and the 12 hour sessions occurred from one hour before sunset to one hour after sunrise (Beier and Barrett, 1993), each diel session roughly corresponds to a mountain lion's movement path over a single night. Thus, this is a pattern at the nightly path level. Net displacement (sometimes calculated in the form of net squared displacement) is the distance from an animal location after a given number of move steps (usually at regular time intervals) to its initial location. It is regarded as a path-level measure of movement (Turchin, 1998). For observed move paths, mean net displacement was calculated by averaging the net displacements across each diel session for each mountain lion at each move. Some diel sessions had more observed movements than others, so as the number of move steps increase the mean is based on fewer diel sessions. For simulated mean net displacement, we used the bootstrap algorithm described by Turchin (1998), except that we bootstrapped the 95 percent confidence intervals from our simulated data separately for each mountain lion, and presented the results as mean net displacement rather than mean net squared displacement. The simulated confidence intervals were created in the R statistical language (R Development Core Team, 2003) by randomly

selecting segments of simulated paths equal in number and length to the number of observed diel sessions and number of observed moves in each diel session, taking the mean at each move step, and repeating the process 5000 times.

The best model for F17 was a neural network with response to vegetation land cover and a directionally-biased, correlated random walk as the default rule of movement. The simulated distributions of move angle, turn angle, and move distance were similar to the observed distributions (Figure 6). Because the bias nodes in the neural network permits directionally biased movement, the simulated data has a move angle distribution similar to the observed data. Notice that the simulated bimodal move angle distribution was created with a neural network-based model and a move effector with only one response state (Figure 6). The best models for M6 and M8 (which, incidentally, were the same model) were structured network-based models with response to vegetation land cover, and a correlated random walk (no directional bias) default rule of movement. For these mountain lions, the simulated turn angle and move distance distributions are similar to the observed distributions (Figures 7 and 8). However, since these models lacked directional bias capability, as expected the simulated move angle distributions are uniform whereas the observed distributions are not. For all mountain lions, the turn angle distributions in both the observed and simulated data indicate a tendency to move in a angle similar to the previous move; therefore, a correlated random walk is an appropriate part of the default movement rule.

Results for comparison of the nightly path-level pattern of net displacement is illustrated in Figure 9. An interesting pattern in comparing the simulated mean net displacement to the observed mean net displacement for all animals is that during the middle of the diel session the observed mean was above the simulated mean, while near the end of the session the observed mean was generally below the simulated mean. This suggests that the mountain lions, on average, went further from their starting location than predicted during the middle of the evening, and then returned

to a location closer to their initial location at the beginning of the evening than expected from the simulations. This suggests that the observed movements of these mountain lions over the diel sessions were more structured in time and space than the formulations of the best model we fit (or only of the other 40 models we considered) for each animal allowed.

We provide an example of a simulated movement path from the best model for each mountain lion (Figure 10). Since the best models only include response to vegetation, which is attractive based on the parameter estimates from the data, they only demonstrate a tendency to move toward vegetation, which provides the only mechanism to avoid urban areas or other land cover types (Figure 10). Therefore, if there is no vegetation land cover that intersects the move agent's detection space, which would occur for example if the agent was surrounded by urban land cover, then no useful information can be acquired from the spatial component to guide movements. The effect of directional bias is clearly visible in the move path for F17 (Figure 10, left), and the simulated move paths tended to be roughly parallel to the major axis of the Santa Ana Mountains. Simulations of this type are useful for evaluating functional connectivity in landscapes not accessible to empirical study.

# 4 Discussion

Our objective in this research is to develop agent-based movement models for large-scale movements of wide-ranging, low-density species such as mammalian carnivores in response to landscapes that have been altered by humans. We have presented our framework for agent-based movement modeling, described an implementation strategy that allows us to instantiate a very large number of alternative models, and demonstrated how to fit and evaluate alternative models using data from mountain lions in the Santa Ana Mountains of coastal southern California. The models we have developed allow for agent perception of its external environment, can take into account internal states and perceptual information, and permit multiple movement responses

under given conditions. In addition to continuing to develop and improve these models, we intend to use these models to evaluate functional landscape connectivity.

We have taken a less common "vector-based" movement approach where the agent is able to move freely in space by drawing move angles and distances from continuous distributions. Many individual-based movement models represent agent movement between adjacent cells in a raster (for examples, see Gustafson and Gardner, 1996; Gardner and Gustafson, 2004; Kramer-Schadt et al., 2004; Morales et al., 2005). We might think of these types of movement models as drawing moves from a multinomial distribution in which the probability of each outcome (movement into a particular adjacent cell) is dependent on environment and agent state. However, the vector-based approach that we have used to model movement is a more natural fit to movement observations at discrete, regular time intervals using methods such as VHF radio or GPS tracking. This correspondence between model and data facilitates the likelihood-based approach to fitting models that we adopted in this research. Using log-likelihood as a basis for calculating fitness, we used a genetic algorithm to fit models to observed data at the move level for each mountain lion. Overall, the likelihood-based approach worked very well in combination with the genetic algorithm. After fitting 41 alternative models for each mountain lion, we used Akaike's Information Criterion ($AIC_c$) to select models that performed best at the move level. Land cover response models were selected over default-only models for each mountain lion, even though we made an effort to construct default-only models that had a chance of out performing the response models; that is, they were not "straw man" null hypotheses. We are unaware of any other move models that have been fit to movement data in this way, or to this degree. Thus, our approach permits an unprecedented ability to fit and simulate models for movement response to landscapes.

We further evaluated the models using a limited pattern-oriented modeling approach, which we found very useful. The move-level patterns we used to evaluate the models were turn angle, move angle, and move distance. All of the models included a

correlated random walk as part of the default movement rule. This was incorporated into the model by passing the previous movement vector back into the network, creating a recurrent connection. This "first-order autocorrelation" in move angles can be described as a distribution of turn angles. In the observed data, mountain lions had non-uniform turn angle distributions that were clustered around 0 radians, indicating a tendency to move in an angle similar to the previous move (a similar pattern was found in previous work (Dickson et al., 2005)). For each mountain lion, the simulated and observed turn angle distributions were similar. Further, the simulated distributions of move distances were similar to those observed for each animal. Thus, the simulated data from the best fitted models were very consistent with the observed move-level patterns that we considered.

When directional bias is included in the model (for example, the AIC-selected model for F17), the simulated and observed move angle patterns are fairly similar (as judged by quantile plots, not shown). If directional bias is not included (as in the best models for M6 and M8), there is no mechanism in the model to generate bias in particular directions, so it is incapable of matching empirical move angle distributions. In the observed data, F17 showed a clearer pattern of directional bias than the males M6 and M8 (Figures 6, 7, and 8). However, we may not always want to include directional bias in a model. For example, directionally biased movement may result from orientation in relation to site-specific distant cues or spatial learning. It may not be appropriate to transfer this pattern of directionally biased movement may to other locations when we use the model to simulate movement to evaluate landscape connectivity. For this reason, future models will allow us to have the option to remove the effect of the bias node of neural networks on move angles.

We detected inconsistencies between the simulated and observed nightly path-level pattern of net displacement for each mountain lion. These inconsistencies suggest that dispersing sub-adult mountain lions may organize their movement activity in time and space to a greater extent than the models we evaluated permit. In the

diel sessions during which data was collected, they tend to move further from their initial location during the middle of the evening and then return to a location nearer their initial location than predicted by the best models. This pattern suggests that spatial memory plays an important role. A possible next step in improving the models is to permit spatial and temporal referencing by passing displacement from the initial location at the beginning of the evening and time of day into the information processing network. We already have implemented the basic means to do this, but we may want to consider mechanistic explanations for how mountain lions spatially and temporally reference their movements.

An important point is that when adopting a pattern-oriented modeling approach, some patterns may be more relevant to the modeling objectives than others. Other researchers have used a pattern-oriented approach with movement models. For example, Kramer-Schadt et al. (2004) used the percent of dispersal habitat used, average maximum distance from the starting point of dispersal, whether or not simulated paths crossed a heavily human populated plain, and move step distribution as patterns. Morales et al. (2005) used daily displacement, turn angle distributions, net squared displacement, and redistribution kernels as patterns to evaluate movement models. Utilization distributions and utilization of different habitat types or landscape elements (e.g., topographic features) may also be useful patterns. Further work should include development of patterns to use in evaluating movement models according to the modeling objectives and the spatial and temporal scales addressed by the models.

As a result of a component-based implementation strategy that includes flexible and exchangeable components, we can instantiate a very wide range of alternative models. Component flexibility means that a component in a model can take on a wide range of configurations. For example, the number of response states in our move effector is only limited by data and computational resources, and the neural and structured networks can be configured to take a wide range of inputs, and the

number of hidden nodes in the neural network can be any natural number (again, only limited by data and computational resources). Component exchangeability refers to the ability to replace one component with another, as we did with the neural network and structured network components. We can implement models that have been revised based on what we have learned from model evaluation in the current iteration of the modeling process due to the exchangeability of the components and extensibility of the software design by linking new components into the agent. Therefore, an important conclusion from this work is that there is a strong connection between model implementation and evaluation. The ability to instantiate many alternative models facilitates model selection and evaluation, and exchangeable components and extensibility facilitates model alternation based on what we learn from the model evaluation.

On theoretical grounds, we expect that the ANNs will probably prove more useful in the future than the structured networks. Fully-connected, feed-forward neural networks have many parameters, and given the size of the data sets we used this worked against them in the model selection process in this paper. However, newer global positioning system tracking methods allow large numbers of observations to be collected per animal, making the neural networks a more viable option. Furthermore, in future work we will implement neural networks capable of instantiating a broader range of network architectures, rather than just the fully-connected, feed-forward topology. This will allow us to create networks with fewer strategically chosen connections between nodes that more directly reflect hypotheses about information processing in animals (Enquist and Ghirlanda, 2005), and therefore have fewer parameters. Still, the structured-network models may be useful in cases where we have fewer observations for each animal, or when we want a more biological interpretation of model parameters.

In general, we believe agent-based modeling approaches are useful in ecological studies and conservation applications. Over the past two decades, the initial hype

over individual-based modeling has given way to a more mature understanding of the strengths and weaknesses of these approaches and development of techniques to address the challenges in using them. The models we have presented here have drawn on these developments, and have confronted the important challenges of agent-based model implementation and evaluation. As a result, we have movement models that can produce realistic movement responses to objects in the landscape and move-level patterns. Further, the results provide guidance for the next iteration in working with these models. Thus, we have developed models that are useful in ongoing studies of animal movement behavior and as a tool for evaluating functional landscape connectivity and other processes.

# References

Ahrens, J. H., and U. Dieter. 1974. Computer methods for sampling from gamma, beta, Poisson and binomial distributions. Computing **12**:223–246.

Bart, J. 1995. Acceptance criteria for using individual-based models to make management decisions. Ecological Applications **5**:411–420.

Batschelet, E. 1981. Circular Statistics in Biology. Academic, New York.

Beier, P. 1993. Determining minimum habitat areas and habitat corridors for cougars. Conservation Biology **7**:94–107.

Beier, P. 1995. Dispersal of juvenile cougars in fragmented habitat. Journal of Wildlife Management **59**:228–237.

Beier, P., and R. H. Barrett, 1993. The Cougar in the Santa Ana Mountain Range, California. Technical report, Orange County Cooperative Mountain Lion Study.

Beier, P., and R. F. Noss. 1998. Do habitat corridors provide connectivity? Conservation Biology **12**:1241–1252.

Beier, P., K. L. Penrod, C. Luke, W. D. Spencer, and C. Cabanero, 2006. South coast missing linkages: restoring connectivity to wildlands in the largest metropolitan area in the United States. *in* K. R. Crooks and M. Sanjayan, editors. Connectivity Conservation. Cambridge University Press, Cambridge.

Bell, W. J. 1990. Searching Behaviour: The behavioral ecology of finding resources. Chapman and Hall, New York.

Bian, L. 2000. Component modeling for the spatial representation of wildlife movements. Journal of Environmental Management **59**:235–245.

Burnham, K. P., and D. R. Anderson. 2002. Model Selection and Multimodel Inference. 2nd edition. Springer, New York.

Campbell, N. A. 1993. Biology. 3rd edition. Benjamin/Cummings Publishing, Redwood City, CA.

Caro, T. 1999. The behavior-conservation interface. Trends in Ecology and Evolution **14**:366–269.

Cheng, R. C. H., and G. M. Feast. 1979. Some simple gamma variate generators. Applied Statistics **28**:290–295.

Crooks, K. R. 2002. Relative sensitivities of mammilian carnivores to habitat fragmentation. Conservation Biology **16**:488–502.

Crooks, K. R., and M. Sanjayan, editors. 2006. Connectivity Conservation. Cambridge University Press, Cambridge.

DeAngelis, D. L., and L. J. Gross, editors. 1992. Individual-Based Models and Approaches in Ecology. Chapman and Hall, New York.

Dickson, B. G., J. S. Jenness, and P. Beier. 2005. Influence of vegetation, topography, and roads on cougar movement in southern California. Journal of Wildlife Management **69**:264–276.

Eiben, A. E., and J. E. Smith. 2003. Introduction to Evolutionary Computing. Springer, New York.

Enquist, M., and S. Ghirlanda. 2005. Neural Networks and Animal Behavior. Princeton Univesity Press, Princeton.

Gardner, R. H., and E. J. Gustafson. 2004. Simulating dispesal of reintroduced species within heterogeneous landscapes. Ecological Modelling **171**:339–358.

Grimm, V., E. Revilla, U. Berger, F. Jeltsch, W. M. Mooij, S. F. Railsback, H. Thulke, J. Weiner, T. Weigand, and D. L. DeAngelis. 2005. Pattern-oriented modeling of agent-based complex systems: lessions from ecology. Science **310**:987–991.

Gustafson, E. J., and R. H. Gardner. 1996. The effect of landscape heterogeneity on the probability of patch colonization. Ecology **77**:94–107.

Haddad, N. M. 1999. Corridor use predicted from behaviors at habitat boundaries. The American Naturalist **153**:215–227.

Hassoun, M. H. 1995. Fundamentals of Artificial Neural Networks. MIT Press.

Holland, J. H., editor. 1992. Adaptation in Natural and Artificial Systems. MIT Press, Cambridge, Mass.

Huston, M., D. DeAngelis, and W. Post. 1988. New computer models unify ecological theory. BioScience **38**:682–691.

Ims, R. A., 1995. Movement Patterns Related to Spatial Structures. *in* L. Hansson, L. Fahrig, and G. Merriam, editors. Mosaic Landscapes and Ecological Processes. Chapman and Hall, London.

Kareiva, P. M., and N. Shigesada. 1983. Analyzing insect movement as a correlated random walk. Oecologia **56**:234–238.

Kramer-Schadt, S., E. Revilla, T. Wiegand, and U. Breitenmoser. 2004. Fragmented landscapes, road mortality and patch connectivity: modelling influences on the dispersal of Eurasian lynx. Journal of Applied Ecology **41**:711–723.

Lorek, H., and M. Sonnenschein. 1999. Modelling and simulation software to support individual-based ecological modelling. Ecological Modelling **115**:199–216.

Maley, C. C., and H. Caswell. 1993. Implementing *i-state* configuration models for population dynamics: an objet-oriented approach. Ecological Modelling **68**:75–89.

Mardia, K. V., and P. E. Jupp. 2000. Directional Statistics. Wiley, New York.

Marsh, L. M., and R. E. Jones. 1988. The form and consequences of random walk models. Journal of Theoretical Biology **133**:113–131.

McLachlan, P., and D. Peel. 2000. Finite Mixture Models. Wiley.

Mitchell, M. 1996. An Introduction to Genetic Algorithms. MIT Press, Cambridge, Mass.

Morales, J. M., D. Fortin, J. L. Frair, and E. H. Merrill. 2005. Adaptive models for large herbivore movements in heterogeneous landscapes. Landscape Ecology **20**:301–316.

Pettifor, R. A., K. J. Norris, and J. M. Rowcliffe, 2000. Incorporating behaviour in predictive models for conservation. *in* L. M. Gosling and W. J. Sutherland, editors. Behaviour and Conservation. Cambridge University Press, Cambridge.

Press, W. H., S. A. Teukolsky, W. T. Vetterling, and B. P. Flannery. 1992. Numerical Recipes in C. 2nd edition. Cambridge.

R Development Core Team, 2003. R: A language and environment for statistical computing. R Foundation for Statistical Computing, Vienna, Austria. URL `http://www.R-project.org`.

Railsback, S. F. 2001. Concepts from complex adaptive systems as a framework for individual-based modeling. Ecological Modelling **139**:47–62.

Reed, R. D., and R. J. I. Marks. 1999. Neural Smithing. MIT Press.

Rice, J. A. 1995. Mathematical Statistics and Data Analysis. Duxbury, Belmont.

Siniff, D. B., and C. R. Jensen. 1969. A simulation model of animal movement patterns. Advanced Ecological Research **6**:185–217.

Soulé, M. E., and J. Terborgh. 1999. Continental Conservation. Island Press, Washington.

Strand, E., G. Huse, and J. Giske. 2002. Artificial evolution of life history and behavior. The American Naturalist **159**:624–644.

Taylor, P. D., L. Fahrig, K. Henein, and G. Merriam. 1993. Connectivity is a vital element of landscape structure. Oikos **68**:571–573.

Tracey, J. A., 2000. Movement of Red Diamond Rattlesnakes (*Crotalus ruber*) in Heterogeneous Landscapes in Coastal Southern California. Master's thesis, University of California, San Diego.

Tracey, J. A., 2006. Animal perception in agent-based models. In prep.

Tracey, J. A., J. Zhu, and K. Crooks. 2005. A set of nonlinear regression models for animal movement in response to a single landscape feature. Journal of Agricultural, Biological, and Environmental Statistics **10**:1–18.

Turchin, P. 1998. Quantitative Analysis of Movement. Sinauer Associates, Sunderland.

Weigand, T., F. Jeltsch, I. Hanski, and V. Grimm. 2003. Using pattern-oriented modeling for revealing hidden information: a key for reconciling ecological theory and application. Oikos **100**:209–222.

Westervelt, J. D., 2002. Geographic Information Systems and Agent-Based Modeling. *in* H. R. Gimblett, editor. Integrating Geographic Information Systems and Agent-based Modeling Techniques for Simulating Social and Ecological Processes. Oxford University Press, Oxford.

Wiens, J. A., N. C. Stenseth, B. Van Horne, and R. A. Ims. 1993. Ecological mechanisms and landscape ecology. Oikos **66**:369–380.

Woodroffe, R., and J. R. Ginsberg. 1998. Edge effects and the extinction of populations inside protected areas. Science **280**:2126–2128.

Woodroffe, R., and J. R. Ginsberg, 2000. Ranging behaviour and vulnerability to extinction in carnivores. *in* L. M. Gosling and W. J. Sutherland, editors. Behaviour and Conservation. Cambridge University Press, Cambridge.

Zollner, P. A., and S. L. Lima. 1999. Search strategies for landscape-level interpatch movements. Ecology 80:1019–1030.

Table 1: Network inputs. R is the number of response states in the effector. For categorical spatial data (land cover, roads, and land form, there is one detector per type, where a type is a set of categories. For continuous data (elevation), there is one detector per layer. For elevation, elevation is calculated as the difference between the elevation of each grid cell in the detection space minus the elevation at the agent's location. All distance inputs are rescaled to kilometers. "Daytime" is the time of day in decimal format (from 0.0 to 1.0), and "yeartime" is the day of year divided by the number of days in the year. The neural net column lists inputs for models that use the feed-forward neural network, and the structured net columns list scalar and vector inputs from the models that use structured networks. Each model may use a subset of the sources of input listed in this table.

| input source | neural net | structured net | |
|---|---|---|---|
| | | scalar | vector |
| internal state ($s_t$) | | | |
| previous move | $x_t - x_{t-1}$ | $l_{t-1}$ | $\cos(a_{t-1})$ |
| | $y_t - y_{t-1}$ | | $\sin(a_{t-1})$ |
| spatial location | $x_t - x_0$ | $\text{dist}(x_t - x_0,\, y_t - y_0)$ | $x_t - x_0$ |
| | $y_t - y_0$ | | $y_t - y_0$ |
| time | | | |
| of day | $\cos(2\pi\text{daytime})$ | | |
| | $\sin(2\pi\text{daytime})$ | | |
| of year | $\cos(2\pi\text{yeartime})$ | | |
| | $\sin(2\pi\text{yeartime})$ | | |
| detector outputs ($d_t$) | | | |
| land cover | $\Delta_{x,i,t}$ | $\text{dist}(\Delta_{x,i,t},\, \Delta_{y,i,t})$ | $\Delta_{x,i,t}$ |
| | $\Delta_{y,i,t}$ | | $\Delta_{y,i,t}$ |
| road | $\Delta_{x,i,t}$ | $\text{dist}(\Delta_{x,i,t},\, \Delta_{y,i,t})$ | $\Delta_{x,i,t}$ |
| | $\Delta_{y,i,t}$ | | $\Delta_{y,i,t}$ |
| land form | $\Delta_{x,i,t}$ | $\text{dist}(\Delta_{x,i,t},\, \Delta_{y,i,t})$ | $\Delta_{x,i,t}$ |
| | $\Delta_{y,i,t}$ | | $\Delta_{y,i,t}$ |
| elevation change | $\Delta_{x,i,t}$ | $\text{dist}(\Delta_{x,i,t},\, \Delta_{y,i,t})$ | $\Delta_{x,i,t}$ |
| | $\Delta_{y,i,t}$ | | $\Delta_{y,i,t}$ |

Table 2: Number of network outputs. The number of outputs produced by an information processing network depends on $R$, the number of response states in the effector, and whether the move effector is in finite mixture model (FMM) or hidden Markov model (HMM) mode. Values used by the move effector to calculated mixing proportions are returned by the network as $u_t$, values used by the effector to calculate transition probabilities are returned as $v_t$, and values used by the effector to calculate von Mises (move angle) parameters are returned by the network as $w_t$.

| Effector response mode | Output vector | Number of network outputs for | | | |
|---|---|---|---|---|---|
| | | mixing proportions | transition probabilities | von Mises parameters | total |
| single | $u_t$ | 0 | 0 | 2 | 2 |
| multiple-FMM | $v_t$ | R - 1 | 0 | 2R | 3R - 1 |
| multiple-HMM | $w_t$ | R - 1 | R | 2R | 4R - 1 |

Table 3: Genetic algorithm parameters. When we fit the models to data, we kept most algorithm parameters fixed. However, we increased the mutation rate ($p_{mut}$) and decreased the variance in the mutation ($\sigma$) linearly as the number of generations since improvement ($g_\Delta$) progressed toward the maximum number of generations allowed without improvement ($G_\Delta$).

| parameter | description | value |
|---|---|---|
| $G$ | max. generations | 50000 |
| $G_\Delta$ | max. generations without improvement | 500 |
| $g$ | current generation | 50000 |
| $g_\Delta$ | generation since improve | 500 |
| $N$ | GA population size | 60 |
| $N_{elite}$ | number elite chromosomes | 10 |
| $p_{tournament}$ | tournament selection parameter | 0.7 |
| $p_{cross}$ | probability of cross over | 0.95 |
| $p_{unif}$ | uniform cross over param. | 0.7 |
| $p_{mut}$ | probability of locus mutation | $0.001 + [g_\Delta\ 0.004]/G_\Delta$ |
| $\sigma$ | variance in locus mutation | $1.0 - [g_\Delta\ 0.9375]/G_\Delta$ |

Table 4: Forty-one alternative models for puma data. Model is an identification number for the models, param is the number of parameters in the model. Network gives the network type where SN = structured net and NN = neural net. Hidden gives the number of hidden nodes. Responses gives the number of effector responses. HMM indicates whether the model used an HMM (T) or FMM (F) to select response states in the effector. Default gives the default movement rule where CRW = correlated random walk, and BCRW = directionally biased correlated random walk. Detectors gives an identification number for the detectors used in the model where detector 1 detects vegetation in the land cover layer (category 7), detector 2 detects urban and water in the land cover layer (categories 1 and 8), and detector 3 detects disturbed land cover (categories 2, 3, 4, 6).

| model | param | network | hidden | responses | HMM | default | detectors |
|---|---|---|---|---|---|---|---|
| 1 | 24 | SN | - | 3 | T | CRW | - |
| 2 | 18 | SN | - | 3 | F | CRW | - |
| 3 | 16 | SN | - | 2 | T | CRW | - |
| 4 | 12 | SN | - | 2 | F | CRW | - |
| 5 | 6 | SN | - | 1 | F | CRW | - |
| 6 | 35 | SN | - | 3 | T | CRW | 1 |
| 7 | 26 | SN | - | 3 | F | CRW | 1 |
| 8 | 23 | SN | - | 2 | T | CRW | 1 |
| 9 | 17 | SN | - | 2 | F | CRW | 1 |
| 10 | 8 | SN | - | 1 | F | CRW | 1 |
| 11 | 35 | SN | - | 3 | T | CRW | 2 |
| 12 | 26 | SN | - | 3 | F | CRW | 2 |
| 13 | 23 | SN | - | 2 | T | CRW | 2 |
| 14 | 17 | SN | - | 2 | F | CRW | 2 |
| 15 | 8 | SN | - | 1 | F | CRW | 2 |
| 16 | 77 | SN | - | 4 | T | CRW | 1, 2, 3 |
| 17 | 57 | SN | - | 4 | F | CRW | 1, 2, 3 |
| 18 | 57 | SN | - | 3 | T | CRW | 1, 2, 3 |
| 19 | 42 | SN | - | 3 | F | CRW | 1, 2, 3 |
| 20 | 37 | SN | - | 2 | T | CRW | 1, 2, 3 |
| 21 | 27 | SN | - | 2 | F | CRW | 1, 2, 3 |

Table 4 continued.

| model | param | network | hidden | responses | HMM | default | detectors |
|---|---|---|---|---|---|---|---|
| 22 | 83 | NN | 4 | 3 | T | BCRW | 1 |
| 23 | 68 | NN | 4 | 3 | F | BCRW | 1 |
| 24 | 61 | NN | 4 | 2 | T | BCRW | 1 |
| 25 | 51 | NN | 4 | 2 | F | BCRW | 1 |
| 26 | 34 | NN | 4 | 1 | F | BCRW | 1 |
| 27 | 67 | NN | 3 | 3 | T | BCRW | 1 |
| 28 | 55 | NN | 3 | 3 | F | BCRW | 1 |
| 29 | 49 | NN | 3 | 2 | T | BCRW | 1 |
| 30 | 41 | NN | 3 | 2 | F | BCRW | 1 |
| 31 | 27 | NN | 3 | 1 | F | BCRW | 1 |
| 32 | 83 | NN | 4 | 3 | T | BCRW | 2 |
| 33 | 68 | NN | 4 | 3 | F | BCRW | 2 |
| 34 | 61 | NN | 4 | 2 | T | BCRW | 2 |
| 35 | 51 | NN | 4 | 2 | F | BCRW | 2 |
| 36 | 34 | NN | 4 | 1 | F | BCRW | 2 |
| 37 | 67 | NN | 3 | 3 | T | BCRW | 2 |
| 38 | 55 | NN | 3 | 3 | F | BCRW | 2 |
| 39 | 49 | NN | 3 | 2 | T | BCRW | 2 |
| 40 | 41 | NN | 3 | 2 | F | BCRW | 2 |
| 41 | 27 | NN | 3 | 1 | F | BCRW | 2 |

Table 5: The five best models for each mountain lion based on $AIC_C$. The model column corresponds to the model column in Table 4 which describes the models. The column $-\ell$ gives the negative log-likelihood values. The top five models for each mountain lion are ranked in ascending order of $AIC_c$.

| mountain lion | rank | model | type | $-\ell$ | $\text{AIC}_c$ | $\Delta_i$ |
|---|---|---|---|---|---|---|
| F17 | 1 | 31 | NN | 60.554 | 196.11 | 0.00 |
| | 2 | 14 | SN | 80.370 | 202.20 | 6.09 |
| | 3 | 12 | SN | 70.474 | 212.18 | 16.07 |
| | 4 | 7 | SN | 70.690 | 212.61 | 16.5 |
| | 5 | 3 | default | 87.049 | 212.65 | 16.54 |
| M6 | 1 | 9 | SN | 102.602 | 243.51 | 0.00 |
| | 2 | 7 | SN | 90.541 | 243.64 | 0.13 |
| | 3 | 30 | NN | 69.046 | 249.28 | 5.77 |
| | 4 | 2 | default | 105.115 | 251.08 | 7.57 |
| | 5 | 1 | default | 98.730 | 254.35 | 10.84 |
| M8 | 1 | 9 | SN | 72.592 | 187.13 | 0.00 |
| | 2 | 8 | SN | 68.229 | 198.01 | 10.88 |
| | 3 | 2 | default | 78.147 | 201.29 | 14.16 |
| | 4 | 1 | default | 68.878 | 202.90 | 15.77 |
| | 5 | 12 | SN | 65.401 | 203.45 | 16.32 |

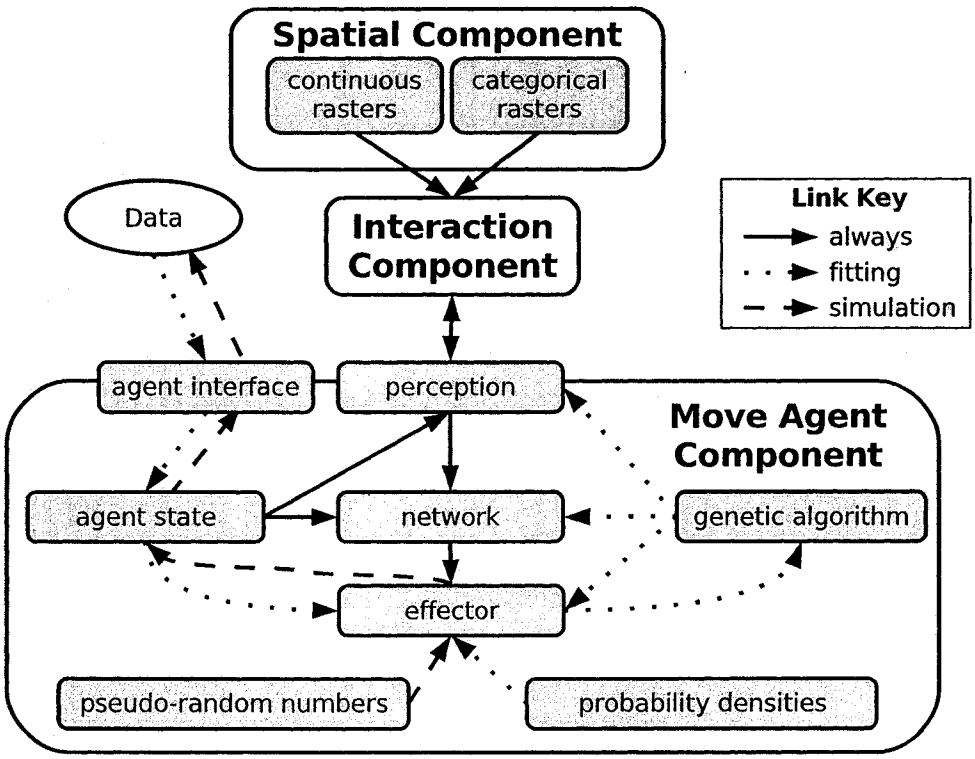


Figure 1: Model components and their interactions. The arrows with solid lines show directions of information flow that occur in both the model fitting program and the simulation program. The arrows with dotted lines show directions of information flow in the fitting program. The arrows with dashed lines show directions of information flow in the simulation program. The components used to construct the move agent are shown as rectangles shaded in gray.

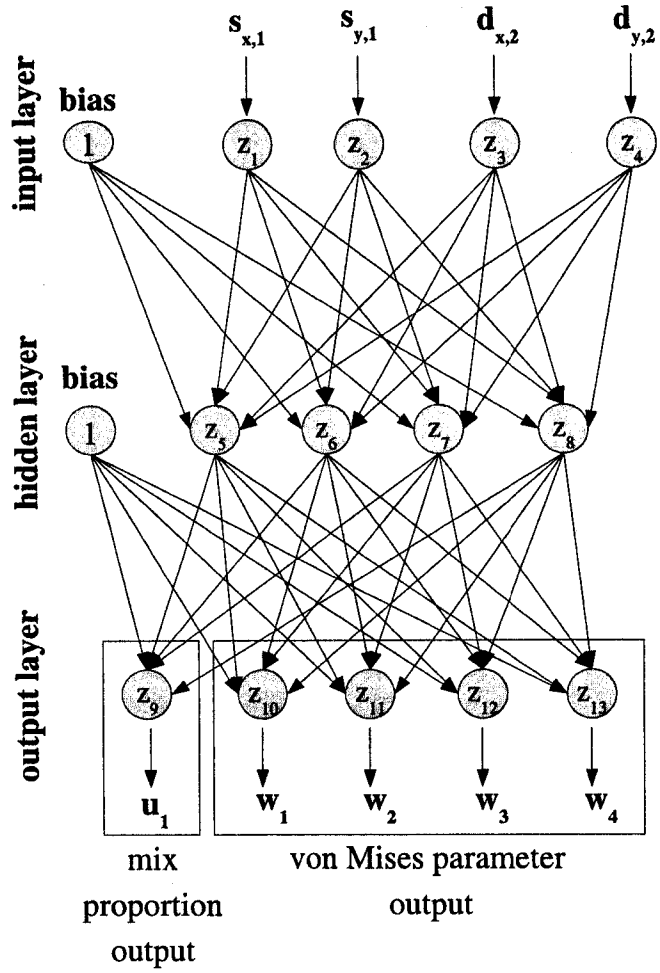


Figure 2: An example of a three layer, fully connected, feed-forward neural network. This example corresponds to a model with outputs from one detector ($d_{x,2}$ and $d_{y,2}$) and the previous agent move vector ($s_{x,1}$ and $s_{y,1}$) as network inputs, and a move effector in finite mixture model mode with two response states. Since the effector uses a FMM, there are no network outputs in $\mathbf{v}_t$. The nodes are illustrated as gray circles, and the connections, each with an associated weight parameter, are illustrated as arrows connecting the nodes.

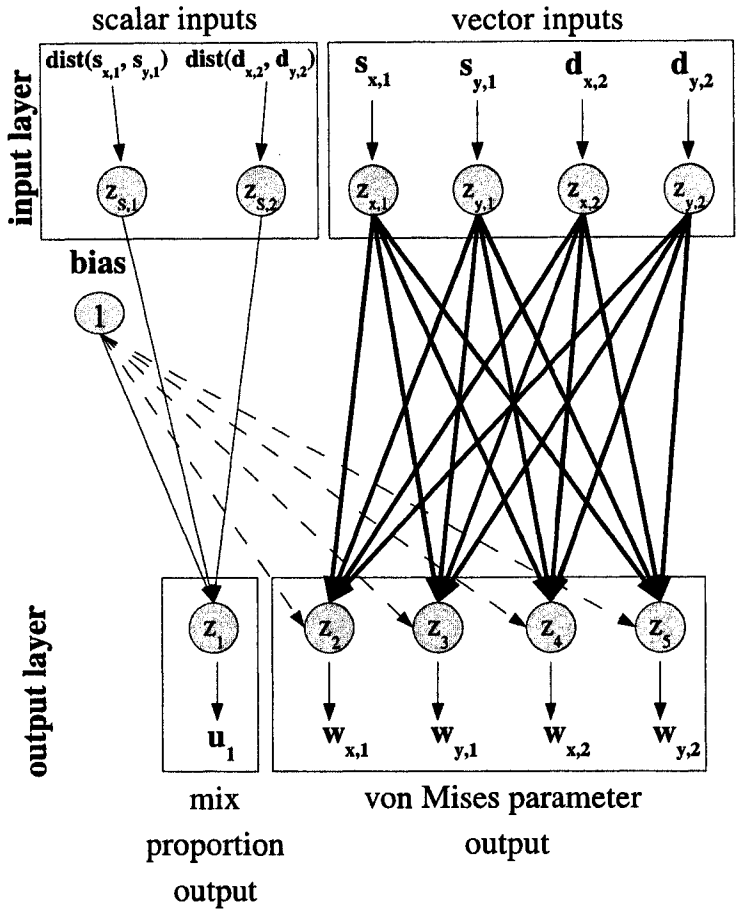


Figure 3: An example of a structured network. This is a structured network that is similar (but not identical) to the FF-ANN illustrated in Figure 2. The nodes are illustrated as gray circles. The thin solid lines between nodes show connections from the bias node and scalar input nodes to the output node corresponding to the mixing proportion. The scalar inputs in this case are simply the lengths of the vector inputs. The thin dashed lines from the bias node show optional connections that, if used, allow the structured network model to incorporate directional bias. The thick solid lines show connections linking vector inputs to outputs used by the effector to calculate von Mises distribution parameters. The weights associated with these connections are determined by functions of the input, and have response angle and response weight parameters (see text for equations). Since the effector uses a FMM, there are no network outputs in $\mathbf{v}_t$.

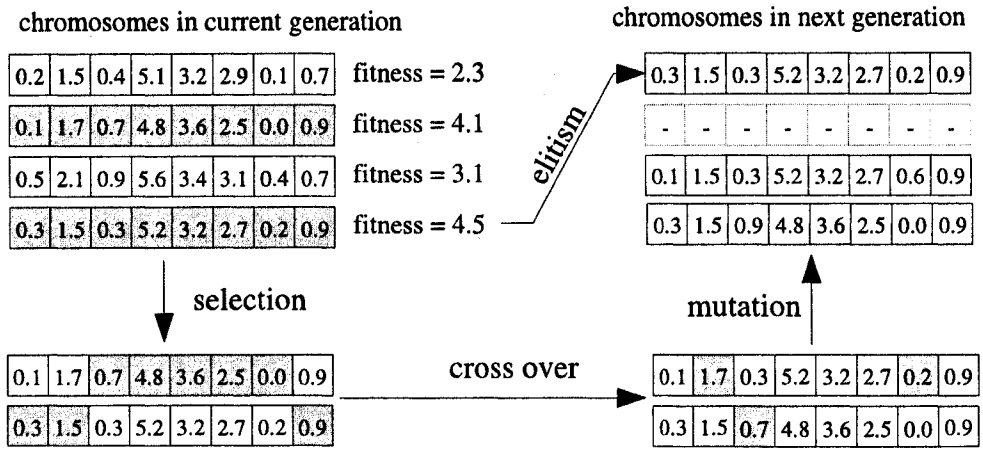


Figure 4: Operations in a genetic algorithm. This figure illustrates the creation of a new population of solutions (top right) from the population in the prior, parent generation (top left). In this small population, we select the highest fitness chromosome and copy it without modification into the new population, which is called "elitism." The remaining three members of the new population are created by selecting two parents based on their fitnesses (shaded chromosomes in the upper left). The parents are recombined using, in this example, a two-point crossover operation, In the lower left, the shaded loci will become part of the second (bottom) "offspring" chromosome in the lower right, and the unshaded loci will become part of the first offspring chromosome. The offspring chromosomes (lower right) created by recombination of the parent chromosomes are then subject to mutation, which will occur in the shaded loci. The resulting chromosomes are added to the population in the next generation (top right). This process of selection-recombination-mutation is repeated until all members of the new population are created. In this example, we only have one more member to create (top right, chromosome with "-"s), so we will only the first offspring created from one more iteration of the selection-recombination-mutation process.

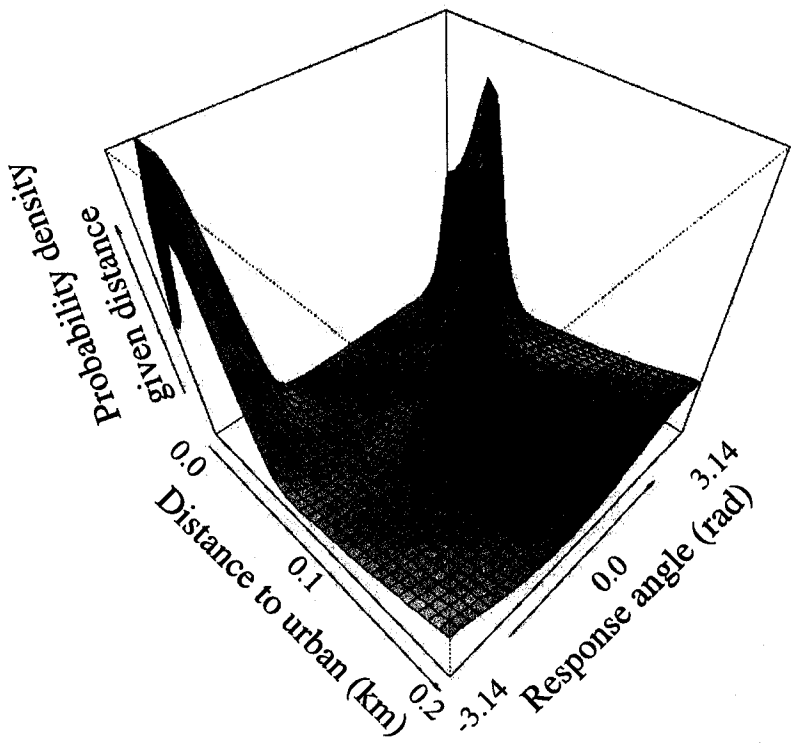


Figure 5: A simple artificial neural network for move angle response to urban edge fit to data for a red diamond rattlesnake *Crotalus ruber*. In this model, the distance to the urban boundary is the covariate. The neural network fitted the mean angle and concentration parameter of a von Mises distribution for response angle to the urban boundary as a function the the covariate. In the figure, the response angle directs the rattlesnake away from the urban boundary with increasing concentration as the distance to the boundary decreases.

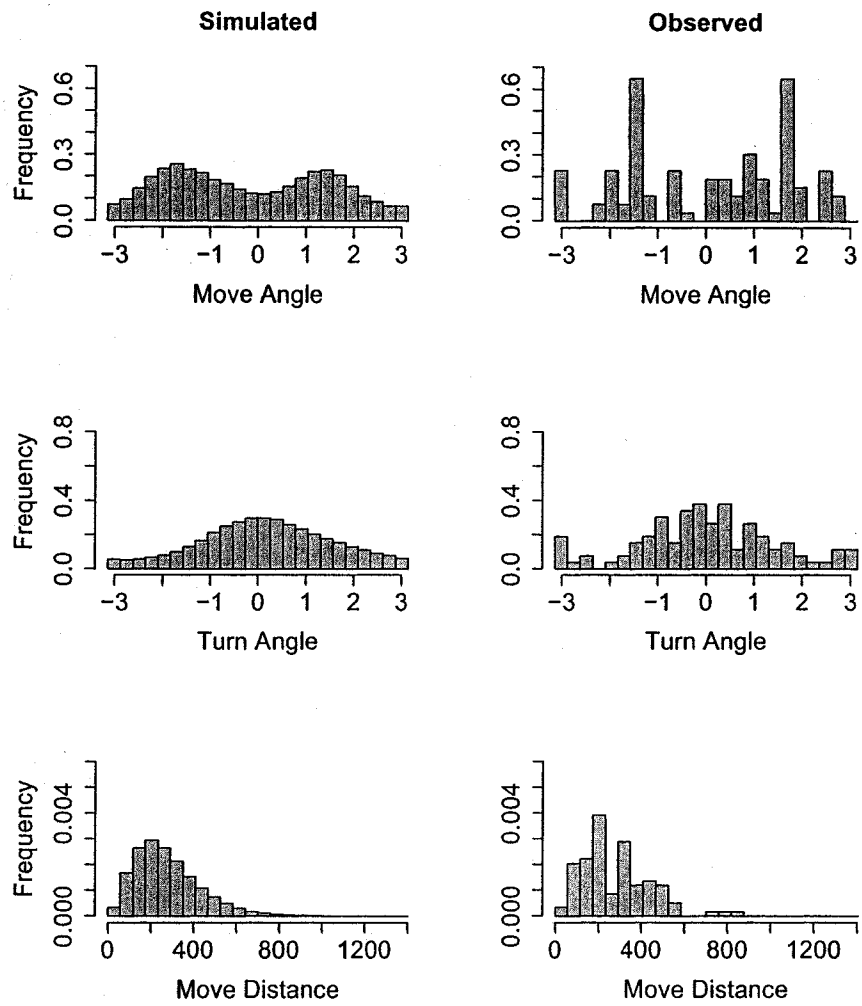


Figure 6: Observed and simulated move angle, turn angle, and move distance distributions for mountain lion F17. The best model for F17 allowed directional bias, so the simulated move angle distribution was able to match the observed distribution. Move angles and turn angles are in radians, and move distance is in meters.

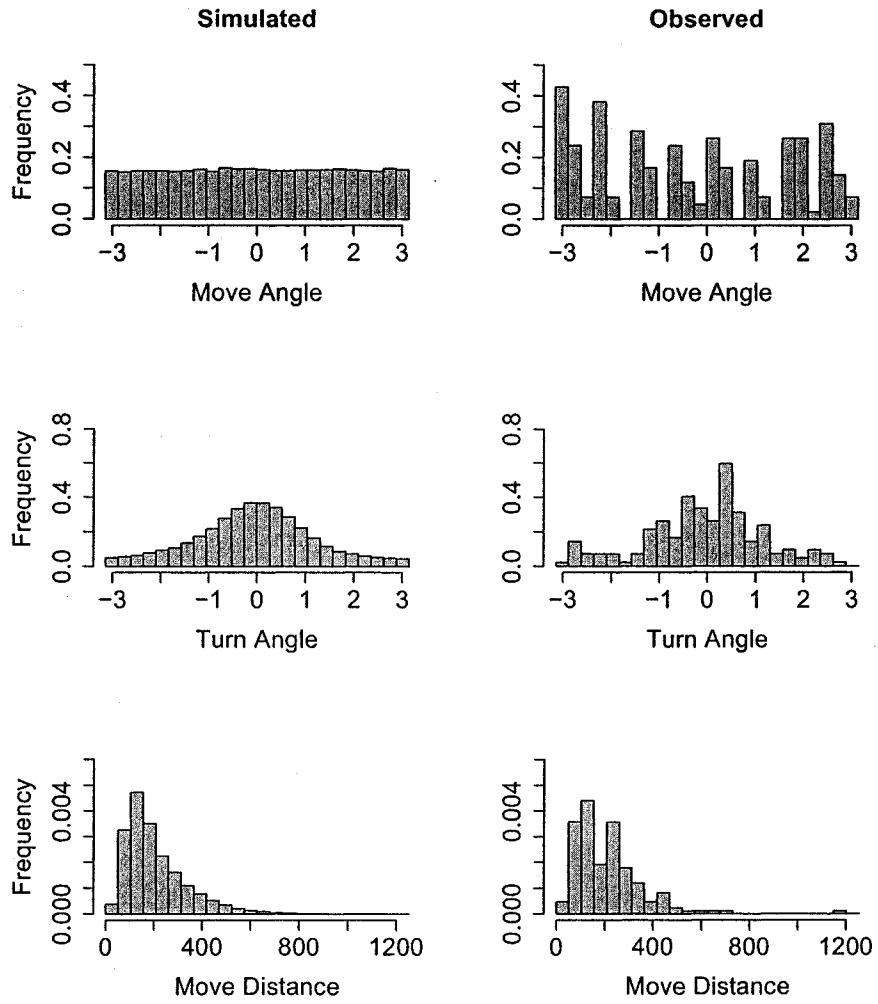


Figure 7: Observed and simulated move angle, turn angle, and move distance distributions for mountain lion M6. The best model for M6 did not allow directional bias, so the simulated move angle distribution is uniform, unlike the observed move angle distribution. Move angles and turn angles are in radians, and move distance is in meters.

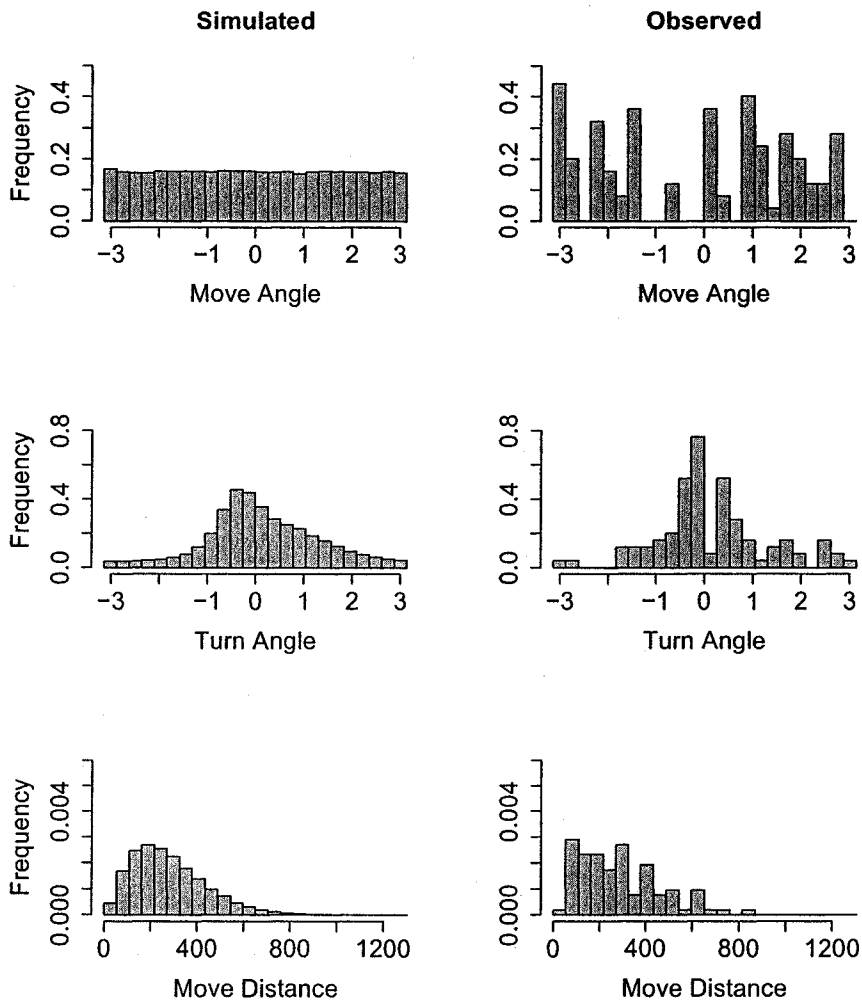


Figure 8: Observed and simulated move angle, turn angle, and move distance distributions for mountain lion M8. The best model for M6 did not allow directional bias, so the simulated move angle distribution is uniform, unlike the observed move angle distribution. Move angles and turn angles are in radians, and move distance is in meters.

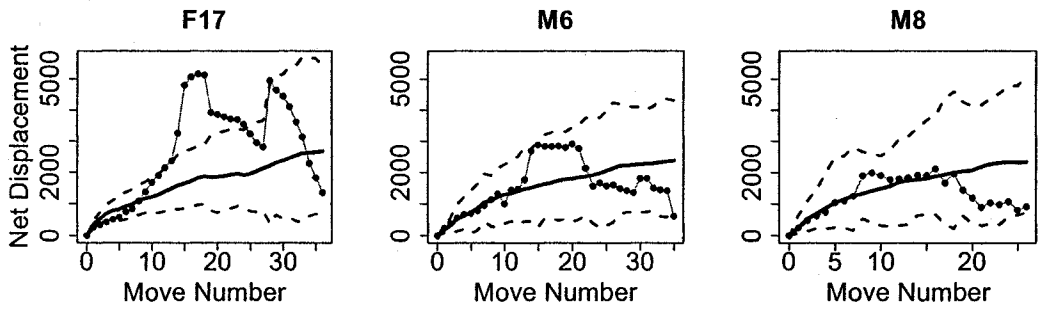


Figure 9: Observed and simulated mean net displacement (meters) for each mountain lion (from left to right F17, M6, and M8). The black points jointed by gray lines are the observed net displacements at each move step (in meters). Net displacement is the distance from the initial location, in this case at the beginning of a diel sampling session, after a given number of move steps. A single move step corresponds to a 15-minute time interval. The thick black line is the mean simulated mean net displacement, and the dashed lines enclose the 95 percent confidence region. For each mountain lion, note that the observed mean net displacement tends to exceed the simulated simulated mean net displacement for intermediate numbers of move steps and fall below the simulated mean for larger numbers of move steps.

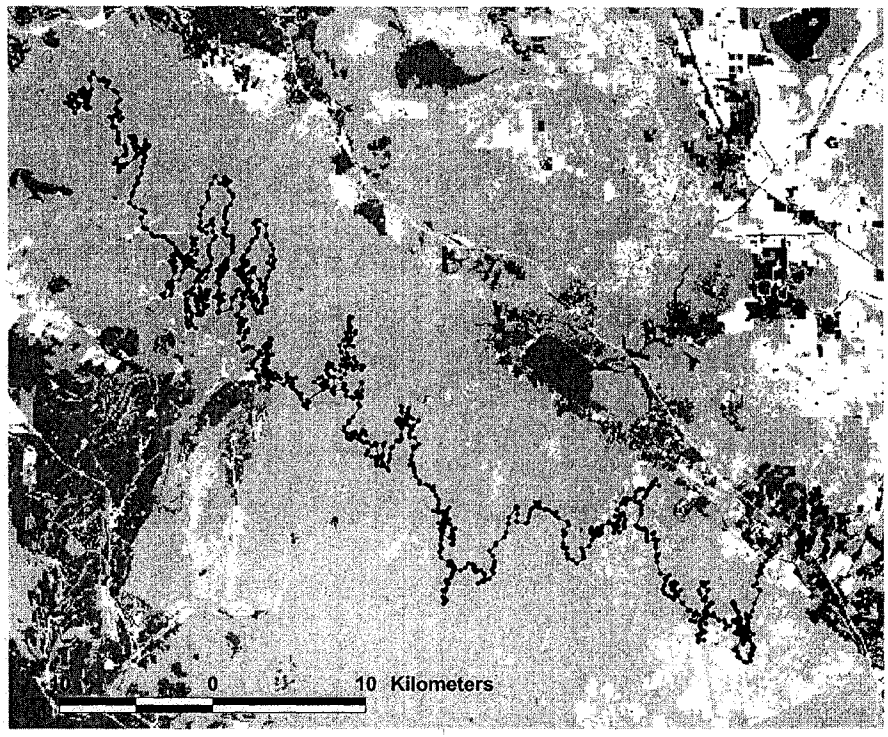


Figure 10: Examples of a simulated move path for mountain lion F17 (left), M6 (center), and M8 (right). The black points joined by black lines is an example of a simulated movement path. The dark gray regions are urban development or water, the light gray regions are vegetation, and the white areas are other land cover types. The best model for F17 was a neural network that was capable of producing directionally biased movement, which is evident in the observed move angles, simulated move angles, and in the simulated paths. The best model for M6 and M8 was a structured network model with a correlated random walk default rule. Each model allows an attractive response to vegetation, and does not respond to other land cover types.

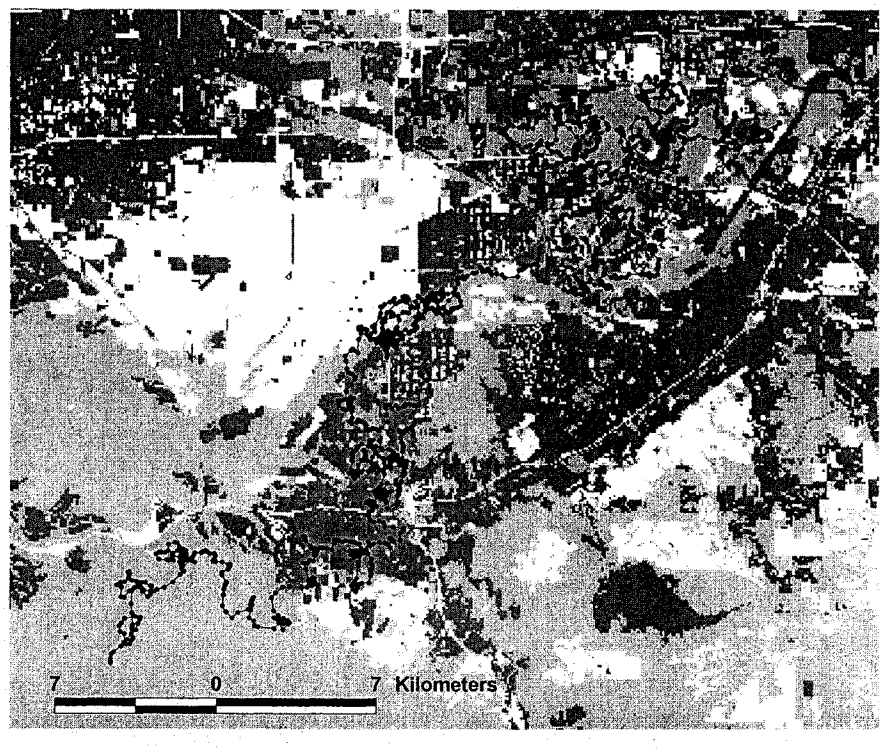


Figure 10 center.

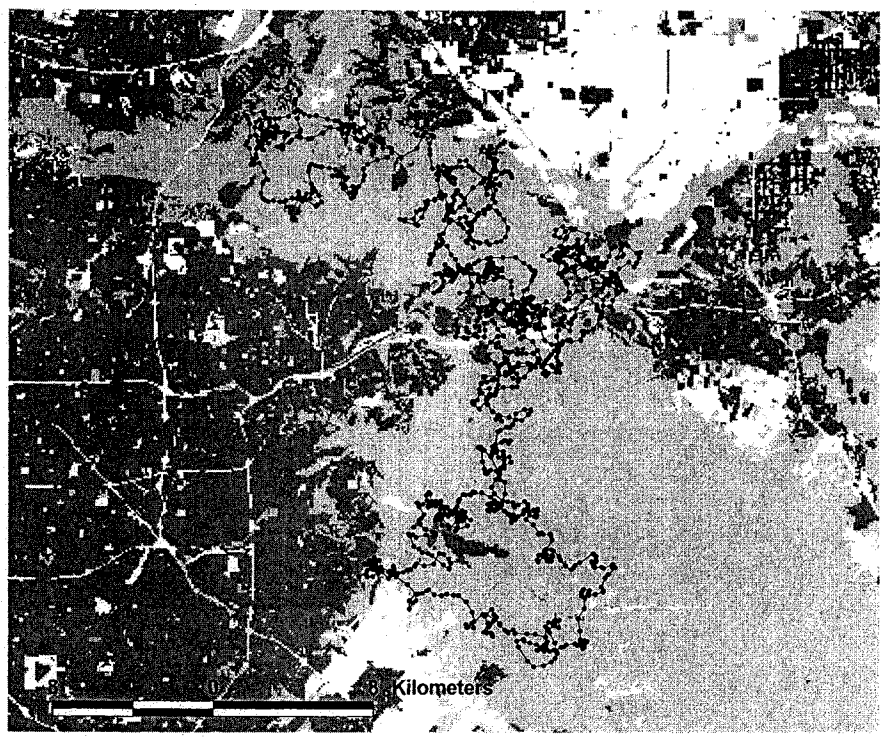


Figure 10 right.